รายงานวิจัยฉบับสมบูรณ์

โครงการ

การประยุกต์ใช้กระบวนการสโทแคสติกและเทคนิคด้านอินเวอร์สโมเดลลิงในการสร้างแบบจำลองคณิตศาสตร์ของแอ่งน้ำบาดาลเชียงใหม่

โดย

ดร. จิรัฏฐ์ แสนทน
ภาควิชาธรณีวิทยา คณะวิทยาศาสตร์ มหาวิทยาลัยเชียงใหม่

สิงหาคม 2553

สัญญาเลขที่ MRG4980079

รายงานวิจัยฉบับสมบูรณ์

โครงการ

การประยุกต์ใช้กระบวนการสโทแคสติกและเทคนิคด้านอินเวอร์สโมเดลลิงในการสร้างแบบจำลองคณิตศาสตร์ของแอ่งน้ำบาดาลเชียงใหม่

โดย

ดร. จิรัฏฐ์ แสนทน
ภาควิชาธรณีวิทยา คณะวิทยาศาสตร์ มหาวิทยาลัยเชียงใหม่

สนับสนุนโดยสำนักงานคณะกรรมการการอุดมศึกษา และสำนักงานกองทุนสนับสนุนการวิจัย
(ความเห็นในรายงานนี้เป็นของผู้วิจัย สกอ. และ สกว. ไม่จำเป็นต้องเห็นด้วยเสมอไป)

Abstract

This research dealt with the application of stochastic methods and inverse modeling technique in setting up a comprehensive regional groundwater flow model of the Chiang Mai basin. Both deterministic and stochastic approaches were used to simulate groundwater flow regime in the semi- to unconsolidated aquifers. The flow model used in this study was a USGS finite-difference groundwater flow program called MODFLOW-2000 and the inverse modeling codes included PEST, UCODE, and PES (one of the package in MODFLOW-2000). Deterministic model simulation indicated that the annual water budget of the basin under steady-state condition was 241 Mm^3. The most sensitive parameters were hydraulic conductivity and recharge. Through stochastic simulation, the model uncertainty was evaluated. The uncertainty in water budget is $\pm$12.1 Mm^3 (95% confidence) and the average error in estimated heads was approximately $\pm$4 m.

บทคัดย่อ

การศึกษาวิจัยนี้ ได้นำวิธีการสโทแคสติกและวิธีการอินเวอร์สโมเดลลิง มาใช้ในการจัดทำแบบจำลองการไหลของน้ำใต้ดินในแอ่งเชียงใหม่ในสเกลระดับภูมิภาค โดยได้ใช้แนวทางการจัดทำแบบจำลองทั้งชนิดดีเทอมินิสติกและสโทแคสติก เพื่อประเมินการไหลของน้ำใต้ดินในชั้นหินอุ้มน้ำที่เป็นตะกอนร่วน และตะกอนร่วนกึ่งแข็ง โปรแกรมที่ใช้ในการจัดทำแบบจำลองคือโปรแกรมประเภทไฟไนต์ดิฟเฟอเรนซ์ ที่มีชื่อว่า MODFLOW-2000 และโปรแกรมที่ช่วยในการปรับแบบจำลองได้แก่ PEST, UCODE และ PES (ซึ่งเป็นแพ็คเกจใน MODFLOW-2000) ผลการจำลองการไหลแบบดีเทอมินิสติกพบว่าสมดุลน้ำในชั้นตะกอนร่วนมีค่าเป็น 241 ล้านลูกบาศก์เมตรต่อปี และตัวแปรที่มีความอ่อนไหวมากที่สุดคือค่าสัมประสิทธิ์ความซึม และอัตราการเติมน้ำใต้ดินโดยธรรมชาติ ส่วนผลการจำลองการไหลแบบสโทแคสติกพบว่า ค่าความไม่แน่นอนของสมดุลน้ำในความเชื่อมั่นระดับ 95% อยู่ที่ ±12.1 ล้านลูกบาศก์เมตร และค่าเฉลี่ยของผลต่างระหว่างเฮดที่คำนวณจากแบบจำลองและเฮดที่วัดได้คือ ±4 เมตร

Table of Contents

List of Figures

List of Tables

Chapter 1

Introduction

Chapter 1: Introduction

1.1. Rationale

The importance of groundwater for the existence of human society cannot be overemphasized. Groundwater is the major source of drinking water in both urban and rural Thailand. Besides, it is an important source of water for the agricultural and the industrial sector. Water utilization projections recently put the groundwater usage at about 50%. Being an important and integral part of the hydrological cycle, its availability depends on the rainfall and recharge conditions. Until recently it had been considered a dependable source of uncontaminated water.

The demand for water has increased over the years and this has led to water scarcity in many parts of the country. The situation is aggravated by the problem of water pollution or contamination. Thailand is heading towards a freshwater crisis mainly due to improper management of water resources and environmental degradation, which has lead to a lack of access to safe water supply to millions of people.

There has been a lack of adequate attention to water conservation, efficiency in water use, water re-use, groundwater recharge, and ecosystem sustainability. An uncontrolled use of the borehole technology has led to the extraction of groundwater at such a high rate that often recharge is not sufficient. The causes of low water availability in many regions are also directly linked to the reducing forest cover and soil degradation.

In rural areas of the Chiang Mai basin, which include Chiang Mai and Lamphun provinces, people still heavily rely upon the availability of groundwater for both domestic uses and agricultural purposes. In an area such as Sankamphaeng, a large cone of depression was discovered during the dry season resulting in a scarcity of water supply for farms and orchards. This indicates a major abuse to groundwater resource where the rate of underground water extraction was significantly more than

natural recharge rate. Therefore, there is the need for better manage groundwater resource of the Chiang Mai basin so that sustainable use can be achieved.

In order to assess and mange groundwater resource more efficiently and more quantitatively, a groundwater model is commonly and, perhaps, inevitably used as a tool for risk assessment and management. It is the main purpose of this research which is to assess the uncertainty in groundwater reserves of the Chiang Mai basin using numerical model. In addition, areas that have high uncertainty in reserves prediction will be delineated using stochastic modeling approach.

1.2. Background

Since the 1960s, numerical ground-water flow models have become increasingly important tools for the analysis of ground-water systems. More recently, ground-water flow models have been combined with optimization techniques to determine water-resource management strategies that best meet a particular set of management objectives and constraints. Optimization techniques are a set of mathematical programs that seek to find the optimal (or best) allocation of resources to competing uses. In the context of ground-water management, the resources are typically the ground- and surface-water resources of a basin and (or) the financial resources of the communities that depend on the water. The management objectives and constraints are stated (or formulated) mathematically in an optimization (management) model. Combined groundwater flow and optimization models have been applied to various ground-water management problems, including the control of water-level declines and land subsidence that could result from ground-water withdrawals, conjunctive management of ground-water and surface-water systems, capture and containment of contaminant plumes, and seawater intrusion.

A number of computer codes have been developed during the past two decades to facilitate linked flow and optimization modeling of ground-water flow systems (Lefkoff and Gorelick, 1987; Greenwald, 1998; Zheng and Wang, 2002; Ahlfeld and Riefler, 2003; Peralta, 2004). These codes differ in the numerical model used to represent the ground-water flow system, the types of ground-water management problems that can be solved, and the approaches used to solve the management problems.

Stochastic models of groundwater flow are based on statistical theories (Dagan, 1986; Gelhar, 1986). They have been applied to determination of head and velocity fields, as well as solute transport problems. Since the early 1980s a very large number of papers have been published, in which many different types of stochastic models of

groundwater flow have been described. In general these papers are difficult for people not trained in the specific mathematics utilized to read and understand. Although most groundwater practitioners who use groundwater models reply upon deterministic rather than stochastic models, the usefulness of stochastic model in simulating groundwater flow (and/or contaminant transport) is tremendous in terms of analyzing uncertainties for better management of groundwater resources.

1.3. Objectives

(1) To develop a well-calibrated groundwater flow model of the Chiang Mai Basin at a regional scale.

(2) To delineate uncertainties in assessing groundwater reserves using stochastic methods.

1.4. The Chiang Mai Basin

The study area covers approximately 2800 km^2 from 18°30′ to 19° north and from 98°45′ to 99°15′ east. The Chiang Mai-Lamphun valley has a kidney shape with mountain ranges on either side which reach a maximum elevation of up to 1685 m to the west and 1025 m to the east of it. The width of this basin reaches more than 25 km in the central part. The inner basin is relatively flat with elevations between 360 and 280 m above mean sea level.

The watershed is harboured by the Ping River, which enters the basin at an elevation of about 320 m in the north and leaves it at about 280 m in the south. Rainfall ranges from less than 800 mm/yr in the valley to more than 1500 mm/yr in the mountains. Precipitation is high between May and October. Potential evaporation mostly exceeds rainfall, except between July and October which is the main period of groundwater recharge.

The domestic water supply of the cities of Chiang Mai, Mae Rim and Doi Saket is based mainly on surface water. All other cities and villages are supplied from groundwater resources, but only some of the larger municipalities have a central water distribution system. Rising demand and increasing sanitary problems has led to increased drilling of groundwater wells since the early 1980s. Previously, the domestic water supply was from hand-dug wells.

The groundwater basin of the **semi- to unconsolidated aquifers** that is being modelled in this research is approximately one-fourth of the area of both provinces. The boundary is delineated using computer software (WMS 7.1®) and illustrated as shaded area (see Figure 1-1). The north-south and east-west lengths of the basin are

approximately 70 and 45 km, respectively. The narrowest portion (width) is about 15-25 km.

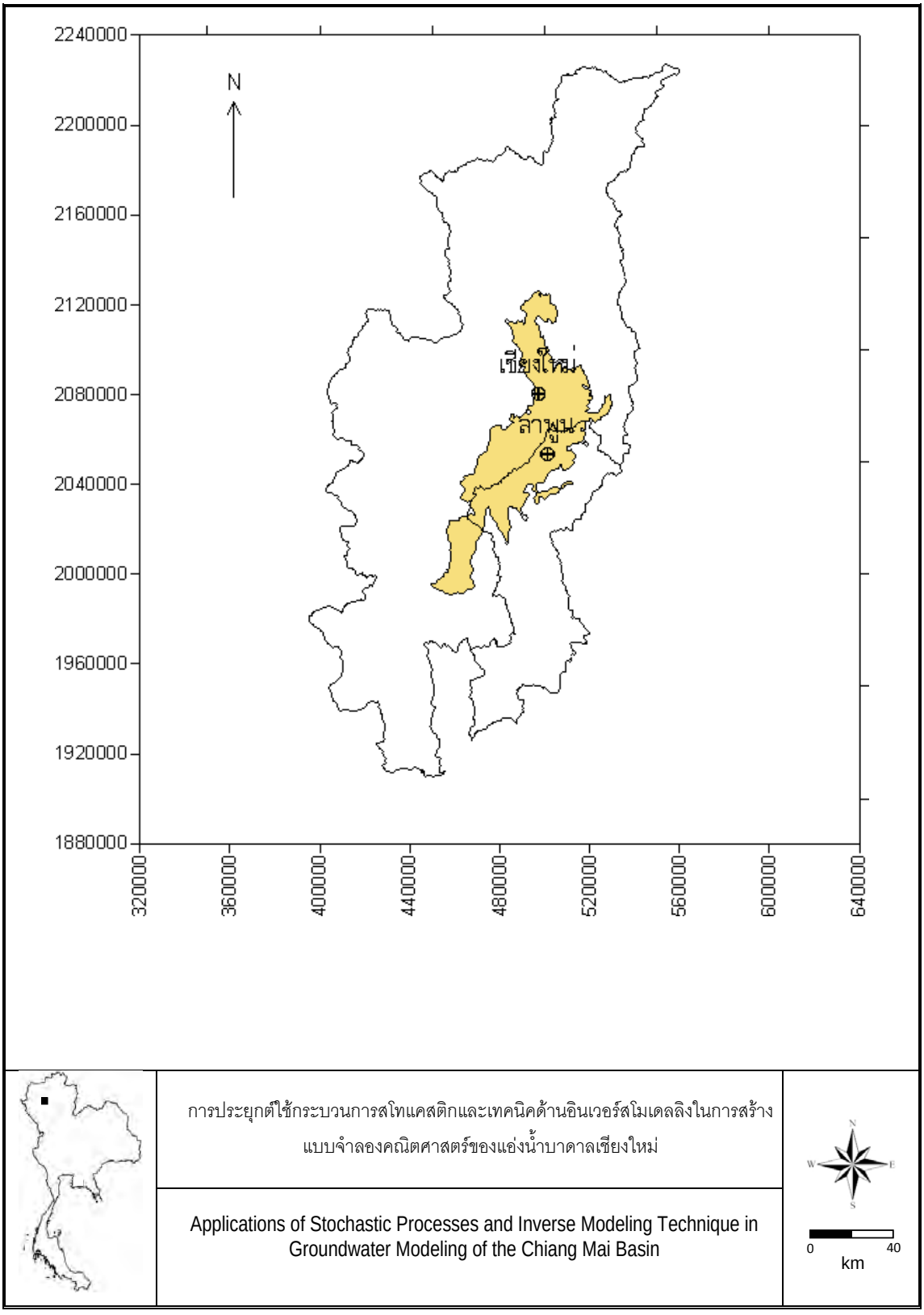

Figure 1-1 The Chiang Mai Basin.

Chapter 2

Chiang Mai Basin

Chapter 2: Chiang Mai Basin

2.1. General Physical Settings and Conditions (DMR, 2000)

Chiang Mai basin is situated within the two provinces, Chiang Mai and Lamphun. The basin that is being considered in this research project refers to a groundwater basin in semi-consolidated and unconsolidated aquifers. These aquifers are primarily Quaternary age.

2.1.1. Chiang Mai Province

Chiang Mai province is bounded by the Union of Myanmar in the north, Chiang Rai, Lampang, and Lamphun provinces in the east, Tak and Lamphun provinces in the south, and Mae Hong Son province in the west, covering 20,107.057 km^2. The province is divided into 24 districts including 204 Tambons, 1,915 villages, 1 city municipality, 28 district municipalities, 184 Tambon administrative organizations, and 7 Tambon councils.

Most of the area consists of forest and mountain range, lying in N-S direction. Thanon Thong Chai and Daen Lao ranges are located in the west, while Khun Tan range is located in the east. The area can be classified into 3 parts:

Flood plain and semi-recent surface: This part is the results from deposition of sediments forms recent channels, such as Ping, Mae Khan, and Fang rivers. It covers 7% of the area.

Undulating to rolling old alluvial terrace: This part is located at higher elevation, 350-600 m, along the rim of flood plain. It was the residual of the old flood plain, and

can be classified into low terrace, middle terrace, and high terrace. It covers 8% of the area.

Residual hills and mountains: This is the main part of the province, coving 85% of the area. The elevation of this part is 600-2,600 m.

There are intermountain basins scatter in this part. Some of the highest mountains in the area are Doi Pha Hom Pok. Doi Luang Chiang Dao, Doi Suthep, and Doi Inthanon.

2.1.2. Lamphun Province

Lamphun is one of the province in Northern Thailand. The area is bounded by Chiang Mai in the north and the west, Lampang in the east, and Tak in the south, covering 4,505.9 km^2. The hilly terrain is 63%, and the plain terrain is 37% of the area. Most of the hilly terrain is in the east and the south of the province. The main plain which is part of the Chiang Mai-Lamphun basin is in the north of the province. Its altitude is 280-310 m (amsl.). The main rivers in the province are Ping, Kuang, Li, and Mae Nam Tha. These rivers have their tributaries covering the province forming catchment area for 966 mm/yr rainfall, which start from May to October.

The province divides into 8 districts which include 51 Tambons and has one provincial administrative organization, 12 Municipals, and 45 Tambon administrative organizations.

2.2. General Geology (DMR, 2000)

Chiang Mai province is located in Shan-Thai micro-plate, and composed of the rocks from Precambrian age to sediments of Recent. The Precambrian rocks consist of gneiss, schist, marble, and calc-silicate. The unit is exposed in the mountains on the west of Ping river from Mae Taeng to Omkoi districts.

The Cambrian rocks consist of sandstone, quartzite, phyllite, and schist. The rocks are exposed in the western range and in the west of Fang basin. The Ordovician rocks consist of limestone and argillaceous limestone with shale and sandstone. They are cropped out in the mountain on the west side of the Ping river, at the west of Fang basin, and at the east of Doi Tao district. The Silurian-Devonian rocks consist of quartzite, phyllite, schist, sandstone, shale, and tuff. The unit is common in the area. The Carboniferous rocks consist of sandstone, shale, conglomerate, and chert. It is common in the north and in the east of the area. The Permian rocks consist of limestone, shale, and sandstone. It is common in the north and in the east of the area. The Triassic and Jurassic rocks consist of sandstone, shale, conglomerate, and lignite. The unit is cropped out in the west of Mae Taeng and Mae Rim districts, at Wiang

Haeng, Mae Chaem, and Omkoi districts. The quaternary sediments consist of sand, silt, clay, and gravel of varying sizes. They are deposited along alluvial plain such as Chiang Mai-Lamphun basin, Fang basin, Phrao basin, Wiang Haeng basin, Mae Chaem basin. The Carboniferous granite is common in the area on the west of the Ping river, and at the north of Fang basin. While the Triassic granite is commonly exposed in both sides of the Ping river, these rocks were deformed and metamorphosed by the movement of the crust, results in tiling, bending, folding, fracturing, or faulting.

Lamphun province is located in Shan-Thai microplate. The rocks are age from Cambrian to Quaternary. In the northern part at Ban Thi, Mae Tha, east of Mueang Lamphun districts, and south of Pa Sang district is mainly composed of sedimentary and meta-sedimentary rocks of Permian and Carboniferous. In the middle and southern part at Ban Hong, south of Mae Tha, Thung Hua Chang, and Li districts is mainly composed of metamorphic rocks of Cambrian, Silurian and Devonian, and sedimentary rocks of Ordovician. Rocks of Carboniferous, Permian-Triassic and Jurassic rocks are seldom exposed. These rocks are extruded by Triassic granitic rock, which cropped out at Khun Tan mountain range and along Li basin. The semi-consolidated rocks of Tertiary were deposited along intermountain basins in Li districtwhich is the dominant of lignite deposit in Thailand. In the Chiang Mai-Lamphun basin where the Tertiary unit was covered by Quaternary sediments. Faults and fractures are dominant in NE-SW direction, including curvature fault at Mae Tha Valley.

2.3. Hydrogeology of Chiang Mai Province (DMR, 2000)

Hydrogeological condition refers to the geological conditions dealing with origin, distribution, movement, quality, survey, and potential evaluation of groundwater. The significant parts are characteristic and compositions of rocks, geological structures, and geological environments. These geological conditions are the criteria for determining the rock properties concerning groundwater storage capacity or generally called hydrogeological property. The significant properties are storage and discharge properties. Naturally, unconsolidated and consolidated rocks have very different geological conditions which result in different hydrogeological properties. Hence, in hydrogeology, the rocks are normally classified into 3 main types which are unconsolidated, semi-consolidated, and consolidated rocks. Following this classification, these two rock types are further subdivided into various hydrogeological units. The classification of hydrogeological units may or may not coincide to the classification of geological units depending on their hydrogeological properties.

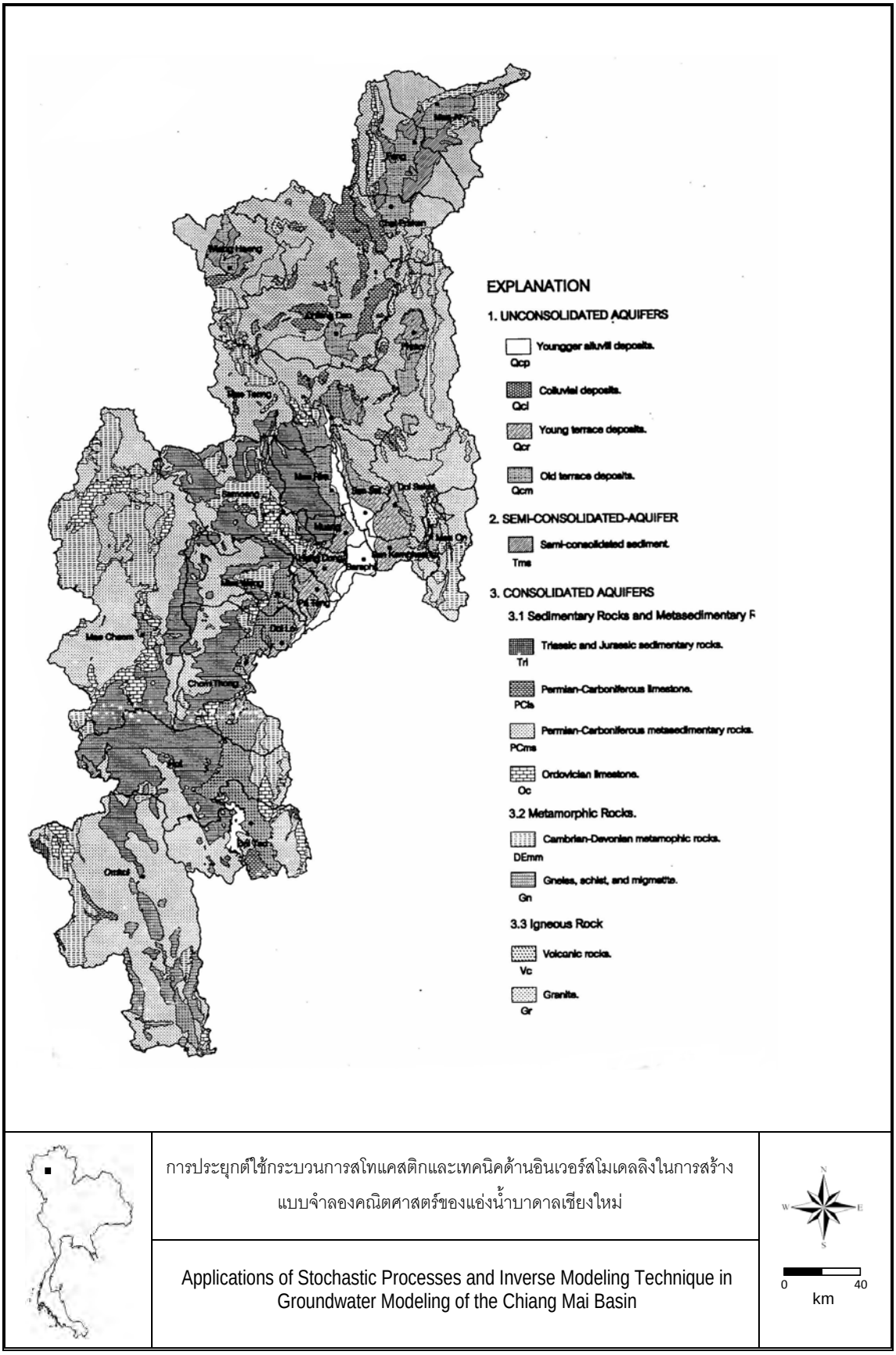

Figure 2-1: Water bearing rocks of Chiang Mai Provinces (DMR, 2000).

The Chiang Mai region comprises of various kinds of rocks of different ages. In addition, they have various geological structures favourable for groundwater storage such as faults, fractures, and folds. The detail of hydrogeological conditions of Chiang Mai Province is illustrated in the map (see Figure 2-1) and described as follows.

2.3.1. Hydrogeologic Units in Unconsolidated Aquifers

The hydrogeologic units in unconsolidated rocks consist of gravel, sand, silt, rock fragment and clay which are loosely cement. Generally, groundwater is stored in inter-granular voids of the sediment grains. The storage capacity of groundwater in the sediment deposits, particularly in those gravel and sand layers, is depending on the following properties.

(1) Thickness of the sediment deposits. The thicker is the better storage capacity.
(2) Sorting of the sediment grain. Well-sorted sediment is better in storage capacity.
(3) Shape of sediment grain. The rounded grain gives good storage capacity.

Unconsolidated rocks of Chiang Mai province can be divided into 3 hydrogeologic units as follows.

Alluvial sediments aquifer (Qcp): consists of gravel, sand, silt, and clay. Groundwater is stored in inter-granular voids of gravel and sand, deposited along the flood plain and meander belts of the Ping river. The average depth to the aquifer is 20-40 m., and well yield is more than 20 m^3/hr.

Young terrace sediments aquifer (Qcr): consists of gravel, sand, silt, clay deposited along narrow terrace next to the Ping river's flood plain which mainly consists of thick clay with some gravel and sand socket to thick gravel and sand bed. Groundwater is stored in inter-granular voids of gravel and sand deposited. The average depth to the aquifer is 30-100 m., and well yield is 10-20 m^3/hr except in the area adjacent to alluvial sediment where may yield more than 20 m^3/hr.

Old terrace sediments aquifer (Qcm): Consists of gravel, sand, silt, and clay deposited along area higher than young terrace deposit. Groundwater is stored in inter-granular voids of gravel and sand deposited. The average depth to the aquifer is 50-250 m., and 300 m. in some area. Well yield is 2-10 m^3/hr.

2.3.2. Hydrogeologic Units in Semi-Consolidated Aquifers

The hydrogeologic units in semi-unconsolidated rocks (Tms) consist of various Tertiary rocks such as shale, oil shale, and lignite. Groundwater is stored in cracks,

fractures, faults, and bedding planes. The average depth to the aquifer is 20-60 m., and well yield is typically less than 2 m^3/hr.

2.3.3. Hydrogeologic Units in Consolidated Aquifers

Most groundwater is stored in spaces of various geological structures i.e. cracks, fractures, faults, and bedding planes, caves, and in weathering zone. The groundwater quantity depends upon size and continuity of these structures. The structures with large cavity and good continuity will store a great amount of groundwater.

The consolidated rocks of Chiang Mai Province can be divided into 8 hydrogeologic units as follows.

Triassic-Jurassic sedimentary rocks aquifer (Tn): consists of sandstone, siltstone and conglomerate. Groundwater is stored in cracks, fractures, faults, and bedding planes. The average depth to the aquifer is 10-40 m., and 70 m in some area. Well yield is generally less than 2 m^3/hr.

Permian-Carboniferous limestone aquifer (PCls): consists of gray to dark gray, massive to bedded limestone with chert nodule.In some part there is shale interbedded. Groundwater is stored in cracks, fractures, faults, caves and bedding planes. The average depth to the aquifer is 12-20 m., and well yield is generally less than 2-10 m^3/hr.

Permian-Carboniferous metasedimentary rocks aquifer (PCms): consists of sandstone, shale, chert, limestone, slate, mudstone, quartzite, phyllite. Groundwater is stored in cracks, fractures, faults, and bedding planes. The average depth to the aquifer is 12-30 m, and well yield is generally less than 2 m^3/hr or nil.

Ordovician limestone aquifer (Oc): consists of gray to dark gray, recrystallized, laminated, argillaceous limestone with interbedded shale in the lower part. Groundwater is stored in cracks, fractures, faults, caves and bedding planes. The average depth to the aquifer is 30-70 m, and well yield is generally 2-10 m^3/hr.

Cambrian-Devonian metamorphic rocks aquifer (DEmm): consists of quartzite, schist, phyllite, gneiss. Groundwater is stored in cracks, fractures, faults, and bedding planes. The average depth to the aquifer is 30-40 m., and well yields are generally less than 2 m^3/hr.

Gneiss, schist, and migmatite (Gn): consists of gneiss, schist, and migmatite. Groundwater is stored in cracks, fractures, faults, and bedding planes. The average depth to the aquifer is 30-80 m., and well yields are generally less than 2 m^3/hr.

Volcanic rock aquifer (Vc): Groundwater is stored in cracks, fractures, faults, and weathering zone. The average depth to aquifer is 30-80 m., and well yield is generally less than 2 m^3/hr.

Granite aquifer (Gr): Groundwater is stored in cracks, fractures, faults, and weathering zone. The average depth to the aquifer is 10-20 m., and well yield is generally less than 2 m^3/hr.

2.3.4. Groundwater Potential of the Chiang Mai Province

Most of the Chiang Mai area are mountainous areas underlain by consolidated aquifers which cover 85% of the area. The important groundwater resources of unconsolidated aquifers consist of alluvial and terrace sediments. These sediments are distributed in the stream channel, flood plain, and higher area along both sides of the Ping river and its tributaries. The well yield of the alluvial sediments is more than 20 m^3/hr. and that of the terrace sediments is 10-20 and 2-10 m^3/hr. The important groundwater resources of consolidated aquifers are Permo-Carboniferous and Ordovician limestone which has the well yields of 10-20 and 2-10 m^3/hr, respectively.

Groundwater quality is generally good. Contents of TDS, hardness, iron, and fluoride are less than 500, 200, 0.5, and 1.0 mg/L, respectively, even though some area shows high content of iron. The depths for groundwater drilling are 30-80 m. in the consolidated aquifers and 10-80 m. in the unconsolidated aquifers, except in the areas of San Pa Tong, Doi Lo, Chom Thong, and Mae Wang districts where depth for groundwater drilling is higher than 120 m.

2.4. Hydrogeology of Lamphun Province (DMR, 2000)

The Lamphun region comprises of various kinds of rocks including both unconsolidated and consolidated rocks with different geochronological order. In addition, they have various geological structures favorable for ground water storage such as faults, fractures, and folds. The details of hydrogeological conditions of Lamphun Province, as illustrated in the map (see Figure 2-2), are described as follows.

2.4.1. Hydrogeologic Units in Unconsolidated Aquifers

The hydrogeologic units in unconsolidated rocks consist of gravel sand, silt, rock fragment and clay which are loosely cement. Generally, groundwater is stored in inter-granular voids of the sediment grains. The storage capacity of groundwater in the sediment deposits, particularly in those gravel and sand layers, is depending on the following properties.

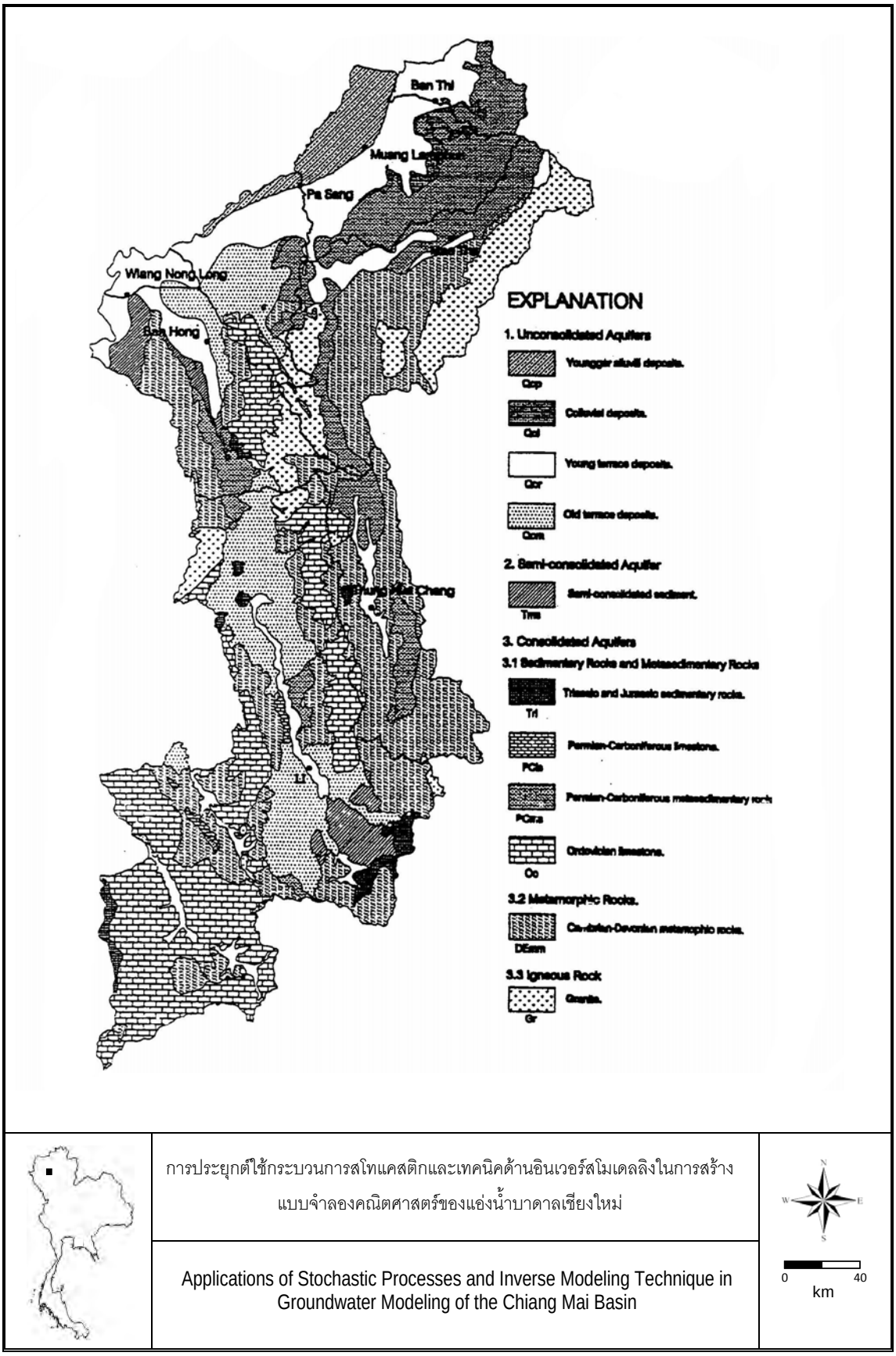

Figure 2-2: Water bearing rocks of Lamphun Provinces (DMR, 2000).

The unconsolidated rocks of Lamphun Province can be divided into 4 hydrogeologic units as follows.

Alluvial sediments aquifer (Qcp) consists of gravel, sand, silt, and clay. Groundwater is stored in inter-granular voids of gravel and sand, deposited along the flood plain and meander belts of the Ping river. The average depth to the aquifer is 20-40 m and well yield is more than 20 m^3/hr. This units distribute in Mueang Lamphun and Pa Sang districts.

Colluvial sediments aquifer (Qcl) consists of gravel, sand, clay and rock fragments. Groundwater is stored in inter-granular voids of gravel and sand deposited along hill slope. The average depth to the aquifer is 15-20 m, and well yield is around 2-10 m^3/hr.

Young terrace sediments aquifer (Qcr) consists of gravel, sand, silt, clay deposited along narrow terrace next to Ping river's flood plain which mainly consists of thick clay with some gravel and sand socket to thick gravel and sand bed. Groundwater is stored in inter-granular voids of gravel and sand deposited. The average depth to the aquifer is 30-100 rn., and well yield is 2-10 m^3/hr except the area adjacent to alluvial sediment such as part of Mueang Lamphun, Pa Sang, Wiang Nong Long, Ban Hong, and Ban Thi districts which may yield more than 20 m^3/hr.

Old terrace sediments aquifer (Qcm) consists of gravel, sand, slit, and clay deposited along area higher than young terrace deposit and in intermontane basin of the Li river. Groundwater is stored in inter-granular voids of gravel and sand deposited. The average depth to the aquifer is 50-250 m., and 300 m. in some area, and well yield is 2-10 m^3/hr except for some area may yield up to 10-20 m^3/hr and more.

2.4.2. Hydrogeologic Units in Semi-consolidated Aquifers

The hydrogeologic units in semi-unconsolidated rocks (Tms) consists of various Tertiary rocks such as shale, oil shale, and lignite. Groundwater is stored in cracks, fractures, faults, and bedding planes. The average depth to the aquifer is 20-30 m, and well yields are generally Leas than 2 m^3/hr.

2.4.3. Hydrogeologic Units in Consolidated Aquifers

Most groundwater is stored in spaces of various geological structures i.e. cracks, fractures, faults, and bedding planes, caves, and in weathering zone. The groundwater quantity depends upon size and continuity of these structures. The structures with large cavity and good continuity will store a great deal of groundwater.

The hydrogeologic units in consolidated rocks of Lamphun province can be divided into 6 hydrogeologic units as follows.

Triassic-Jurassic sedimentary rocks aquifer (Tn): consists of sandstone, siltstone and conglomerate. Groundwater is stored in cracks, fractures, faults, and bedding planes. The average depth to the aquifer is 20-40 m., and well yields are generally less than 2 m^3/hr.

Permian-Carboniferous limestone aquifer (PCls): consists of gray to dark gray, massive to bedded limestone with chert nodule. In some part there is shale interbedded. Groundwater is stored in cracks, fractures, faults, caves and bedding planes. The average depth to the aquifer is 20-60 m, and well yields are generally 2-10 m3/hr. However, in case of large cavity, well yield can be more than 20 m^3/hr.

Ordovician limestone aquifer (Oc) consists of gray to dark gray, recrystallized, laminated, argillaceous limestone with interbedded shale in the lower part. Groundwater is stored in cracks, fractures, faults, caves and bedding planes. The average depth to the aquifer is 30-70 m., and well yields are generally around 2-10 m^3/hr. However, in case of large cavity, well yield can be around 10- 20 m^3/hr or more.

Permian-Carboniferous metasedimentary rocks aquifer (PCms) consists of sandstone, shale, chert, limestone, slate, mudstone, quartzite, phyllite. Groundwater is stored in cracks, fractures, faults, and bedding planes. The average depth to the aquifer is 30-80 m., and well yields are generally less than 2 m3/hr or nil.

Cambrian-Devonian metamorphic rocks aquifer (DEmm) consists of quartzite, schist, phyllite, gneiss. Groundwater is stored in cracks, fractures, faults, and bedding planes. The average depth to the aquifer is 40-70 m., and well yields are generally less than 2 m^3/hr.

Granite rocks aquifer (Gr): Groundwater is stored in cracks, fractures, faults, and weathering zone. The average depth to the aquifer is 10-50 m., and well yields are generally less than 2 m^3/hr.

2.4.4. Groundwater Potential of the Lamphun Province

In Lamphun 32% of the area is covered by unconsolidated rocks which are good aquifer especially in the area of Chiang Mai-Lamphun basin which store 485 million m^3 and can be developed for 97 million m^3/yr (Wongsawat, 1999). Other 18% of the area is limestone which is good aquifer, yield groundwater enough for utilization in many purposes. Other 15% of the areas are sandstone and shale which give moderate yield. The other 35% are igneous and metamorphic rocks contain less amount of water.

The quality of groundwater is in good and moderate classes, though iron and fluoride content is quite high in some area. The depth for drilling is in 40-60 in. in general, except in the eastern rim of Lamphun basin where the depth is 80- 120 m, or even more in the northern part.

2.5. Chiang Mai Basin: A Closer Look (Margane and Tatong, 1999)

2.5.1. Geology

The Chiang Mai basin is an intermontane basin that was formed, like similar basins in Thailand, between the late Cretaceous and the early Tertiary during a period of transtensional faulting following the collision of the Indian with the Eurasian plate (Bunopas and Vella 1983, Bunopas and Vella 1992, Polachan and Sattayarak 1989). The dominant tectonic features are N–S extensional faults, NW–SE dextral shear faults, and NE–SW sinistral shear faults. A sequence of Precambrian to Permian sedimentary rocks is exposed in the area around the basin. West of the basin, these rocks were intruded by granites (Carboniferous and Triassic). East of the basin, there are volcanic rocks.

Evaluation of geological mapping data (Chaimanee, 1997) and gravity data (Wattananikorn et al., 1995), structural interpretation of satellite images, lithological logs, geophysical borehole logs and hydrogeological data reveals that continuous down-faulting since the late Cretaceous has governed the sedimentation pattern. On the basis of geophysical data, the basin fill reaches a thickness of about 2000 m (Wattananikorn et al., 1995). In the areas with high subsidence rates, sand and gravel have been deposited with high accumulation rates during the Quaternary. The more stable blocks are dominated by the deposition of slopewash sediments (colluvium) consisting mainly of clay and silt. In some areas almost no down-faulting or even uplift has occurred, as evidenced by the preservation of gravel beds at higher elevations (‘High Terrace’). In the area downstream of the Mae Kuang dam from the foot of the mountains down to the area east of Chiang Mai, sand and gravel beds interfingered with clayey and silty units were deposited in the form of alluvial fans by the Kuang River and its tributaries. Such interfingering units are observed throughout this area, providing evidence of the rapid change of the courses of the streams and rivers. As observed in outcrops and lithological logs, sand and gravel beds can be traced mostly only over short distances.

2.5.2. Hydrogeology

Configuration of the Groundwater System and Aquifer Characteristics

It is extremely difficult to delineate the sedimentary units in the basin because correlation is mostly not possible. Previous hydrogeological models, which proposed that the aquifer system consists of a number of terraces (Chuamthisong, 1971; Buapeng et al., 1995), could not be confirmed. However, it is possible to delineate areas or blocks with a distinct sedimentation pattern. On the basis of lithological characteristics, the upper part of the Chiang Mai basin down to a depth of around 200 m can be subdivided into the following zones (Figure 2-3):

(1) Central Alluvial Channel
(2) Mae Kuang Alluvial Fan
(3) Nam Wang–Nam Mae Khan sub-basin
(4) Zone of Colluvial Deposits
(5) High Terrace deposits

The distinctive lithology of each of these zones results in a very different hydrogeology of the aquifer complexes. However, adjacent aquifer complexes are certainly interconnected hydraulically. The aquifer complexes can be characterized as follows:

Central Alluvial Channel

The central part of the Chiang Mai basin is dominated by the deposition of sand and gravel transported under high energy conditions by the Ping River. This is the area where according to the structural interprettation the main down-faulting occurs. Clayey strata are present throughout the sequence but form only a very minor component. Wells in this area are relatively shallow (average depth: about 50 m). In most cases adequate yields with low drawdown (high specific well capacities) have been reached within the top 30 m of the sediments. The Central Alluvial Channel is the area of highest groundwater exploitation potential. Specific well capacities per meter of screen length (i.e., normalized SC) are between 10 and about 100 m/d. Average screen length is around 6 m. Little data is available on hydraulic conductivities from pumping test evaluations; most of the data is from the area around Mae Rim district, with hydraulic conductivities between 20 and about 200 m/d.

Groundwater quality is commonly very good, with total dissolved solids (TDS) mostly less than 250 mg/L. The fluoride and iron concentrations are generally low,

especially in the upper part of the aquifer, owing to high oxygen concentration and flow velocities.

The future development of groundwater resources for central water supplies should be concentrated in this zone. However, it has to be emphasized that the vulnerability of this aquifer to groundwater pollution is high, due to the lack of a continuous cover of clayey/silty sediments. Therefore, measures leading to protection of these groundwater resources are highly recommended. For example, industrialplants and landfills for waste disposal should be legally banned in these areas, along with other activities hazardous to groundwater quality.

Mae Kuang Alluvial Fan

In the area between the villages of San Sai, Doi Saket and San Kamphaeng districts, sand and gravel interfingering with silt and clay. Especially in the northern half of this area, sand and gravel prevail. This sedimentation pattern was created by the alluvial fan of the Kuang and the Huai Bon rivers. The average depth of wells in this area is about 50 m. Specific well capacities per meter screen length vary considerably from one area to the other, from about 1 m/d to about 20 m/d, providing evidence of the rapid lateral changes in lithology. Hydraulic conductivity values range between about 5 and about 100 m/d. Groundwater quality is mostly good. Only in the southern part have elevated TDS values been observed. The vulnerability of the aquifer to pollution is highly variable. In the area between San Kamphaeng and San Sai districts, a thick cover of clay silt provides adequate protection against groundwater pollution. This is supported by a geoelectric sounding profile prepared by the Groundwater Division of DMR.

Nam Wang–Nam Mae Khan sub-basin

Evidence for the existence of a down-faulted block has been found from the tectonic interpretation of satellite images and gravity data from the area west of San Pa Tong district. Continuous subsidence in this sub-basin has led to the accumulation of predominantly sand and gravel. This interpretation is supported by hydrogeological data that indicate high specific well capacities per meter screen length of as much as about 50 m/d. However, values are quite different from one point to the other and it seems that lower values are confined to the margins and lower parts of this comparably small sub-basin, whereas high values are found in the northwestern part.

Zone of Colluvial Deposits

Clayey and silty colluvial deposits predominate in the area east of the Kuang River from the southern limit of the project area to the Huai Bon river in the north (approximately UTM northing 2,080,000). Sand and gravel beds occur only in limited areas as channel deposits of the eastern tributaries of the Kuang river, which have relatively small catchment areas. In a few wells, undated consolidated rocks have been reached (described as limestone and shale), indicating that the bottom of the basin in some areas is quite shallow. The specific well capacity per meter screen length of wells in this area ranges from less than 0.1 to about 3 m/d. However, higher values may be expected locally – in alluvial channels of the tributaries. Hydraulic conductivity values are generally less than 1 m/d. Wells are often quite deep (as much as 200 m) and screened at several depth intervals in order to obtain a suitable amount of water. Monitoring of wells shows a relatively large lowering of the water table of up to 1 m/yr. This indicates that the recharge rate, especially in deeper parts of the aquifer, is less than the abstraction rate. The high fluoride content in this area of up to 16.5 mg/L provides further proof of low flow velocities (high residence time).

Colluvial deposits have been mapped in several other areas along the foot of the mountain ranges. Very few water wells have been drilled in most of these areas, but in general specific well capacities and hydraulic conductivities are low.

High Terrace deposits

Sediments classified as ‘High Terrace’ deposits (Qth) occur along the western margin of the basin. On the eastern margin, such deposits have been mapped only in a very small area (north of UTM northing 2,091,500). These deposits consist of sand and gravel beds intercalated with silt and clay, probably deposited during the Late Pliocene to early Quaternary. The sand and gravel beds have a relatively high clay content (mainly kaolinite) and are indulated. The high clay content of ‘High Terrace’ deposits results in a very low specific well capacity, which is clearly reflected on the map of the groundwater exploitation potential (see Figure 2-3). Specific well capacity per meter screen length is usually less than 1 m/d. Groundwater monitoring data from this area indicate a rapid lowering of water levels. In the deeper part of this aquifer complex, water levels have in some cases dropped considerably and the difference between the piezometric head in the shallow part of the aquifer and the deeper part is more than 35 m in some places, indicating that the recharge rate of these resources is very low.

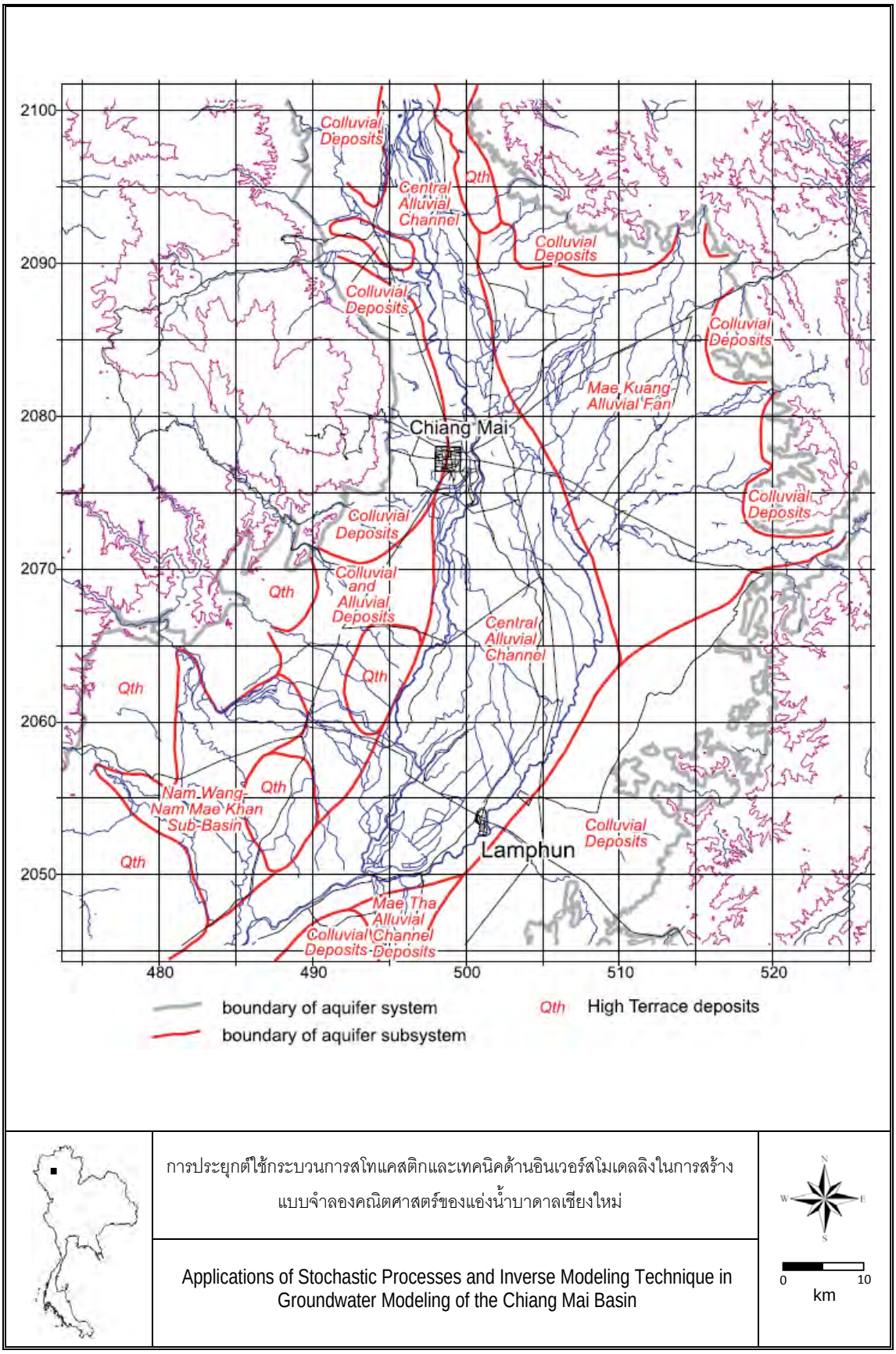

Figure 2-3 Subdivision of aquifer system in Chiang Mai basin (Margane and Tatong, 1999)

2.6. Hydraulic Properties of Unconsolidated Aquifers in Chiang Mai Basin

Determination of aquifer hydraulic properties is a basic component of most groundwater supply and contaminant-transport investigations. A frequently used method for estimating hydraulic properties is graphical type-curve analysis of aquifer tests, in which dimensionless type curves derived from an assumed analytical model of ground-water flow to a pumped well are used to analyze time-drawdown measurements of hydraulic head in observation wells and piezometers. These analyses are done to estimate the transmissivity and storativity of confined aquifers or the hydraulic conductivity and specific yield of water-table (unconfined) aquifers. An alternative approach to dimensionless type-curve analysis is to generate dimensional time-drawdown curves from the analytical model that are compared directly to the measured values. In this approach, the hydraulic properties of the model are adjusted in a series of model simulations until the model-calculated drawdowns closely match the measured values. This procedure is called model calibration and can be done graphically, as in the dimensionless type-curve approach, or automatically by use of a parameter-estimation technique.

Many analytical models have been developed for evaluation of axial-symmetric flow to a well that pumps from a confined or water-table aquifer. The ability of these models to represent realistic field conditions such as well-bore storage and skin, partial penetration of wells, and, in the case of a water-table aquifer, drainage from the unsaturated zone, has steadily improved since the pioneering work of Theis (1935), who presented a transient analytical model of flow to a fully penetrating well in a confined aquifer. Recently, Moench (1997) developed an analytical model of flow to a partially penetrating, finite-diameter well in a homogeneous, anisotropic water-table aquifer. The model accounts not only for well-bore storage and skin at the pumped well, but also for delayed drawdown response of an observation well. By including these factors, it is possible to accurately evaluate the specific storage of a water-table aquifer from early-time drawdown data in observation wells and piezometers. It is also theoretically possible to use the model to interpret pumped-well data. For confined aquifers, the model expands upon the work of Dougherty and Babu (1984) and allows for anisotropic hydraulic conductivity. For unconfined aquifers, the model expands upon the early work of Boulton (1954, 1963) and of Neuman (1972, 1974) and allows for well-bore storage and skin, delayed piezometer response, and delayed drainage from the unsaturated zone.

This research project uses a modified computer program WTAQ to evaluate hydraulic conductivity of the pumping test data. WTAQ is based on Moench's (1997) analytical model for axial-symmetric flow in a confined or water-table aquifer. WTAQ calculates dimensionless or dimensional drawdowns that can be used with measured drawdowns at observation points to estimate hydraulic properties of confined and water-table aquifers. WTAQ can be used to estimate both horizontal and vertical hydraulic conductivity, specific storage, and specific yield of a water-table aquifer by graphical, type-curve methods and by an automatic parameter-estimation method.

2.6.1. Pumping Tests Results in Chiang Mai Basin

Pumping test wells in the study area were drilled by Department of Groundwater Resources, Ministry of Natural Resources and Environment. Although there are a number of test wells drilled in the study area, covering all aquifer zones, only 41 test wells drilled in 5 aquifer zones are selected for further pump test analysis (Uppasit, 2004).

These are 17 wells in the Central Alluvial Channel, 2 wells in the Colluvial and Alluvial Deposits, 15 wells in the Colluvial Deposits, 6 wells in the Mae Kuang Alluvial Fan and one well in the Nam Wang-Nam Mae Khan Sub-basin. Details of the pumping test wells, calculated transmissivities and hydraulic conductivities, and calculated specific yield values are shown in Table 2-1, respectively. Locations of the pumping test wells are shown in Figure 2-4. The specific yield ranges from 0.0766 to 0.3280. Due to the lack of observation well, all pumping test data are from measurement in the pumped well itself (single-well pumping test). Radius of the pumped well is used as distance from the pumped well to the observation well. The accuracy of the estimating aquifer specific yield using the single well pump test is therefore low.

These pumping test data will be re-analyzed using WTAQ (Barlow and Moench, 1999) program and an inverse modeling code, UCODE (Poeter and Hill, 1998) to obtain anisotropy of the aquifer materials. There still is the need to obtain more data in the areas where no pumping well is available.

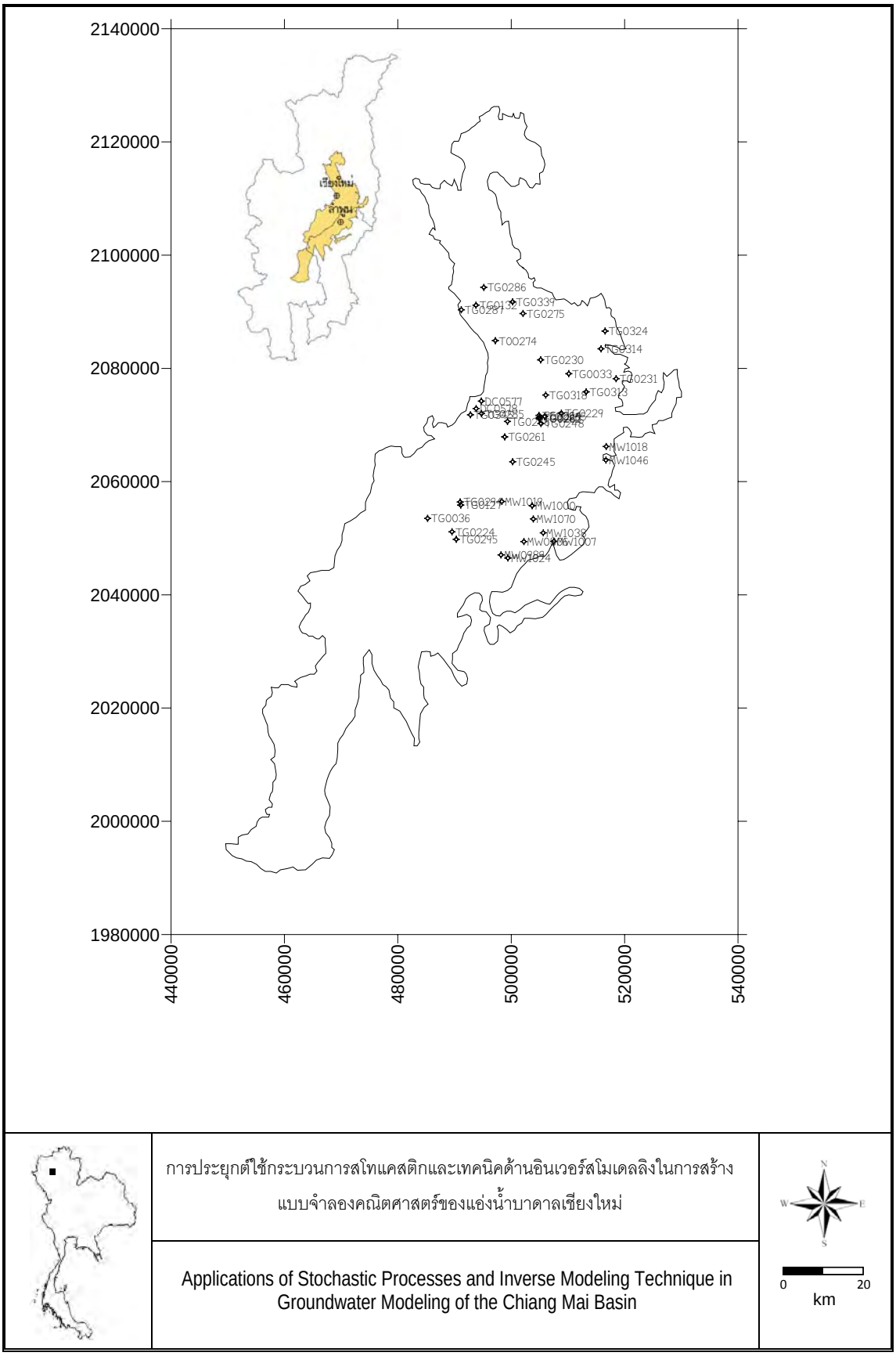

Figure 2-4: Locations of pumping test (*from* Uppasit, 2004).

Table 2-1: Pumping tests wells and results (Uppasit, 2004).

Well No.	Well Name	UTM E	UTM N	Aquifer	T [m^2/d]	K [m/d]	S [-]
1	MW1000	503700	2055730	Central Alluvial Channel	1.605	0.1338	0.1316
2	MW1019	498350	2056490	Central Alluvial Channel	7.959	0.9949	0.2547
3	TG0224	489554	2051135	Central Alluvial Channel	2.361	0.1816	0.0936
4	TG0245	500250	2063500	Central Alluvial Channel	2.486	0.6215	0.2996
5	TG0246	499334	2070620	Central Alluvial Channel	16.89	2.111	0.1936
6	TG0248	505233	2070249	Central Alluvial Channel	1.285	0.1606	0.2818
7	TG0261	498850	2067900	Central Alluvial Channel	1.283	0.1603	0.2695
8	TG0262	504944	2071101	Central Alluvial Channel	0.8728	0.2909	0.2695
9	TG0263	504950	2071330	Central Alluvial Channel	4.291	0.7152	0.2965
10	TG0264	504890	2071700	Central Alluvial Channel	2.51	0.4183	0.234
11	TG0265	505890	2071500	Central Alluvial Channel	2.115	0.3525	0.2898
12	T0O274	497200	2084900	Central Alluvial Channel	1.062	0.1771	0.2885
13	TG0286	495160	2094300	Central Alluvial Channel	6.827	1.707	0.2706
14	TG0287	491200	2090350	Central Alluvial Channel	2.657	0.3321	0.2698
15	TG0295	490300	2049800	Central Alluvial Channel	0.2589	0.0324	0.0766
16	TG0318	506092	2075286	Central Alluvial Channel	39.42	9.856	0.2705
17	TG0339	500246	2091752	Central Allivial Channel	3.865	0.4832	0.198
18	TG0127	491100	2055850	Colluvial and Alluvial Deposits	1.854	0.206	0.2047
19	TG0294	491000	2056400	Colluvial and Alluvial Deposits	11.75	0.9794	0.1532
20	DC0577	494730	2074220	Colluvial Deposits	7.092	0.2955	0.2693
21	DC0578	493810	2072900	Colluvial Deposits	0.1077	0.0045	0.2591
22	MW0806	502232	2049409	Colluvial Deposits	0.0802	0.0134	0.2103
23	MW0989	498205	2047046	Colluvial Deposits	0.4004	0.0334	0.1668
24	MW1007	507520	2049450	Colluvial Deposits	6.307	0.1828	0.2842
25	MW1018	516750	2066200	Colluvial Deposits	0.7351	0.0981	0.2934
26	MW1024	499420	2046510	Colluvial Deposits	2.924	0.2437	0.0977
27	MW1038	505650	2050950	Colluvial Deposits	0.0602	0.0013	0.1646
28	MW1046	516700	2063800	Colluvial Deposits	2.394	0.1228	0.328
29	MW1070	503898	2053398	Colluvial Deposits	3.247	0.5412	0.2779
30	TG0132	493786	2091157	Colluvial Deposits	5.985	0.3741	0.2273
31	TG0285	494750	2072020	Colluvial Deposits	1.19	0.1488	0.2968
32	TG0314	515838	2083455	Colluvial Deposits	2.721	0.0403	0.2647
33	TG0324	516555	2086587	Colluvial Deposits	7.244	0.1932	0.1578
34	TG0345	492810	2071800	Colluvial Deposits	1.933	0.2416	0.0703
35	TG0033	510149	2079062	Mae Kuang Alluvial Fan	29.6	1.315	0.2265
36	TG0229	508838	2072079	Mae Kuang Alluvial Fan	5.543	0.462	0.0975
37	TG0230	505194	2081506	Mae Kuang Alluvial Fan	11.17	1.862	0.265
38	TG0231	518500	2078175	Mae Kuang Alluvial Fan	9.549	1.592	0.1829
39	TG0275	502080	2089690	Mae Kuang Alluvial Fan	5.016	0.836	0.2921
40	TG0313	513220	2075850	Mae Kuang Alluvial Fan	16.33	0.8163	0.275
41	TG0036	485255	2053502	Nam Wang-Nam Mae Khan	143.4	7.965	0.2788

2.7. Hydrometeorological Data

Hydrometeorological data includes precipitation, humidity, windspeed, evaporation, evapotranspiration, etc. Some of these data will be used as input data for groundwater model discussed in the next chapter. Table 2-2 shows some 30-yr average climatological data of the Chiang Mai basin. The data were derived from all meteorological stations located within the Chiang Mai basin.

Table 2-2: Climatological data of the Chiang Mai basin (30-yr average).

	Maximum	Minimum	Annual
Rainfall (mm)	224.4 (Aug)	7.7 (Jan)	1,134.0
Pan Evaporation (mm)	203.1 (Apr)	97.1 (Dec)	1686.7
Temperature (°C)	29.4 (Apr)	21.1 (Dec)	25.8
Relative Humidity (%)	82.0 (Sep)	52.5 (Apr)	71.3

2.7.1. Potential Evapotranspiration (ET_p)

The process of direct evaporation from soil and transpiration from growing plants are the primary component of the hydrologic cycle that returns precipitated water to the atmosphere as vapour. Since it is almost impossible to separate evaporation from transpiration, both processes are usually combined and called evapotranspiration which is normally expressed as a depth of water, mm.

In groundwater study, potential evapotranspiration (ET_p) is required. ET_p is the evapotranspiration that would occur under given climatic condition (maximum rate) if here were unlimited moisture supply. A number of empirical equations have been developed for estimating ET_p from available meteorological data. Table 2-3 shows the value of monthly ET_p calculated using Penman's equation.

2.7.2. Groundwater Recharge

Groundwater recharge pattern describes the duration and time needed for recharge water to reach the aquifer. The pattern serves as additional information to groundwater management.

Uppasit (2004) determined the duration for recharge water to infiltrate and reach groundwater (i.e., percolation) of the Chiang Mai basin using available meteorological data as shown in Table 2-3. It is clear that the recharge duration of the aquifer is July to September (on average) with the recharge rate of 218.56 mm/yr. This number however represents the entire amount of water that recharges all existing aquifers. In reality, different aquifer units will have different recharge amount.

Therefore, Uppasit (2004) uses the method of water-level fluctuation to determine (i.e. distribute) the amount of recharge in each of the unconsolidated aquifers (see Table 2-4).

Table 2-3: Calculation of effective rainfall from ET_p and precipitation (Uppsit, 2004).

Month	Precipitation (mm)	ET_p (mm)	Soil Moisture Deficit (mm)	Effective Rainfall (mm)
Jan	7.02	92.16	85.14	-
Feb	7.94	116.39	108.45	-
Mar	19.89	150.85	130.96	-
Apr	54.41	177.13	122.72	-
May	161.35	165.38	4.03	-
Jun	126.79	144.05	17.26	-
Jul	159.24	130.89	-	28.35
Aug	236.22	123.63	-	112.59
Sep	207.85	130.24	-	77.61
Oct	113.39	129.47	16.08	-
Nov	48.48	107.76	59.28	-
Dec	17.12	88.84	71.72	-
Total	1,159.70	1,556.79	615.66	218.55

Table 2-4: Calculation of recharge in unconsolidated aquifers (Uppsit, 2004).

Aquifer	Effective Rainfall (mm)	Recharge		Average Recharge (% of Annual Rainfall)
		(mm/yr)	% of Annual Rainfall	
Central Alluvial Channel	232.14-335.19	65.20-240.87	5.62-20.77	13
Colluvial and Alluvial Deposits	332.79	15.38-23.22	1.33-2.00	2
Colluvial Deposits	210.85-335.54	90.43-251.86	7.80-21.71	15
Mae Kuang Alluvial Fan	241.63-264.67	51.20-95.51	4.42-8.24	6
Wang-Mae Khan Sub-basin	260.41	0.37-13.93	0.003-1.20	1
Total		0.37-251.86	0.003-21.71	11

Chapter 3

Groundwater Flow Model: Deterministic

Chapter 3: Deterministic Groundwater Flow Model

3.1. Groundwater Models

Mathematical models, used commonly in groundwater studies, are an attempt to represent groundwater flow processes by mathematical equations. The precise language of mathematics provides a powerful mechanism for expressing a tremendous quantity of information in an amazingly simple and compact way. Naturally, the starting point in modeling is a clear understanding of the processes involved. In terms of the flow of groundwater, one mainly needs to consider two dominant processes: flow in response to hydraulic potential gradients and the loss or gain of water from sinks or sources (e.g. pumping or injection, or gains and losses in storage). Mathematical models rely upon the solution of the basic equations of groundwater flow which is a combination of Darcy's Law and mass balance equation. Equation (3-1) illustrates a partial differential equations describing groundwater flow in three-dimensional domain. The parameters K and S_s are hydraulic conductivity and specific storage, respectively. The hydraulic head h is a function of both space and time. The parameter W refers to source/sink within the domain (i.e., groundwater systems) of interest.

$$K_x \frac{\partial^2 h}{\partial x^2} + K_y \frac{\partial^2 h}{\partial y^2} + K_z \frac{\partial^2 h}{\partial z^2} = S_s \frac{\partial h}{\partial t} \pm W \qquad (3\text{-}1)$$

With proper boundary and initial conditions given, solution to (3-1) can be obtained. However, analytical solution to (3-1) is generally not available due to the complexity of the problems and heterogeneity of the aquifers. Numerical model must

be used, in such case, to be able to make use of the mathematical model presented in (3-1). Numerical solution to the flow, heat, or mass transport equations require that they be recast in an algebraic form. These recast equations are numerical approximations and the answers obtained are also approximations. The equations a most commonly in matrix form and they are solved on a digital computer. Numerical models are one of the most important development in hydrogeology in the last 15 years.

A numerical groundwater flow model is the mathematical representation of an aquifer in a computer. Using the basic laws of physics that govern groundwater flow, we instruct the computer to consider the physical boundaries of the aquifer, recharge, pumping, interaction with rivers, or other phenomenon to model the behaviour of the aquifer over time. Many types of numerical model for groundwater flow simulation are available. In this research, a program MODFLOW will be used in conjunction to stochastic methods and inverse modeling to assess groundwater resources of the Chiang Mai basin. Anderson and Woessner (1992) suggested step-by-step for successful modeling of groundwater as shown in Figure 3-1.

3.1.1. MODFLOW

MODFLOW is a computer program that simulates three-dimensional ground-water flow through a porous medium by using a finite-difference method (McDonald and Harbaugh, 1988). MODFLOW was designed to have a modular structure that facilitates two primary objectives: ease of understanding and ease of enhancing. Ease of understanding was an objective because U.S. Geological Survey technical managers generally believe that modellers should understand how a model works in order to use it properly. Ease of enhancement was an objective because experience showed that there was a continuing need for new capabilities.

MODFLOW was originally documented by McDonald and Harbaugh (1984). As with most computer programs that are used over a long time period, MODFLOW underwent several overall updates. The second version of MODFLOW is documented in McDonald and Harbaugh (1988), and this version is often called MODFLOW-88 to distinguish it from other versions. A third version is called MODFLOW-96 (Harbaugh and McDonald, 1996a and 1996b).

In addition to the enhancements and updates, the U.S. Geological Survey developed two major extensions to MODFLOW—MODFLOWP (Hill, 1992) and MOC3D (Konikow and others, 1996). MODFLOWP and MOC3D solve equations in addition to the ground-water flow equation. MODFLOWP solves a MODFLOW calibration problem by calculating values of selected input data that result in the best

match between measured and model calculated values, and MOC3D solves the solute-transport equation for concentration.

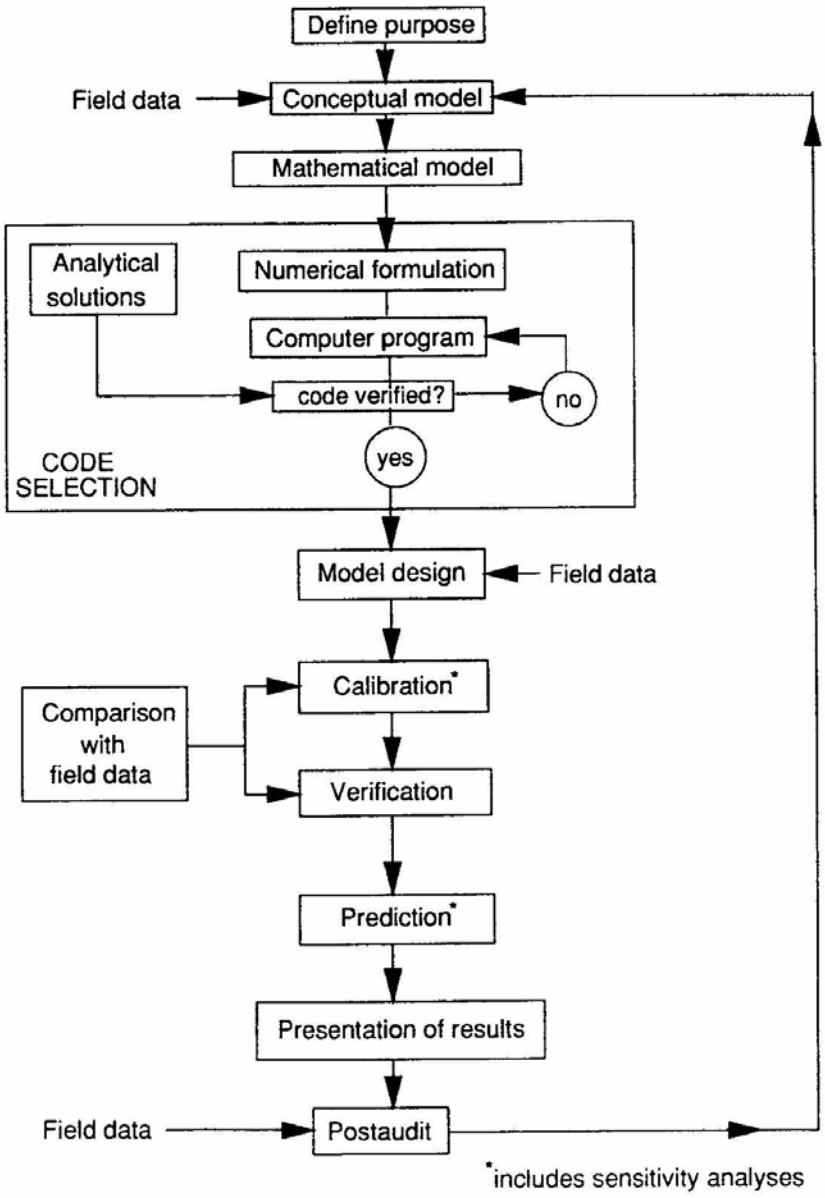

Figure 3-1 Steps in a protocol for model application (Anderson and Woessner, 1992).

Although MODFLOW was originally designed to facilitate change, its design concepts did not include solving equations other than the ground-water flow equation. As a result, incorporating capabilities such as those added through MODFLOWP and MOC3D was not as straightforward from the programmer's or user's perspective as were the other enhancements that dealt only with the ground-water flow equation. Therefore, MODFLOW-2000 has been developed to facilitate the addition of multiple types of equations. Ease of understanding continues to be included as an objective of

the design. There is also an objective to minimize changes that would impact existing MODFLOW users.

For many data input quantities, MODFLOW-2000 allows definition using parameter values, each of which can be applied to data input for many grid cells. In combination with new multiplication and zone array capabilities, the parameters make it much easier to modify data input values for large parts of a model. Defined parameters also can have associated sensitivities calculated and be modified to attain the closest possible fit to measured hydraulic heads, flows, and advective travel. This is accomplished using the Observation, Sensitivity, and Parameter-Estimation Processes of MODFLOW-2000, which are documented by Hill and others (2000).

The main objectives in designing MODFLOW were to produce a program that can be readily modified, is simple to use and maintain, can be executed on a variety of computers with minimal changes, and has the ability to manage the large data sets required when running large problems. The MODFLOW report includes detailed explanations of physical and mathematical concepts on which the model is based and an explanation of how those concepts was incorporated in the modular structure of the computer program. The modular structure of MODFLOW consists of a Main Program and a series of highly-independent subroutines called modules. The modules are grouped in packages. Each package deals with a specific feature of the hydrologic system which is to be simulated such as flow from rivers or flow into drains or with a specific method of solving linear equations which describe the flow system such as the Strongly Implicit Procedure or Preconditioned Conjugate Gradient. The division of MODFLOW into modules permits the user to examine specific hydrologic features of the model independently. This also facilitates development of additional capabilities because new modules or packages can be added to the program without modifying the existing ones. The input/output system of MODFLOW was designed for optimal flexibility.

3.1.2. MODFLOW Add-Ons

Many computer codes have been developed to be used with MODFLOW. The codes are often called packages, models or sometimes simply programs. Packages are integrated with MODFLOW, each package deals with a particular technique for solving the system of equations or a specific feature of the hydrologic system to be simulated. A model or program is not embedded in MODFLOW, but communicates with MODFLOW through data files. Some popular Package, Models, and Programs are given below.

Direct Solution (DE4): This package provides a direct solver using Gaussian elimination with an alternating diagonal equation-numbering scheme.

Horizontal-Flow Barrier (HFB): Simulates thin, vertical low-permeability geologic features (such as cutoff walls) that impede the horizontal flow of ground water.

Interbed-Storage (IBS): Simulates storage changes from both elastic and inelastic compaction in compressible fine-grained beds due to removal of groundwater.

Reservoir (RES): Simulates leakage between a reservoir and an underlying groundwater system as the reservoir area expands and contracts in response to changes in reservoir stage.

Streamflow-Routing (SFR): Account for the amount of flow in streams and to simulate the interaction (leakage) between surface streams and groundwater.

Time-Variant Specified Head (CHD): This package was developed as a part of the Interbed-Storage package to allow constant-head cells to take on different values for each time step.

3.1.3. Steps in Model Setup

Anderson and Woessner (1992) suggested steps in successful setting up a groundwater model as shown in Figure 3-1. Generally, one should begin with establishing the purpose of setting up a groundwater simulation; usually a predictive model. Then, using field data in both geology and hydrogeology aspects, to establish the conceptual model which includes defining the hydrostratigraphic units and proper boundary conditions. Next step, convert the conceptual model into a set of partial differential equations describing the system with appropriate boundary and initial conditions. This is called a mathematical model. Next, the problem domain is discretized in to pieces of blocks (in finite difference method) as seen in Figure 3-2 and model is executed.

Next crucial step, and perhaps the most important, is to calibrate the model using field observations. This is to make sure that model can capture flow field conditions. The model calibration, which has traditionally been achieved using trial-and-error approach, should be done systematically using automatic parameter estimation (e.g. Poeter and Hill, 1998). Finally, a validated model can be used to predict system behaviour or to assess groundwater resources.

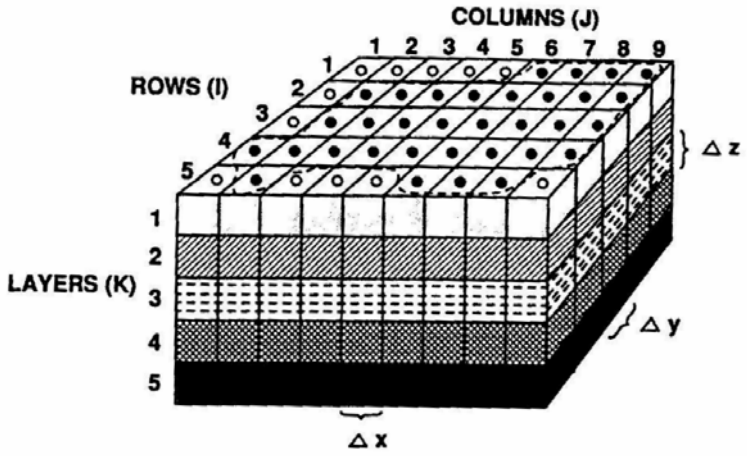

Figure 3-2 Grid system used in MODFLOW setup (Anderson and Woessner, 1992).

3.2. Conceptual Model

Setting up a proper conceptual model of the groundwater system is very important because it will dictate how good the approximation will result from a numerical model (in this case, MODFLOW). Good practice for modellers is always to start with a clear picture of a site's conceptual model.

The Chiang Mai groundwater basin is a semi-closed basin where groundwater can only flow in and flow out in the north and south boundaries, respectively. The east and west boundaries are bounded by mountains (Figure 1-1). Areas inside the basin boundary are a zone of natural recharge and, of course, a zone of groundwater extraction. Surface water runoffs include Ping and Kuang rivers which flows generally from north to south. The general groundwater flow direction is from north, east, and west to south which is similar to the flow of surface water.

Five semi- to unconsolidated deposits (described earlier in Chapter 2) of the Chiang Mai basin can be grouped into three hydrostratigraphic units: (1) Floodplain deposits aquifer which has a thickness of 50 m. The upper aquifer is unconfined with an average thickness of 30 m. The bottom 20 m of an aquifer is confined. (2) Low terrace deposits aquifer has an average thickness of 150 m which can be divided into two sub-units: an unconfined aquifer having a thickness of 30 m is located in the east and west parts of the floodplain deposits. The deeper aquifer located beneath the floodplain deposits is confined. (3) High terrace deposits aquifer having an average thickness of 300 m. The unconfined part of this aquifer is approximately 30 m thick whereas the aquifer beneath the low-terrace deposits is confined.

Figure 3-3 shows conceptual model of the Chiang Mai basin. The problem domain is similar to Figure 2-3 where the north and south ends of the aquifers were

cutoff in order to put the general-head boundary conditions for simulating inflow/outflow of groundwater. Groundwater generally flows from east and west side of the basin toward the central plain and flows southward out of the aquifer system.

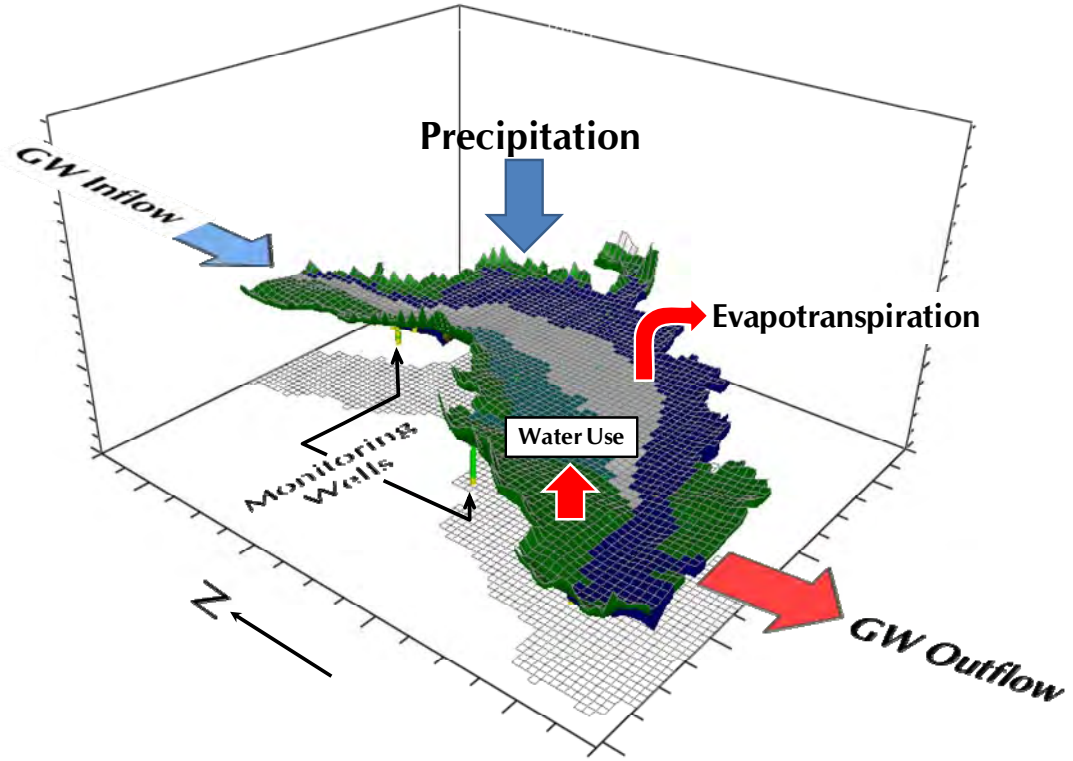

Figure 3-3 Conceptual model of the Chiang Mai basin
(modified from DGR, 2003)

3.3. Numerical Model

The conceptual model in Figure 3-3 is converted into a numerical model using three graphical user interface (GUI) versions of MODFLOW called PMWIN Pro® 7, GMS® 6.5 and Visual MODFLOW® 4.2. Each of them has weaknesses as well as strengths. This research utilizes all three GUI programs in order to accomplish model setup & execution, model calibration, and the stochastic groundwater modeling (discussed in Chapter 4). The domain (aquifer system) is discretized into a set of square finite-difference grid with the dimension of 1000×1000 m^2 (71 columns, 80 rows). The area outside unconsolidated aquifer is considered inactive (see Figure 3-4). The aquifer system is divided into four model layers with varying thicknesses and hydraulic conductivity fields. The hydraulic conductivity field for all four model layers are shown in Figure 3-5.

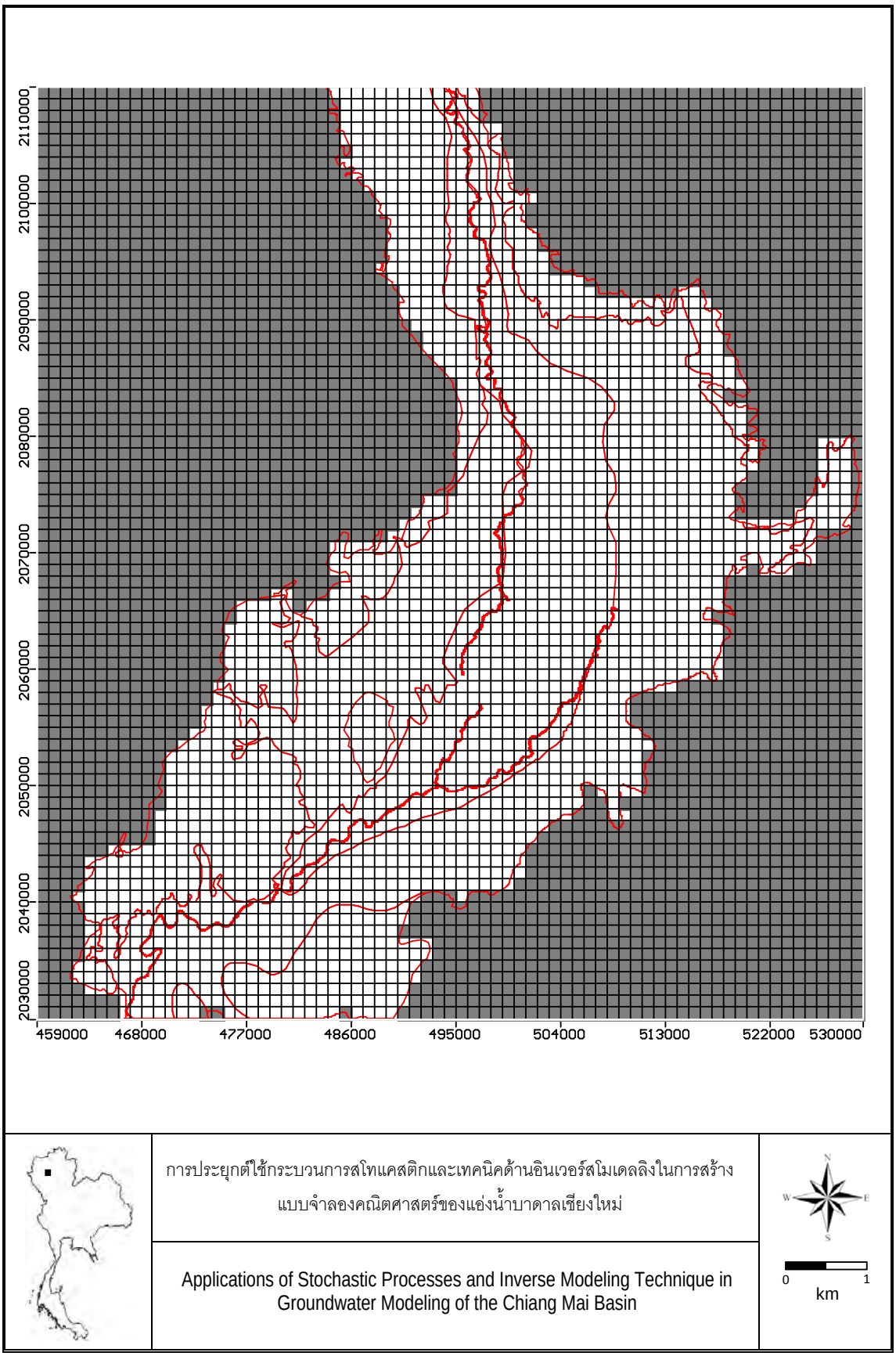

Figure 3-4 Model domain showing active/inactive cells.
(modified from DGR, 2003)

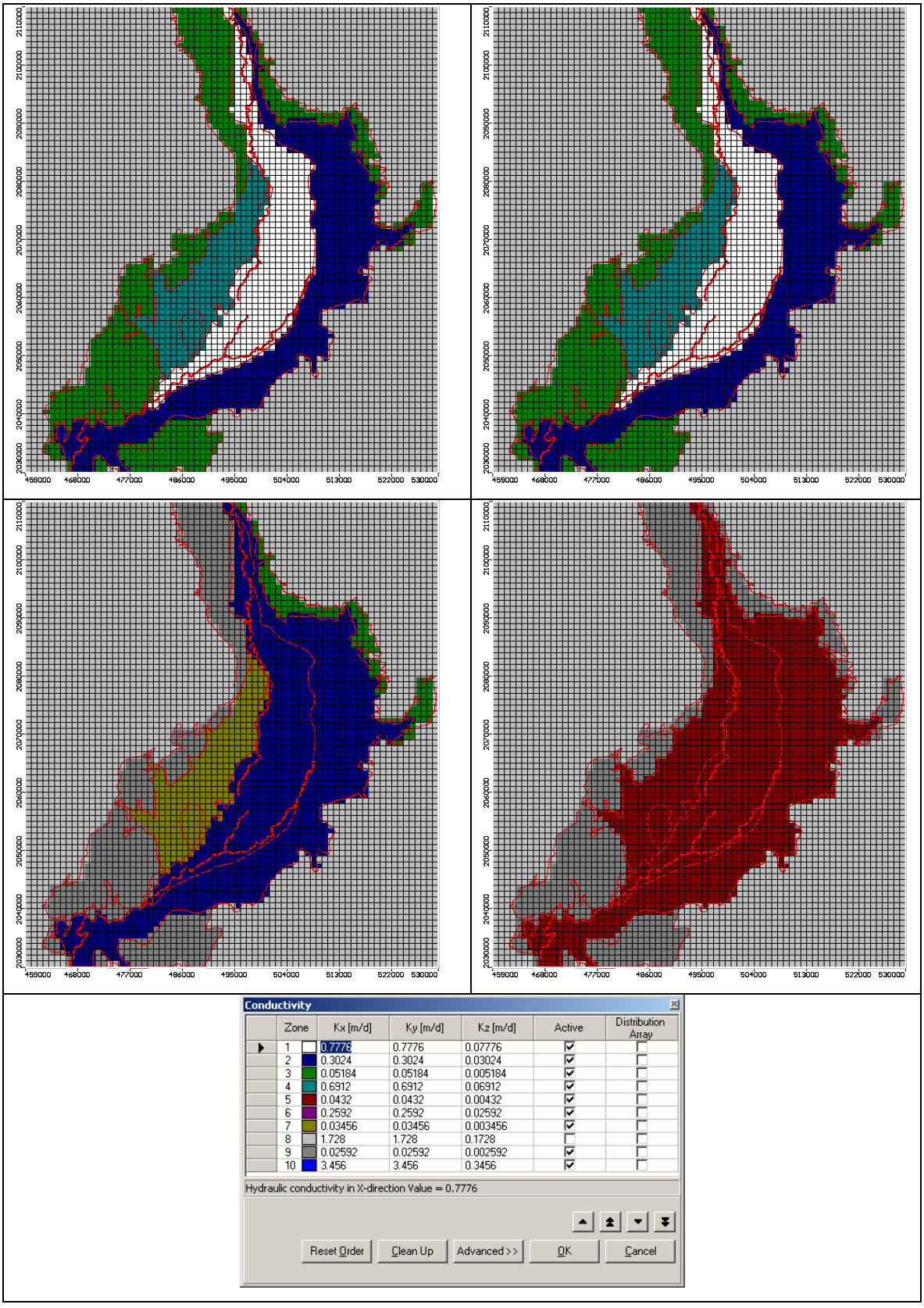

Figure 3-5 Hydraulic conductivity zones.
(modified from DGR, 2003)

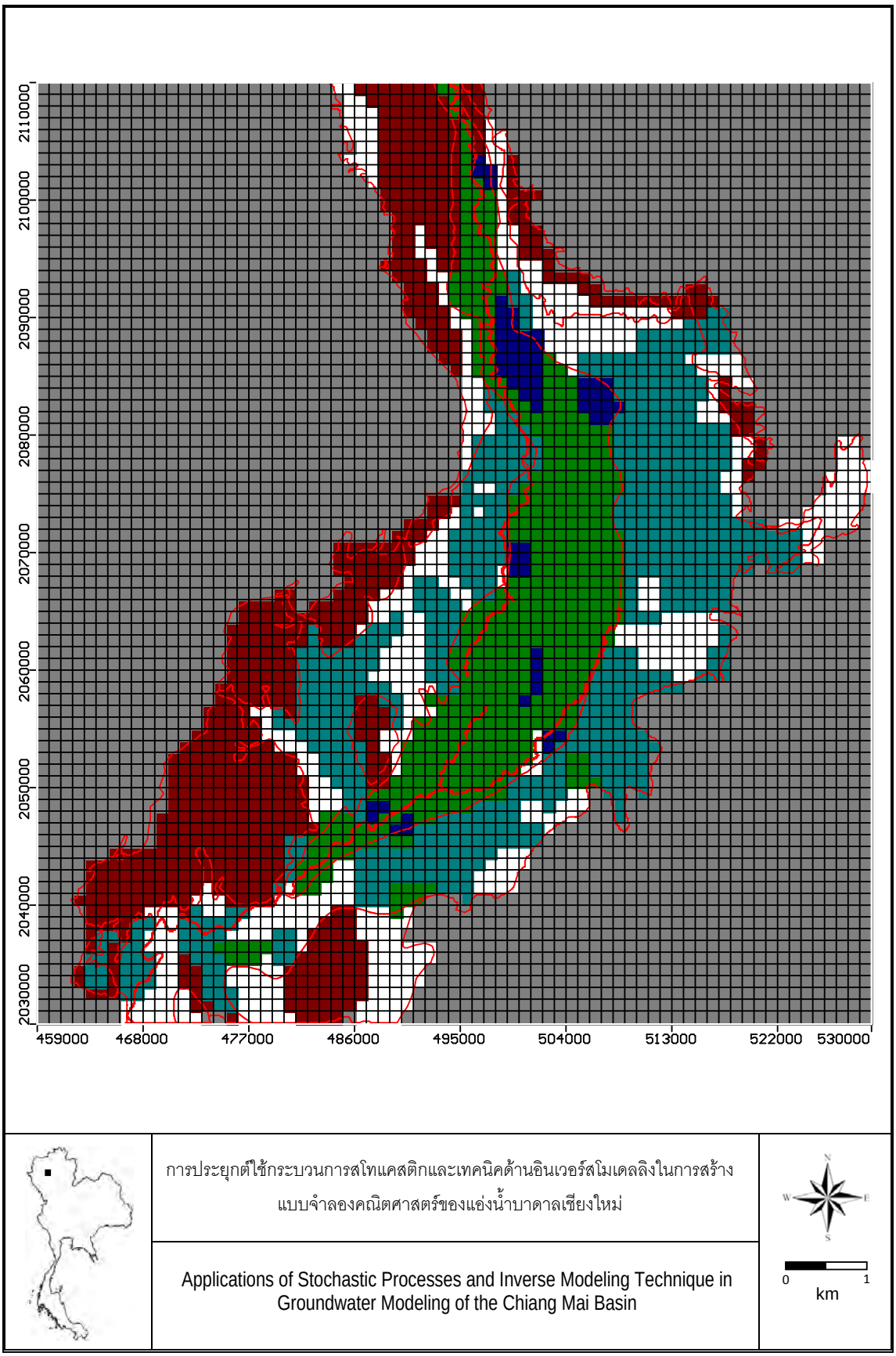

Figure 3-6 Recharge zones.
(modified from DGR, 2003)

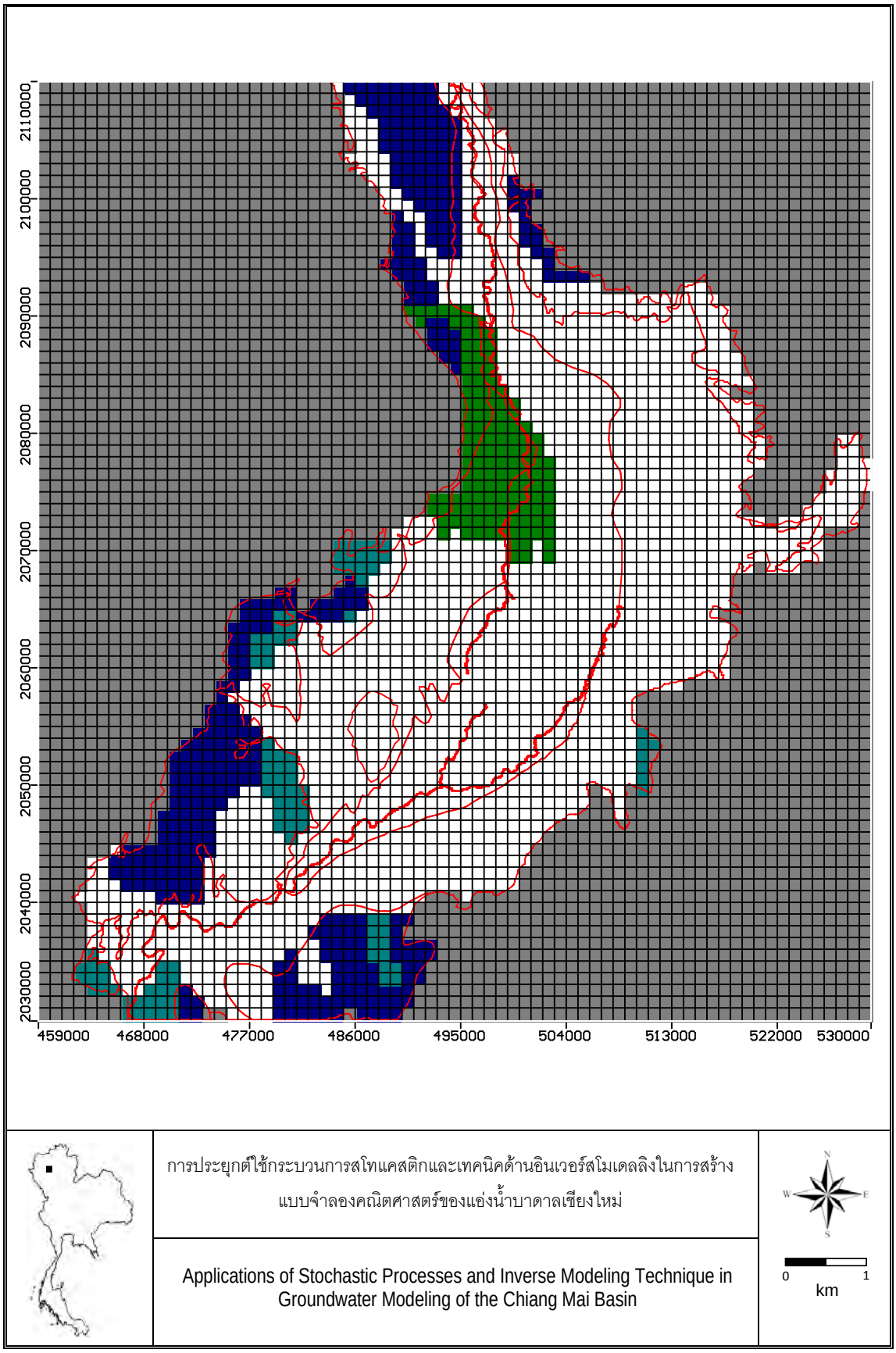

Figure 3-7 Evapotranspiration zones.
(modified from DGR, 2003)

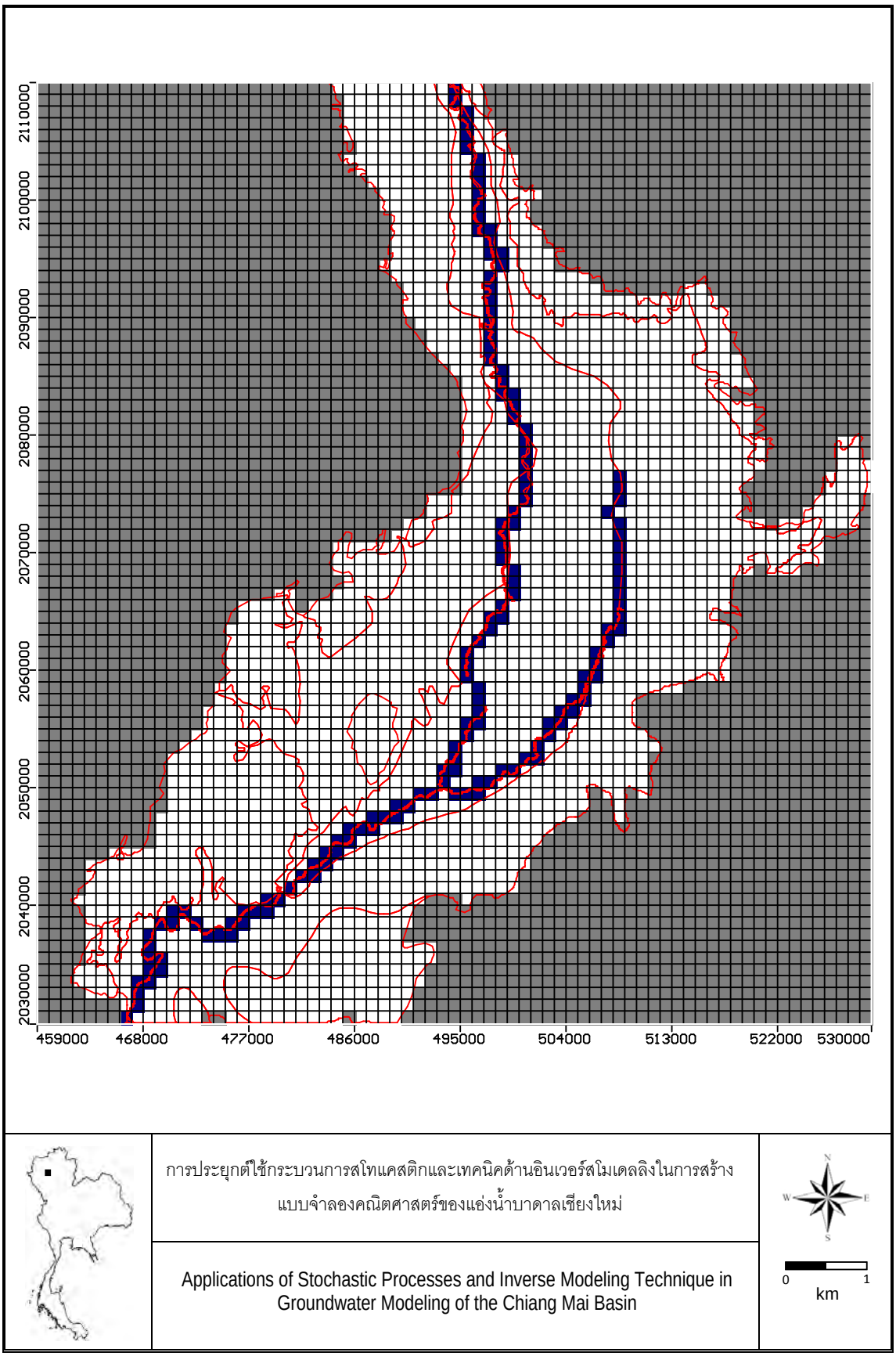

Figure 3-8 River cells (Ping and Kuang rivers).
(modified from DGR, 2003)

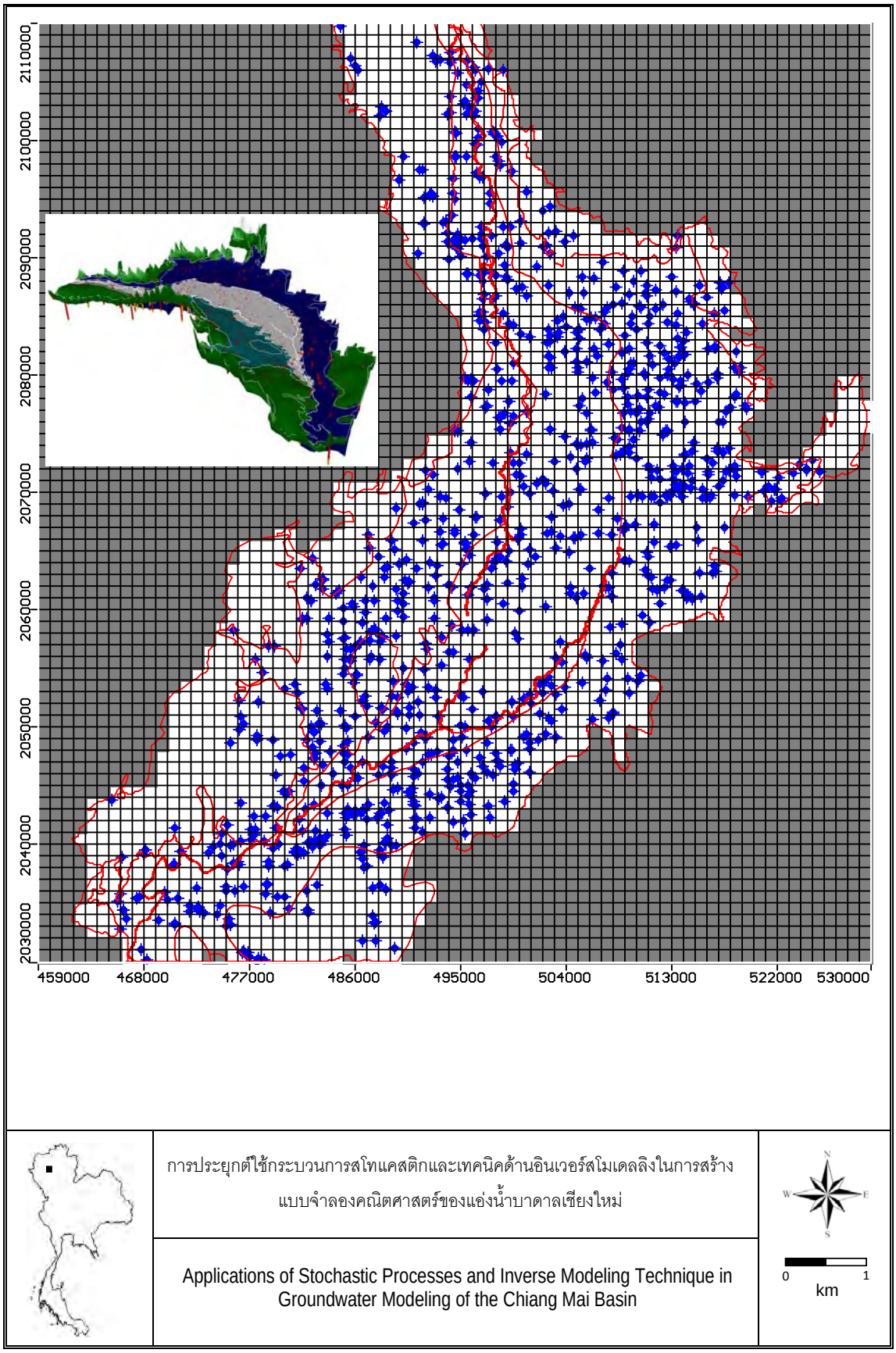

Figure 3-9 Pumping wells.
(modified from DGR, 2003)

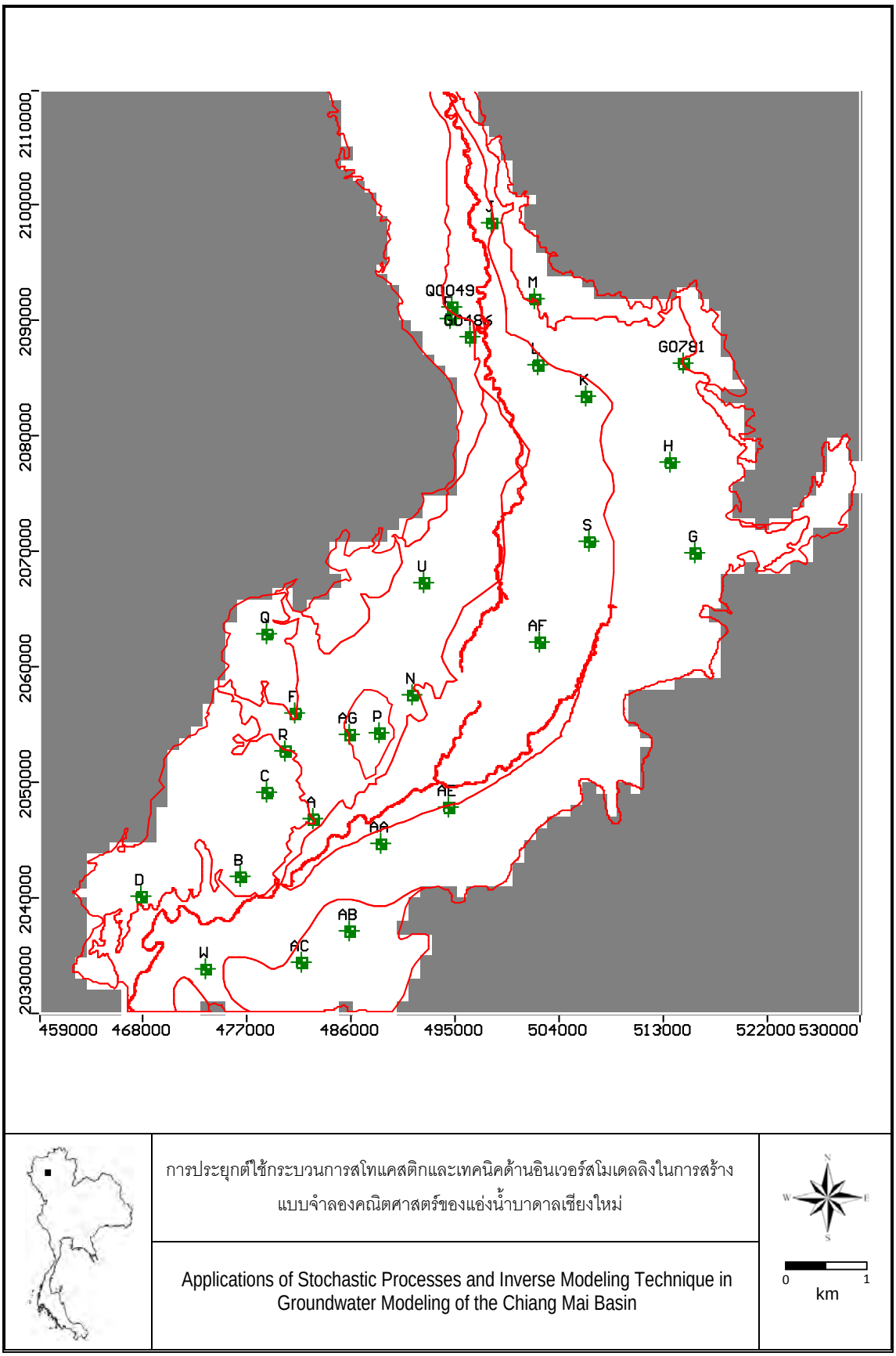

Figure 3-10 Locations of head observation wells.
(modified from DGR, 2003)

The distributions of recharge zone, evapotranspiration zone, river cells, pumping wells, and head observation wells are illustrated in Figure 3-6 to Figure 3-10, respectively. The measured hydraulic heads (h_{obs}) used to calibrate groundwater flow model were obtained from field measurements of 28 monitoring wells (see Figure 3-10 and Table 3-1 for locations and well detail) starting from year 2004 to 2009. The model is transient and has 48 stress periods. The length of each stress period is one month (in accordance with calendar) and was divided into five time steps in each period.

Table 3-1 Twenty-eight observation wells used in model calibration.

Well Name	UTM E (m)	UTM N (m)	Screen Elev. (m, asl.)
G0486	496290	2088600	268.0
G0781	514700	2086250	273.0
Q0049	494640	2091250	280.0
A	482649	2046827	124.0
B	476401	2041786	149.2
C	478730	2049147	136.0
D	467855	2040036	120.4
E	494565	2090158	200.8
F	481125	2056040	162.5
G	515698	2069886	121.1
H	513656	2077663	197.0
J	498070	2098550	212.0
K	506367	2083422	210.0
L	502177	2086173	262.0
M	501833	2091882	200.0
N	491273	2057538	105.0
P	488470	2054271	170.1
P	488470	2054271	256.1
Q	478730	2062849	89.0
R	480246	2052724	16.0
S	506589	2070819	135.0
U	492252	2067279	139.0
W	473326	2033863	128.0
AA	488533	2044619	126.0
AB	485829	2037083	124.0
AC	481735	2034399	126.5
AE	494401	2047786	101.0
AF	502239	2062077	102.0
AG	485778	2054178	131.0

After setting up all required input files (i.e., packages), the model was tested and made sure whether it can be executed properly. The intitial model excution or run may or may not be able to simulate the measured hydraulic heads of 28 observation wells. The model calibration is, a very important step of groundwater modeling, is then required so that model is able to match the observed heads. Next section will describe

the process of inverse modeling which is essential for a very large and complex hydrogeologic settings like Chiang Mai basin.

3.4. Model Calibration

3.4.1. Introduction

Despite their apparent utility, formal sensitivity and parameter-estimation methods are used much less than would be expected – sensitivity analyses and calibrations conducted using trial-and-error methods only are much more commonly used in practice. This situation has arisen partly because of difficulties inherent in inverse modeling, which are related to the mathematics used, the complexity of the simulated systems, and the sparsity of data in most situations; and partly due to a lack of effective inverse models that make the inherent and powerful statistical aspects of inverse modeling widely understandable. Recent work (for example, Poeter and Hill, 1997) has clearly demonstrated that inverse modeling, though an imperfect tool, provides capabilities that help modelers take greater advantage of the insight available from their models and data. Expanded use of this technology requires sophisticated computer programs that combine the ability to represent the complexities typical of many ground-water situations with statistical and optimization methods able to reveal the strengths and weaknesses of calibration data and calibrated models.

The Model Calibration is to use hydraulic heads from observation wells and observed flows from streams and compare to model computed values. It has traditionally been done using a trial-and-error method that iteratively adjusts model parameters until the model computed values match the field observed values to an acceptable level of agreement. In many cases, calibration can be achieved much more rapidly with an inverse model. Currently there are three automatic inverse models available: MODFLOW 2000 PES process (Hill et al., 2000), PEST (Doherty, 1994), and UCODE (Poeter and Hill, 1998). An inverse model is an internal process (MODFLOW 2000 PES process) or an external utility (PEST/UCODE) that automates the parameter estimation process. The inverse model systematically adjusts a user-defined set of input parameters until the difference between the computed and observed values is minimized. All three algorithms are similar although they are different in details. In this research, a program UCODE and PEST will be used to calibrate ground water models.

3.4.2. UCODE

UCODE is designed to allow inversion using existing algorithms (called application models in this work) that use numerical (ASCII or text only) input, produce

numerical output, and can be executed in batch mode. Specifically, the code was developed to: (1) manipulate application model input files and read values from application model output files; (2) compare user-provided observations with equivalent simulated values derived from the values read from the application model output files using a weighted least-squares objective function; (3) use a modified Gauss-Newton method to adjust the value of user selected input parameters in an iterative procedure to minimize the value of the weighted least-squares objective function; (4) report the estimated parameter values; and (5) calculate and print statistics to be used to (a) diagnose inadequate data or identify parameters that probably cannot be estimated, (b) evaluate estimated parameter values, (c) evaluate how accurately the model represents the actual processes, and (d) quantify the uncertainty of model simulated values.

Application models executed by UCODE can include pre-processors and post-processors as well as models related to the processes of interest (physical, chemical, and so on), making UCODE extremely powerful. In general, graphical user interfaces cannot be used directly with UCODE, but can be adapted with relatively little effort.

A flowchart of UCODE is presented in Figure 3-11. It describes the steps listed in the flowchart and introduces the most commonly used UCODE input files. The input files introduced are the universal, prepare, and extract files (one of each is needed for each UCODE run), the function file (optional, one may be used for each UCODE run), and template files (one or more are used for each UCODE run). The application model(s) executed by UCODE can include only one process/simulation model, a sequence of such models, or any combination of pre-processors, process/simulation models, and post-processors. Each application model needs to be set up to run in batch mode.

UCODE initializes a problem by reading the following information: (1) solution control information, commands needed to execute the application model(s), and observations from the universal file; (2) instructions from the prepare file, template files and, perhaps, a function file, which are used to create application model input files with starting or updated parameter values; and (3) instructions from the extract file for calculating simulated equivalents for each observation from numbers extracted from the application model output files. This information is stored for later use.

Parameter-estimation iterations are needed to solve the nonlinear regression problems for which UCODE is designed. In UCODE, parameter-estimation iterations begin by substituting the starting parameter values into the template files using instructions from the prepare file to create application model input files. UCODE then performs one execution of the application model(s) based on commands provided by

the user. Next, for each observation, UCODE extracts one or more values from the application model output and, using instructions from the extract file, calculates an equivalent simulated value to be compared to the observation. Equivalent simulated values are referred to simply as simulated values in the remainder of this section. Examples of calculating simulated values from extracted values are described below. The simulated values calculated at this step of each parameter-estimation iteration are called unperturbed simulated values because they are calculated using the starting or updated parameter estimates. The unperturbed simulated values are subtracted from the observations, and these differences are called residuals. The residuals are weighted, squared, and summed to produce the sum-of-squared-weighted residuals objective function, which is used by the regression to measure model fit of the observations.

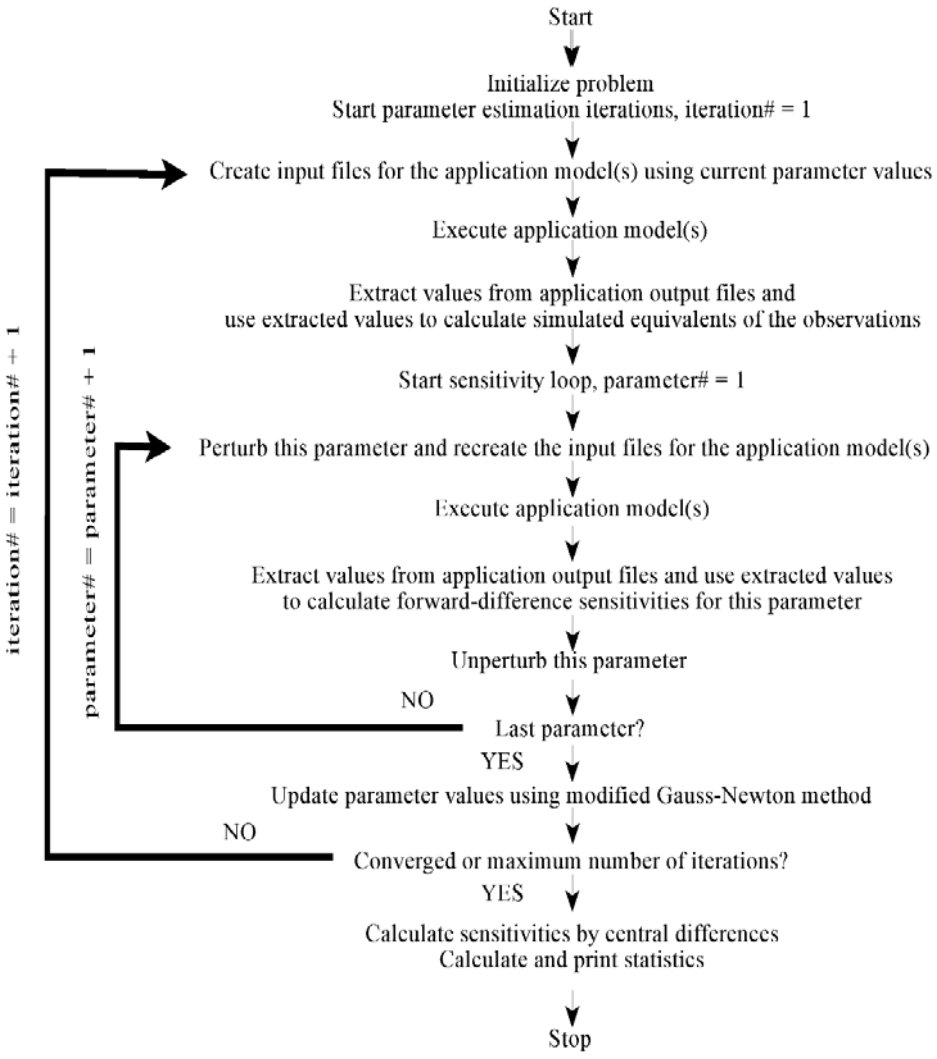

Figure 3-11 Flowcharte for estimating parameters with UCODE (Poeter and Hill, 1998).

To calculate sensitivities of the simulated values to the parameters, the application model(s) are executed once again for each parameter, and each time the value of one parameter is slightly different (perturbed) than its unperturbed value. The differences between perturbed simulated values and the unperturbed simulated values are used to calculate forward-difference sensitivities, as described below. Alternatively, the application model(s) can be executed yet again for each parameter (not shown in fig. 1) and sensitivities can be calculated using more accurate central differences, but this added accuracy is rarely needed to perform parameter-estimation iterations. Once the residuals and the sensitivities are calculated, they are used in a computer program which is specified by name in the universal file and performs a single parameter estimation iteration. UCODE is distributed with the nonlinear regression code MRDRIVE, which updates the parameter values using one iteration of the modified Gauss-Newton method as described by Hill (1998). The last step of each parameter-estimation iteration involves comparing two quantities against convergence criteria: (1) the changes in the parameter values and (2) the change in the sum-of-squared-weighted residuals. If the changes are too large and the maximum number of parameter-estimation iterations has not been reached, the next parameter-estimation iteration is executed. If the changes are small enough, parameter estimation converges. If convergence is achieved because the changes in the parameter values are small (1 above), the parameter values are assumed to be the optimal parameter values – that is, the values that produce the best possible match between the simulated and observed values, as measured using the weighted least-squares objective function. If convergence is achieved because the changes in the objective function are small, it is less likely that the estimated parameters are optimal and further analysis generally is needed. If parameter estimation does not converge and the maximum number of iterations has not been reached, the updated parameter values are substituted into the template files, and the next parameter-estimation iteration is performed. When parameter estimation converges or the maximum number of iterations has been reached, sensitivities are calculated using the more accurate central-difference method. The additional accuracy is needed to achieve a sufficiently accurate parameter variance-covariance matrix, from which a number of useful statistics are calculated. If parameter estimation converged, the final parameter values are considered to be optimized. Once a model is calibrated, it can be used to make predictions for management or other purposes. UCODE can calculate linear confidence and prediction intervals that approximate the likely uncertainty in predictions simulated using the application models and optimized parameter values.

3.4.3. PEST

Similar to UCODE, an inverse algorithm PEST (Parameter ESTimation)is a nonlinear parameter estimation package developed by Doherty (1994). The major difference between PEST and UCODE is that, in PEST, optimum parameter values can be constrained to lie between individually-specified upper and lower bounds. This is implemented using a mathematically advanced algorithm that actually regularizes the parameter estimation problem as bounds are imposed.

Many application models will produce nonsensical results or may cease with run-time error if certain input parameters fall outside the permissible range. For example, the hydraulic conductivities of any geologic materials may fall within a reasonable range (minimum, maximum). The estimation of K from inverse modeling, without posing upper and lower limits, could result in a value that is far away from the reasonable range. Therefore, posing the lower and upper bounds for adjustable parameters will eliminate this problem.

3.5. Simulation Results

3.5.1. Model Calibration Results

The model was setup using three graphical user interface programs (GUIs) of MODFLOW that include Processing MODFLOW, Visual MODFLOW, and GMS. After using GUIs to construct the groundwater flow model, a series of input files (ASCII format) were exported and ready for excution in DOS environment. Both PEST and UCODE programs were subsequently coupled with MODFLOW-2000 to calibration the transient groundwater flow model. The calibration results of some observation wells were illustrated in Figure 3-12. It is obvious that the calibrated model can capture observed hydraulic heads exceptionally well in some observation wells whereas others cannot be matched satisfactorily. This problem is commonly found in a simulation/calibration of regional-scale groundwater flow model. Nevertheless, the error in observation is still in an acceptable range (90% confidence).

During and after model calibration, sensitivity analyses results could also be obtained from a set of output files (`*.rec, *.sen, *.dss`). It was found that parameter sensitivities are different between parameter groups. The hydraulic conductivities, storage coefficients, and recharge are the top most sensitive whereas general head boundary conductances, riverbed conductances, and maximum evapotranspiration rates are less sensitive suggesting that hydrogeologic chracterization of hydraulic properties (K, S) must be performed carefully.

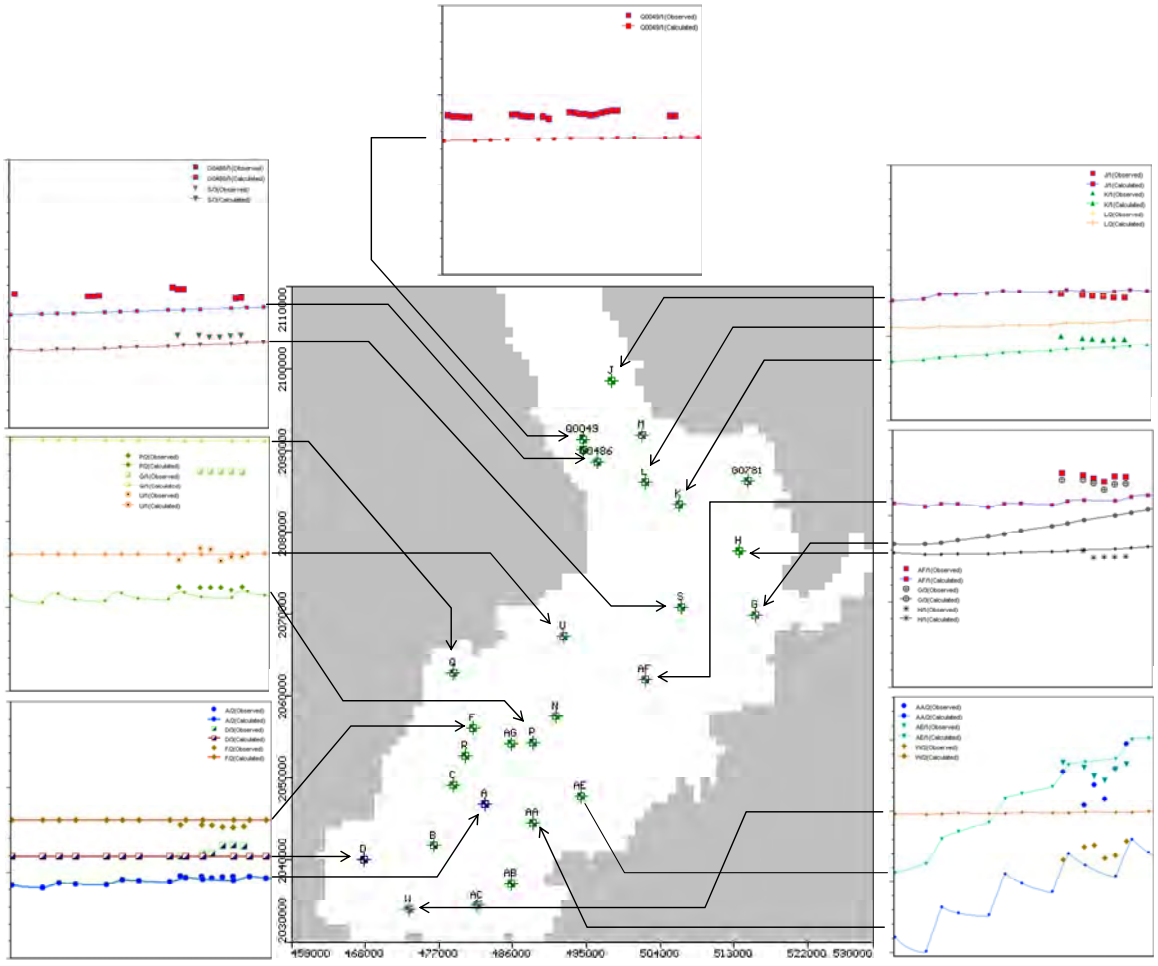

Figure 3-12 Example of model calibration results.

Figure 3-13 illustrates the distribution of hydraulic heads in the top model layer at the end of December 2009 simulation year.

3.5.2. Water Budget

After model calibration is completed, the water budget of the basin can be calculated. Table 3-2 shows the water budget of the basin during entire 2009.

Table 3-2 Water budget of the Chiang Mai Basin (Year 2009)

IN (million m^3)		OUT (million m^3)	
Recharge	231.4	Pumping Well	72.7
GHB (inflow)	0.06	GHB (outflow)	0.18
River (into aquifer)	9.92	River (out of aquifer)	16.5
		ET	151.6
Total	241.4	Total	241.0

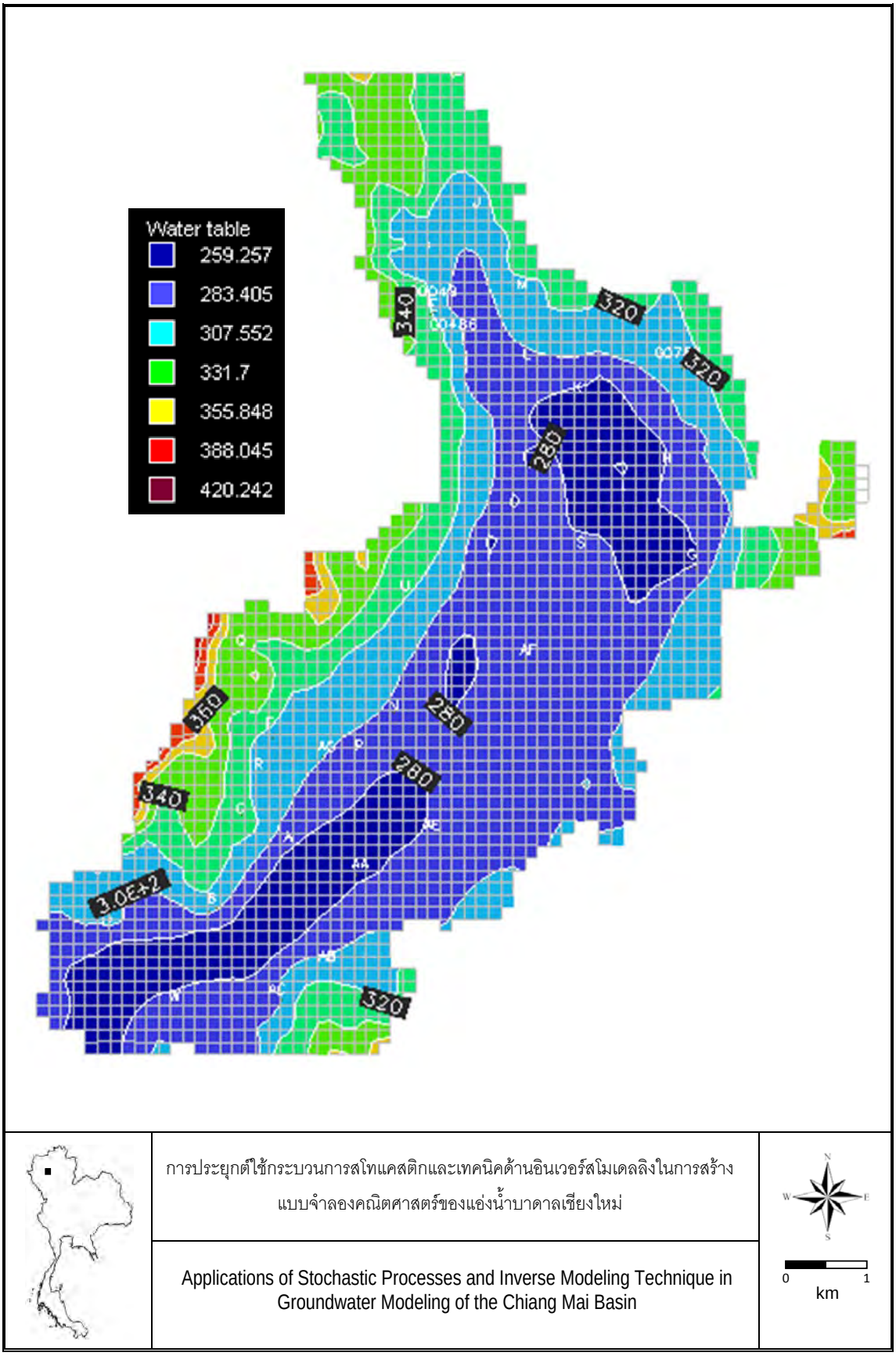

Figure 3-13 Distribution of hydraulic heads in the basin (end of December 2009).

Chapter 4

Groundwater Flow Model: Stochastic

Chapter 4: Stochastic Groundwater Flow Model

4.1. Rationale for Using Stochastic Approach

It is well known that, at a field scale, geological formations are heterogeneous, and the groundwater flow and solute transport processes in the formation are considerably affected by the heterogeneity of the formation properties. In the last two decades, many stochastic theories have been developed for groundwater flow and solute transport in heterogeneous porous media (Gelhar, 1983). In development of the theories, it is common to assume that the spatial distributions of the medium properties can be characterized by one single correlation scale. This assumption was based on some field studies, as well as on the notion of the existence of a discrete hierarchy of scales of heterogeneity, with disparity between the scales such that when modeling groundwater flow and solute transport at one scale, variations at other scales can either be averaged out (if other scales are much smaller), or be modeled as a deterministic trend (if other scales are much larger). However, hydraulic properties of many natural media exhibit heterogeneity at multi-scales, where the heterogeneity at any scale cannot be averaged out, nor be treated as a deterministic trend.

Heterogeneity is one of the primary factors which complicates the characterization and remediation of contaminated aquifers. Prior to addressing the assessment of groundwater resource potential, the subsurface hydraulic environment must be evaluated. This includes understanding the mechanisms that create subsurface variability, the significant parameters, range of parameter values, and quantification of the spatial variation.

Examination of the processes that create heterogeneity in the subsurface can provide insight to the distribution and range of material properties. The spatial variability of the subsurface is a function of constantly changing atmospheric conditions (Gelhar, 1993). Runoff, sediment transport, deposition of materials and infiltration all reflect the unpredictable nature of weather. These processes occurring over geological time periods create variations in the deposition of materials. In addition structural processes occurring over the same extended time scales insure that fractures are formed providing preferential flow channels of water. Variation in terrain that was historically exposed and becomes buried results in formations promoting or impeding the movement of water in the subsurface.

There are many studies which have documented the variability of field parameters such as porosity, grain size distribution, and hydraulic conductivity in the subsurface (Peck, 1983; Gelhar, 1986). The impact of heterogeneity has been observed in many field studies (Mackay et al., 1986). It would be virtually impossible to deterministically capture all of the variation in these systems, even relatively small systems, especially since scaling, the size at which a system is studied determines which features dominate flow and transport, remains an issue.

Efficient analysis of flow requires selection of the most sensitive material property parameters. There are many different parameters that can be used to describe the subsurface: porosity, grain-size distribution, hydraulic conductivity, dispersivity, suction-saturation relationships, relative permeability, entry pressure and sorption coefficients. The logistics of collecting and evaluating the spatial distribution of once of these parameters, much less all of them, would be a considerable task. For this reason, it is important to evaluate which are the most significant n terms of flow and transport in heterogeneous media. To assess sensitivity of different parameters, Warran and Price (1964) studied variations in porosity. In addition, Naff (1978) studied variations in local dispersion coefficient. The impact of variations in both porosity and dispersivity was minimal in comparison to variations of hydraulic conductivity. Although many of the parameters listed are highly correlated, hydraulic conductivity is typically used to describe the variability since it mot efficiently captures the impact of subsurface heterogeneity on flow and transport. Variations of conductivity dominate the overall movement and spread of a conservative solute (Dagan, 1984).

4.2. Stochastic Theory

4.2.1. Introduction

The daunting task of deterministically characterizing the subsurface has led many investigations to resort to stochastic methods (Freyburg, 1986). For flow and transport in the subsurface, hydraulic conductivity is the constitutive parameter typically treated as a random space function. Treating hydraulic conductivity as a random space function results in values of flux and head being random variables. Instead of treating these parameters as deterministic, they are described in terms of statistical properties. For example, hydraulic conductivity is described in terms of its probability density function (PDF): $f_k(k)$, which is defined by (4-1).

$$f_k(k)\delta k = P\left[k < K < k + \delta k\right] \tag{4-1}$$

The PDF is the probability that the random variable, K, will have a value between k and $k + \delta k$. The PDF completely specifies the properties of the continuous random variable. When the distribution is normal it can be completely characterized by its first two moments: the mean and variance. Instead of referring to an individual value, the expected value, mean (μ) and its expected range of variation, variance (σ^2) are used to represent hydraulic conductivity. Equations (4-2) and (4-3) relate the PDF to μ and σ^2.

$$\mu_k = E\left[K\right] = \int_{-\infty}^{+\infty} k f_k(k)dk \tag{4-2}$$

$$\sigma_k^2 = E\left[\left(K - \mu_k\right)^2\right] = \int_{-\infty}^{+\infty} \left(k - \mu_k\right)^2 f_k(k)dk \tag{4-3}$$

The mean and variance provide overall statistics independent of spatial organization. The spatial structure is described by the covariance. Between any two conductivities K_1 and K_2, located at points x_1 and x_2 respectively, the covariance is:

$$\mathrm{cov}\left(K_1,K_2\right) = E\left[\left(K_1 - \mu_1\right)\left(K_2 - \mu_2\right)\right] = \int\left(K_1 - \mu_1\right)\left(K_2 - \mu_2\right) f_k(k_1,k_2)\partial k_1 \partial k_2 \tag{4-4}$$

The covariance function measures the linear relationship between the values of conductivity at the two points. If K_1 and K_2 are independent then the covariance will be zero. When the separation distance, $|x_1 - x_2|$, reduces to zero, equation (4-4) reduces to the variance. For groundwater investigations higher order terms are not typically used to describe the PDF for two reasons. First of all, they are more susceptible to sampling noise or error, require much more effort to generate and are more difficult to interpret. Secondly, investigations have found the conductivity to be log-normally distributed (Freeze, 1975). The log-normal distribution can be fully characterized using its first two moments.

The correlation scale (λ) provides another measure of spatial relation. It is the distance of separation at which the correlation equals $1/e$: the separation at which the correlation has decreased to 0.367 (Gelhar, 1993). This is typically used as the separation distance at which the correlation starts o become insignificant. For example, in a layered system the horizontal structure persists over very long distance. This tendency is reflected in a large value of horizontal correlation scale (λ_x), while the relatively thin layers, having great deal of variation over small vertical distances, are characterized with a much smaller vertical correlation scale (λ_z). Although the concept of structure within a random field may seem contradictory there are many examples of field data demonstrating structure in heterogeneous systems (Greenholtz et al., 1988) as well as a number of books explaining the theoretical concepts (Gelhar, 1993; Dagan, 1989).

In the same way that many aspects of statistics assume an underlying normal distribution, stochastic analysis requires that the random field is stationary and that it satisfies the ergodic assumption. Stationarity, as it typically applied to subsurface hydrology, requires that the mean is constant and to covariance is only a function of separation. The condition of stationarity essentially rules out any large spatial trends in the aquifer material and requires that the spatial correlation between points be constant for a given distance anywhere in the system. The ergodic assumption addresses the issue of whether expectations of a random distribution can be applied to a single realization: the single realization which was sampled is equated to the expected value of the theoretical distribution. The collection of all possible outcomes of the theoretical distribution is called the ensemble. If an aquifer is stationary, the expected transport of a solute in an ensemble of aquifers with the assigned statistical properties approximates the individual field conditions. This hypothesis is likely to be satisfied if the scale of the flow system is large in comparison to the correlation scale of the aquifer.

4.2.2. Stochastic Equations: Eulerian Reference Frame

Stochastic techniques provide mechanism for handling the variability found in many natural systems. For a site satisfying stationarity and ergodicity the spatial statistics of the hydraulic conductivity distribution can be computed and these properties incorporated into the governing equations. Stochastic concepts can be applied to flow and transport in groundwater in a wide variety of ways. Governing equations are typically derived in a Eulerian framework but solution of the stochastic partial differential equations can often benefit by evaluating in a different frame of reference. The Eulerian reference observes variations of head, velocity and concentration with time at fixed points in space. This is the easiest to visualize: information at various points in the field and how the values change with time. Examples of successful applications of these techniques applications of these techniques include places such as Borden and Cape Cod (Freyburg, 1986; Sudicky, 1986; Garabedian et al., 1991; Mackay et al., 1994). Other references such as Lagrangian and solute flux, will be discussed later.

Treating hydraulic conductivity as a random space field (RSF), allows the stochastic nature of an aquifer to be incorporated into the governing equations for flow and transport. The first step is to evaluate the steady-state groundwater flow equation (4-5) with hydraulic conductivity as a RSF.

$$\frac{\partial}{\partial x_i}\left(\mathbf{K}\frac{\partial \phi}{\partial x_i}\right) = 0 \text{ , when } i = 1,2,3 \qquad (4\text{-}5)$$

In (2-5) **K** is the isotropic hydraulic conductivity tensor, ϕ is the hydraulic potential, x_i is the i^{th} coordinate direction and the repeated i index implies a summation. Differentiating the product and dividing through by hydraulic conductivity in (4-5) produces (4-6).

$$\frac{\partial^2 \phi}{\partial x_i^2} + \frac{\partial \ln \mathbf{K}}{\partial x_i}\frac{\partial \phi}{\partial x_i} = 0 \text{ , when } i = 1,2,3 \qquad (4\text{-}6)$$

In this form the logarithm of hydraulic conductivity occurs naturally. The impact of the heterogeneity is manifested entirely through gradients in ln K. When ln K is constant, as in the homogeneous case, the head equation reduces to the Laplace equation. This form is advantageous because ln K is often normally distributed: the distribution can be completely characterized by just the mean and variance. In addition

the variance of ln K wil always be less than K. For these reasons it is beneficial to use ln K in the analysis (Gelhar, 1993). To perform the analysis of perturbations, ln K is decomposed into its mean and fluctuation components (4-7).

$$\left.\begin{aligned} \ln K &= F + f \\ E[\ln K] &= F = \ln K_g \\ E[f] &= 0 \end{aligned}\right\} \tag{4-7}$$

Where E[ ] represents the expected value operator, K_g is the geometric mean of conductivities and f is the random fluctuation of hydraulic conductivity about the mean. This decomposition can then be used in (4-6) and expectations taken to produce the equation describing the mean field head distribution (4-8).

$$\frac{\partial^2 H}{\partial x_i^2} + \frac{\partial F}{\partial x_i}\frac{\partial H}{\partial x_i} + E\left[\frac{\partial f}{\partial x_i}\frac{\partial h}{\partial x_i}\right] = 0\,, \tag{4-8}$$

where ϕ has been decomposed as follows:

$$\left.\begin{aligned} \phi &= H + h \\ E[\phi] &= H \\ E[h] &= 0 \end{aligned}\right\} \tag{4-9}$$

Equations (4-8) can then be subtracted from (4-6) which results in the equation for head fluctuations (4-10).

$$\frac{\partial^2 h}{\partial x_i^2} + \frac{\partial F}{\partial x_i}\frac{\partial h}{\partial x_i} + \frac{\partial f}{\partial x_i}\frac{\partial h}{\partial x_i} = E\left[\frac{\partial f}{\partial \mathbf{x}_i}\frac{\partial h}{\partial \mathbf{x}_i}\right] - \frac{\partial f}{\partial \mathbf{x}_i}\frac{\partial h}{\partial \mathbf{x}_i} \cong 0\,, \tag{4-10}$$

In (4-10), the difference between the product of head perturbations with ln K fluctuations and the expected value of their product is assumed to be close to zero. This is reasonable since the head perturbations are produced by the ln K fluctuations. If the ln K fluctuations are small then the head perturbations will also be small and the product of these two terms will be even smaller (Gelhar, 1993).

4.2.3. Variograms

The variability in K within aquifers is generally not purely random but also displays an underlying correlation structure. Spatial correlation of hydraulic conductivity is due to geologic stratification such as lenses and layers. The correlation scale is a characteristic length of the average spatial persistence of ln K. A geostatistical tool for the quantification of spatial structure is the experimental semi-variogram.

Variograms are useful for identifying the underlying spatial structure and identifying trends in K. The classical experimental semivariogram estimator, $\gamma(h)$, for Gaussian data is calculated as the mean-squared differences between sample values at specified separation distances in the x direction,

$$\gamma(h) = \frac{1}{2n(h)} \sum_{i=1}^{n(h)} \left[K(x_i + h) - K(x_i) \right]^2 , \qquad (4\text{-}11)$$

Where $\gamma(h)$ is the variogram statistics, $K(x_i)$ is the ln K at the point x_i, h is the separation distance between observations and n(h) is the number of data pairs separated by the distance h. Henceforth, the semivariogram estimator is referred to simply as the variogram. If the ln K data is statistically homogeneous (stationary) then the variogram is dependent only on h. Variograms are calculated in the appropriate coordinate directions, i.e. a two-dimensional aquifer can be described by variograms in the horizontal and vertical directions.

A typical variogram for a stationary process is shown in Figure 4-1. The variogram is related to the covariance function for a stationary process as shown. For small separations in the x direction, the correlation between pairs is strong and the variogram statistic is small. If the variance does not approach zero toward zero separation then there exists a nugget effect. This implies that there is a correlation in K at a scale smaller than the smallest separation. Points at increasing separations have lower correlation and the variogram will approach a constant plateau, called the sill. The separation at which the sill is reached determines the range of the variogram

If the process is nonstationary, the variogram may increase indefinitely resulting in an upward trend at the tail. The number of pairs decreases with increasing separation and there may only be in erratic variation at the tail of the variogram. Therefore it is common practice to examine the variogram for separations up to one half of the maximum separation given than the sample consists of at least 30 pairs. This portion of the variogram is the most meaningful in the statistical sense.

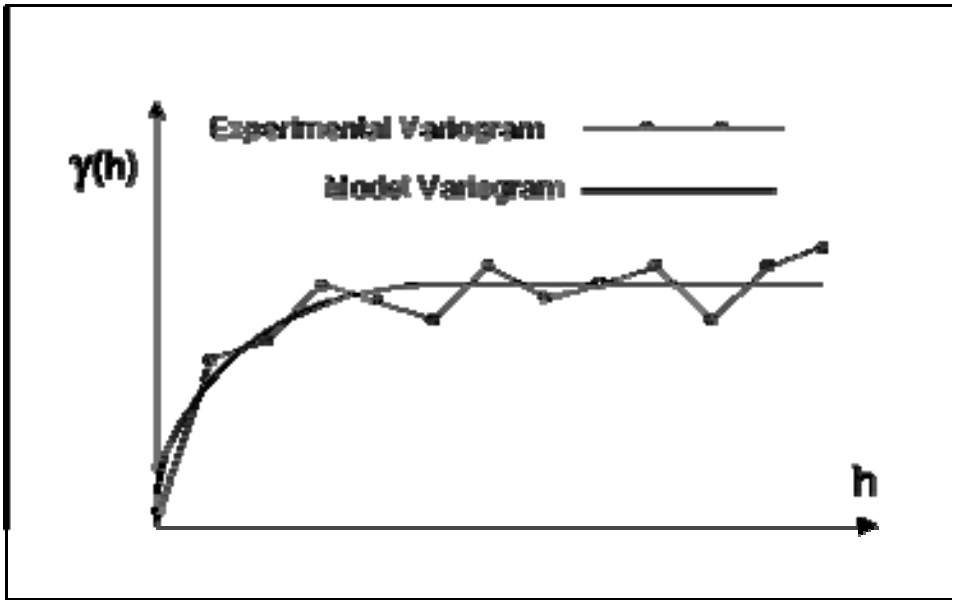

Figure 4-1 Typical variogram for a stationary process.

The theoretical variogram is estimated by the negative exponential model;

$$\gamma(h) = \sigma_s^2 \left[1 - e^{-h/\lambda}\right], \tag{4-12}$$

where σ^2 is the variogram sill and λ is the correlation scale. The exponential model can be fit to the experimental variograms by minimizing sum of squares of the difference between the two. The correlation lengths may be roughly estimated as the separation distance at which the variogram increases to the level

$$\gamma(h) = \sigma^2 \left[1 - e^{-1}\right], \tag{4-13}$$

4.3. Stochastic Modeling of Groundwater Flow of the Chiang Mai Basin

4.3.1. Overview

Prior to constructing a stochastic groundwater flow model of the Chiang Mai basin, the variogram of ln K must be calculated using hydraulic conductivity measured from the field tests (e.g., pumping and slug tests). Hundreds of pumping and slug tests have been conducted in Chiang Mai basin (DGR, 2003) and they are therefore ready for this analysis. The field-measured hydraulic conductivities were then categorized into four model layers. Each layer has its own variogram, correlation lengths, mean and

variance of ln K. Then, a geostatistical program called Field Generator (Chiang, 2005) was used to generate 10 hydraulic conductivity fields for all layers. Each field is called realization. Ten realizations of K field will then be used to setup groundwater flow models in MODFLOW-2000. Uncertainties in flow budget as well as errors in model calibration can then be calculated.

4.3.2. Vairogram of Hydraulic Conductivity

The variograms of hydraulic conductivity field of the Chiang Mai basin were calculated using Surfer® 7.0 program (see Figure 4-2).

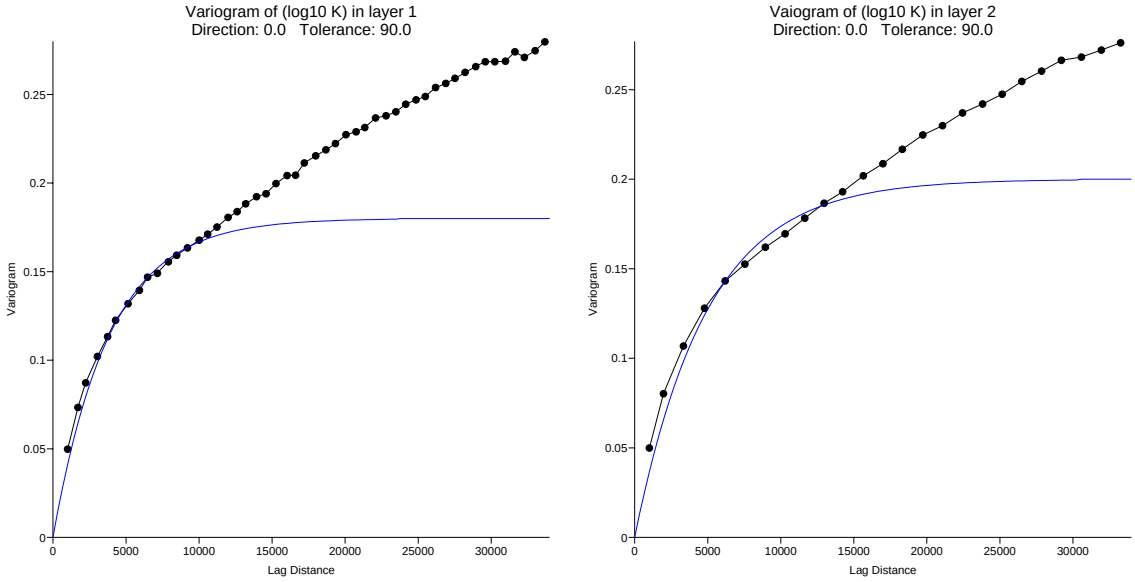

Layer 1 (↑) Layer 2 (↑)

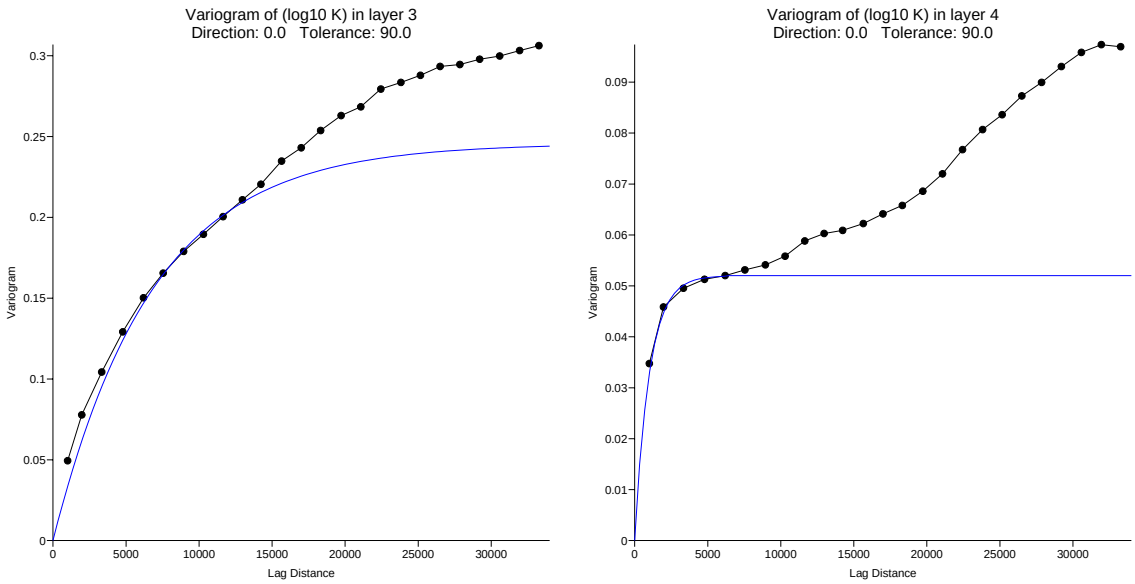

Layer 3 (↑) Layer 4 (↑)

Figure 4-2 Variogram of [log K] for all model layers.

4.3.3. Hydraulic conductivity Field

The hydraulic conductivity field of all model layers can be generated from program Field Generator®. Figures 4-3 to 4-6 show inputs for the program for generating hydraulic conductivity field for ten realizations. Groundwater flow model was then setup to simulate groundwater flow and its budget as well as calibration errors can be obtained.

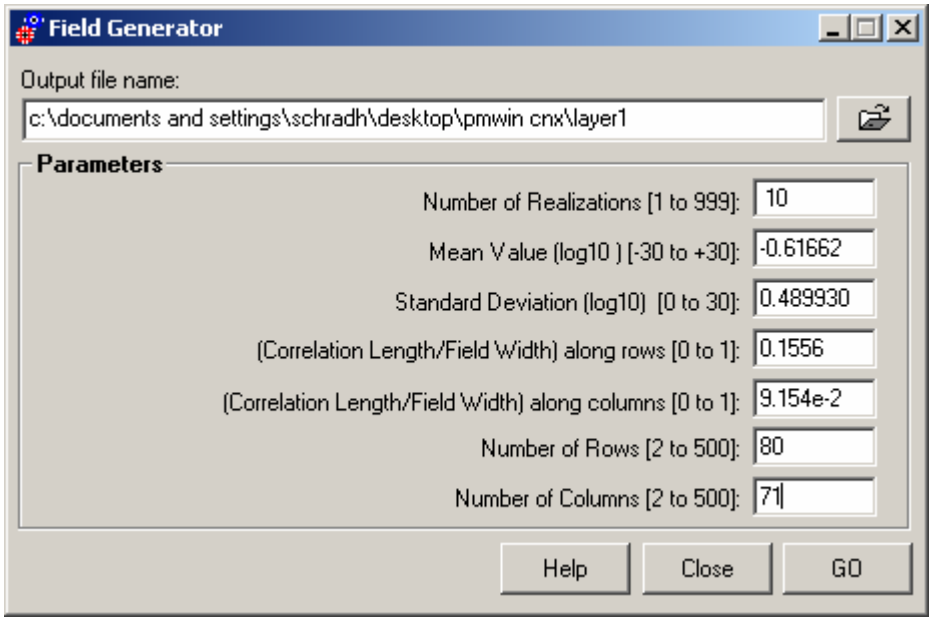

Figure 4-3 Parameters used for generating hydraulic conductivity field in layer 1.

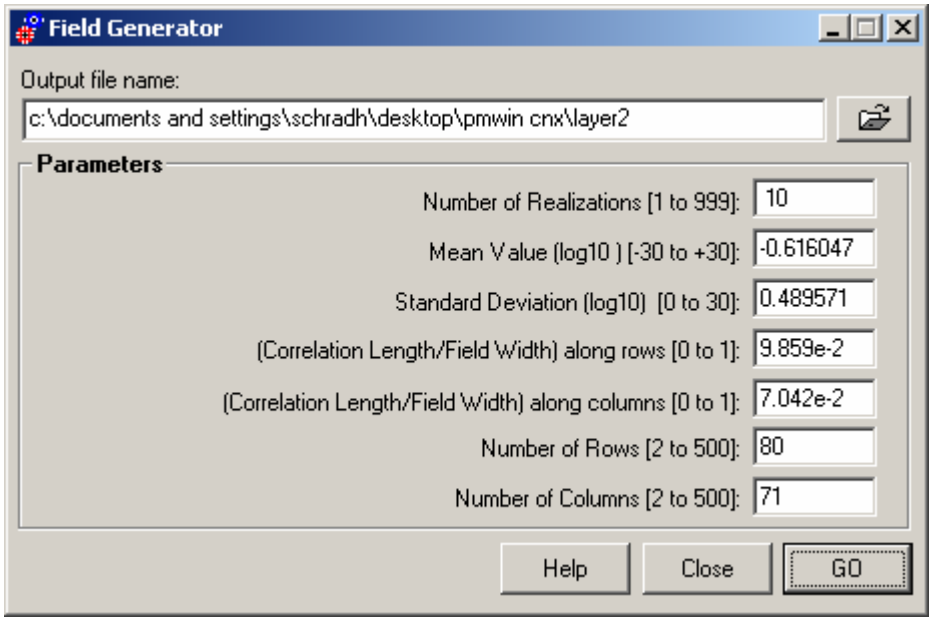

Figure 4-4 Parameters used for generating hydraulic conductivity field in layer 2.

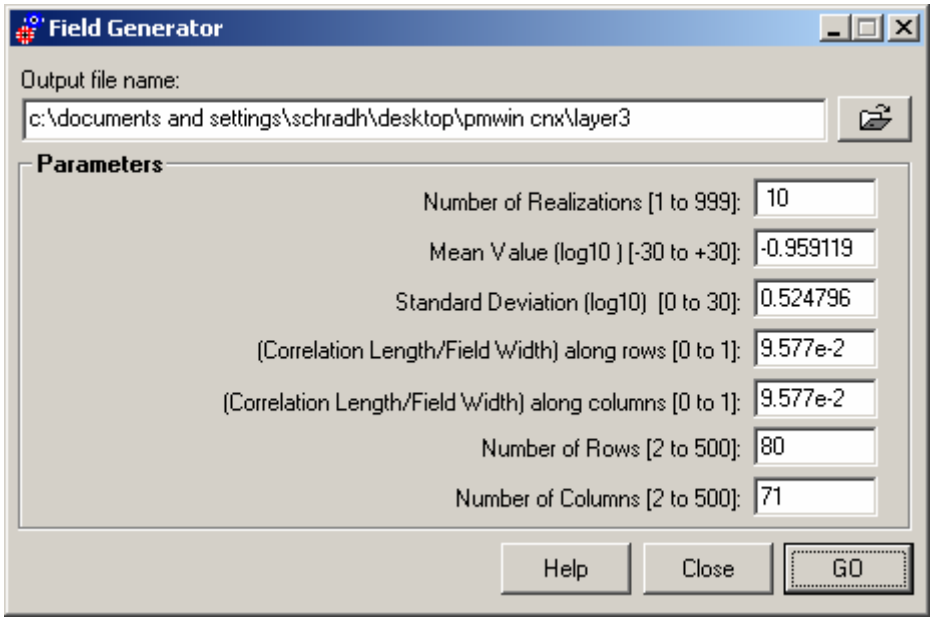

Figure 4-5 Parameters used for generating hydraulic conductivity field in layer 3.

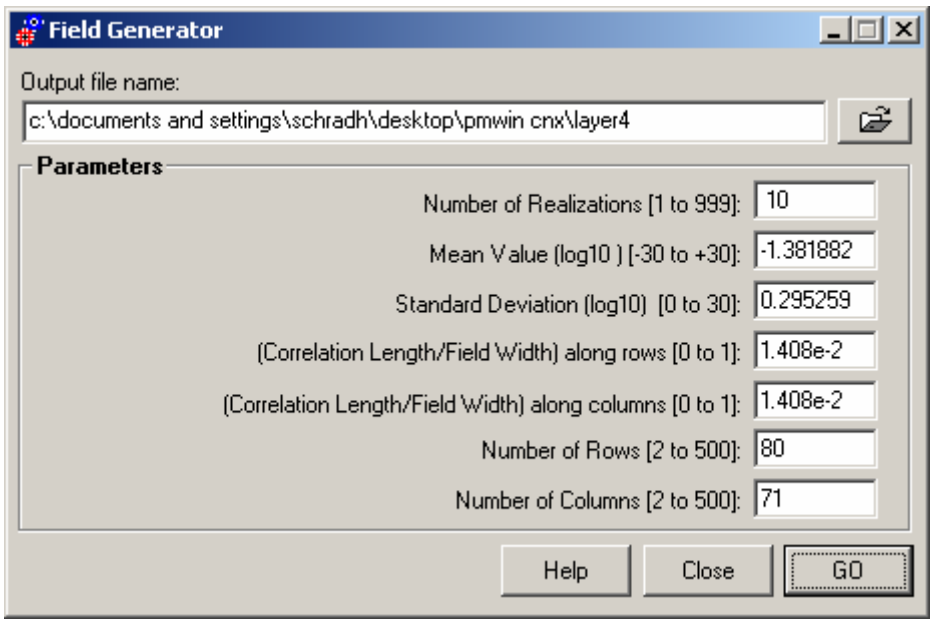

Figure 4-6 Parameters used for generating hydraulic conductivity field in layer 4.

Figures 4-7 to 4-16 represent the hydraulic conductivity field of all four layers in 10 realizations used in the stochastic simulations of groundwater flow in Chiang Mai basin (darker color means larger K value). The simulated water table for all realizations are illustrated in Figures 4-17 to 4-26. Appendix B lists the groundwater budget and calibration errors for all realizations.

Figure 4-7 Hydraulic conductivity field for all layers in realization #1.

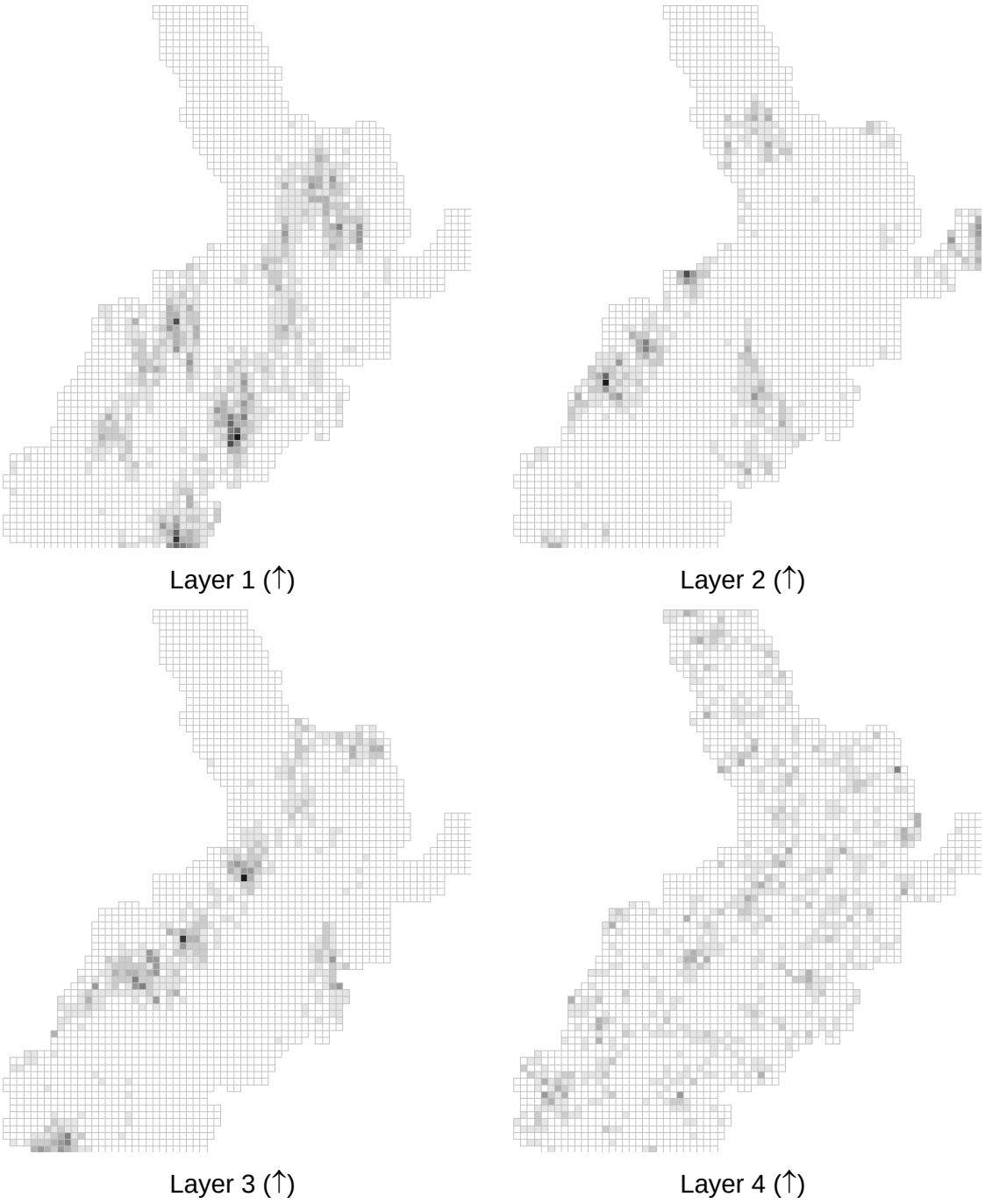

Figure 4-8 Hydraulic conductivity field for all layers in realization #2.

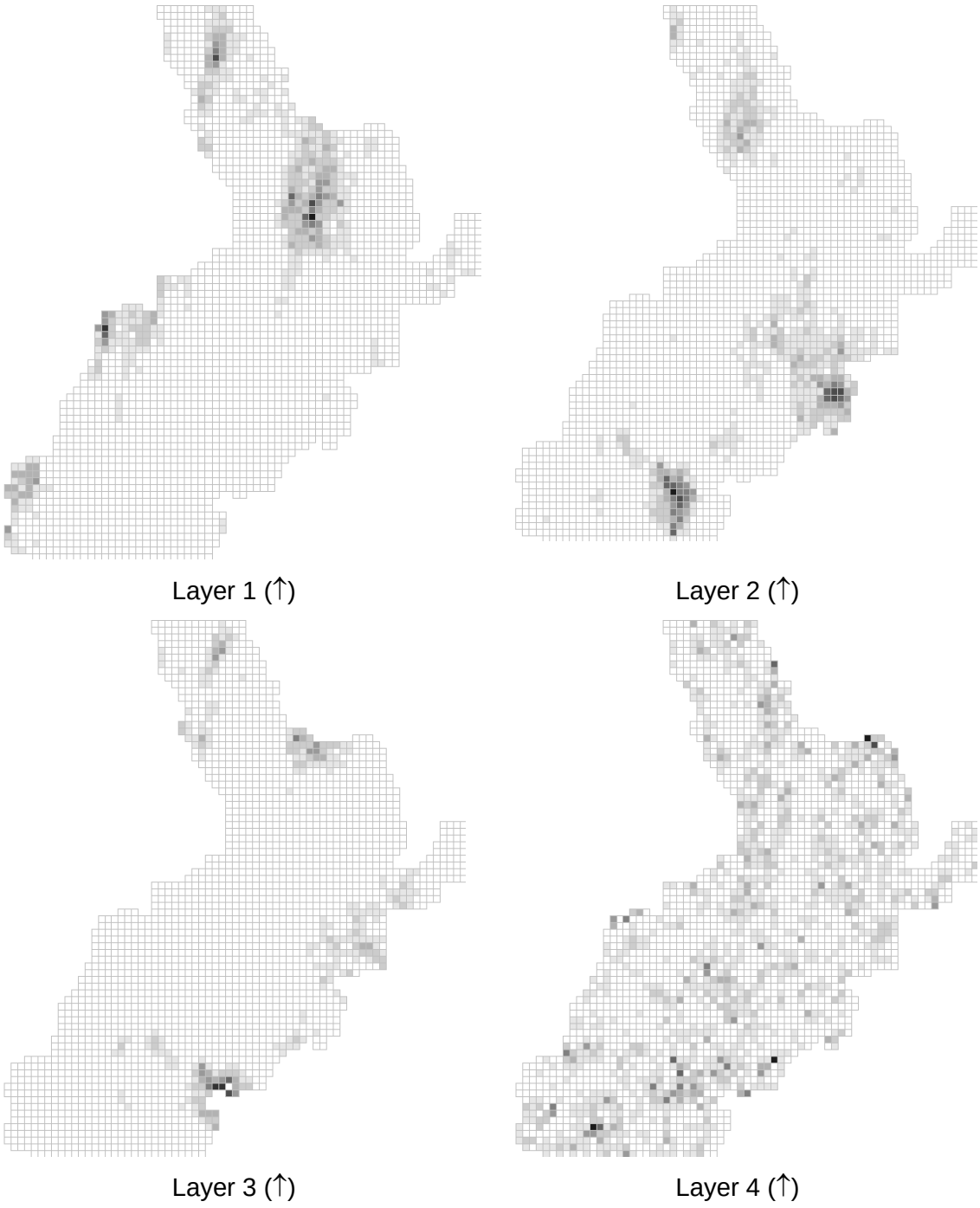

Figure 4-9 Hydraulic conductivity field for all layers in realization #3.

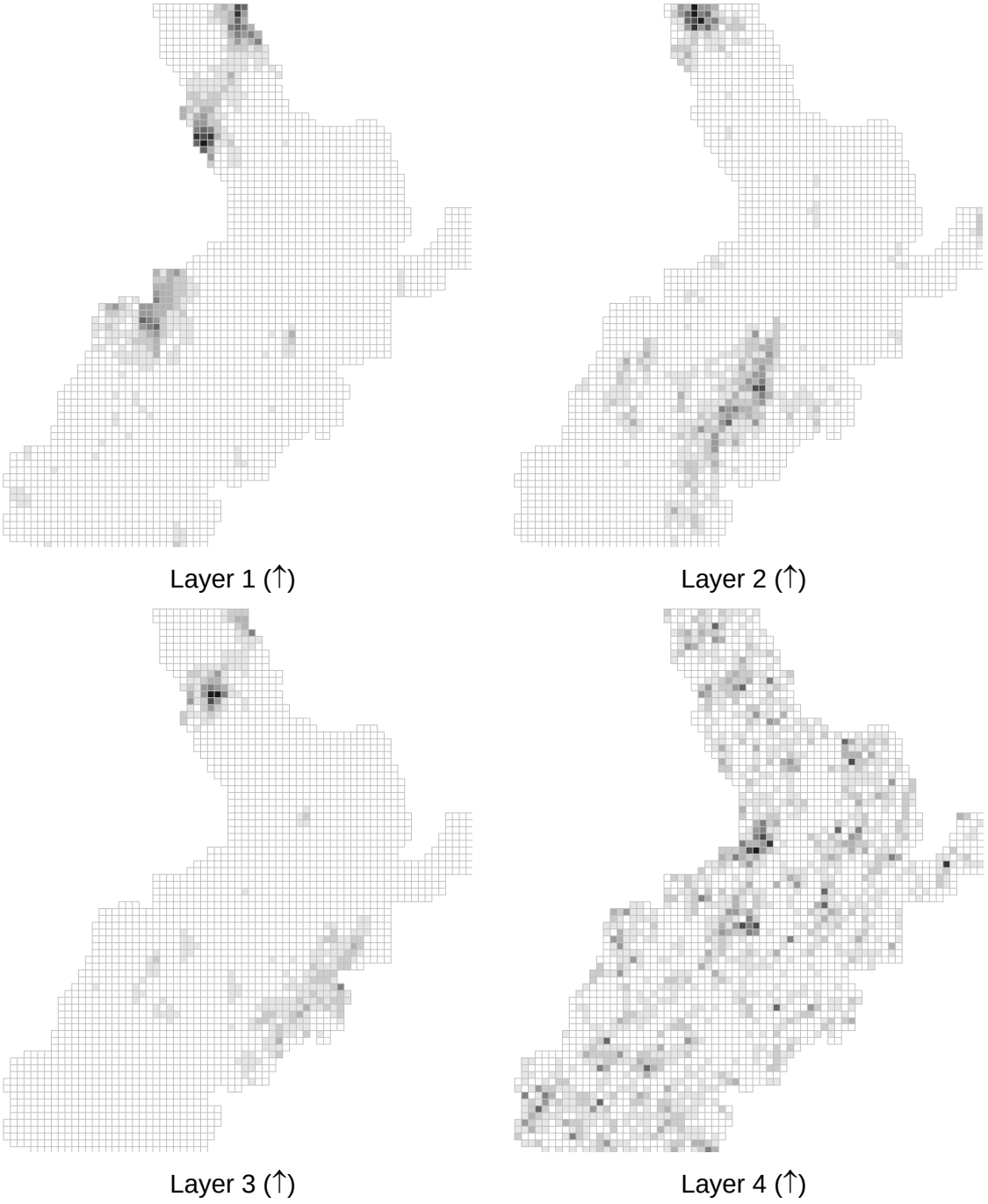

Figure 4-10 Hydraulic conductivity field for all layers in realization #4.

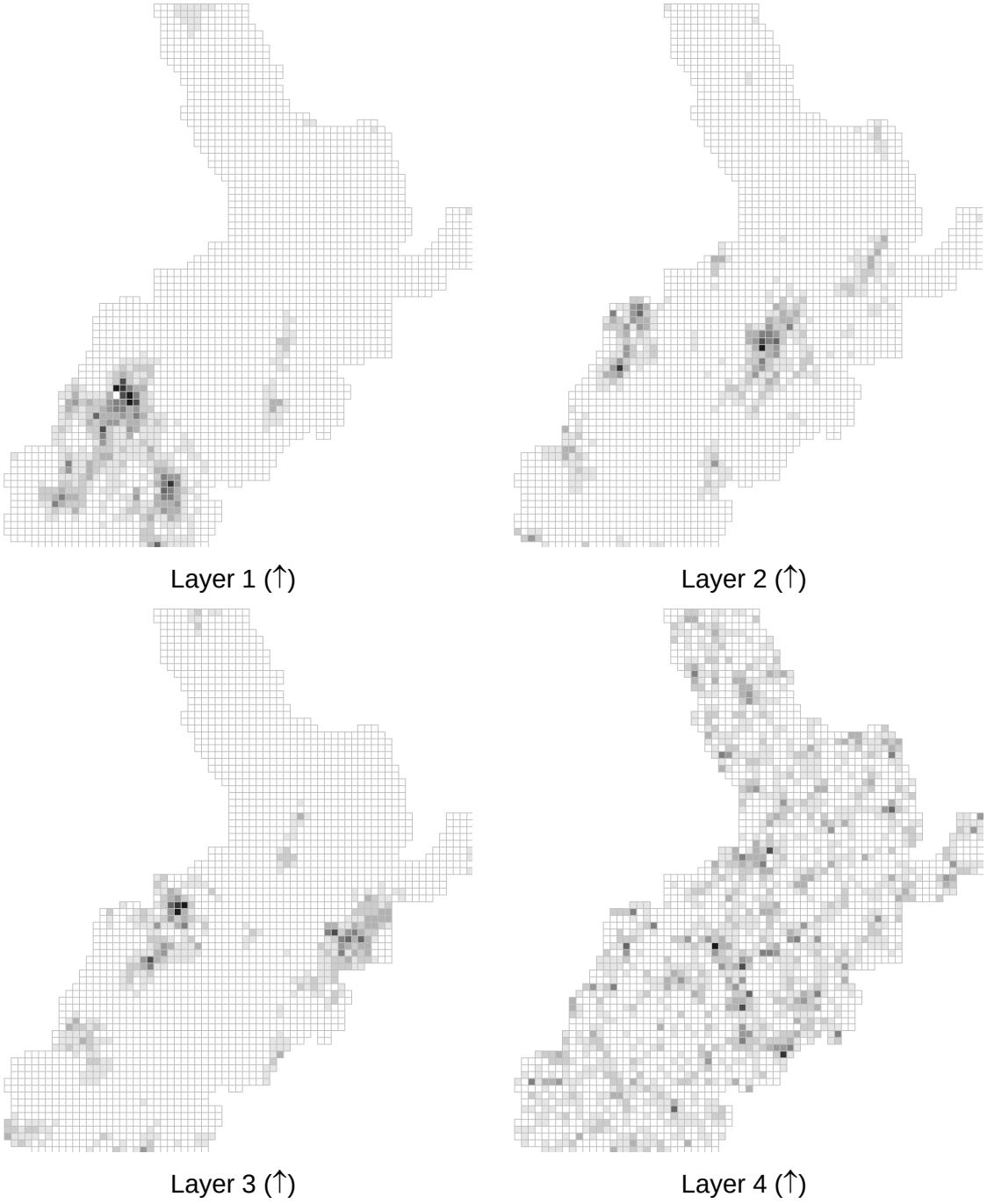

Figure 4-11 Hydraulic conductivity field for all layers in realization #5.

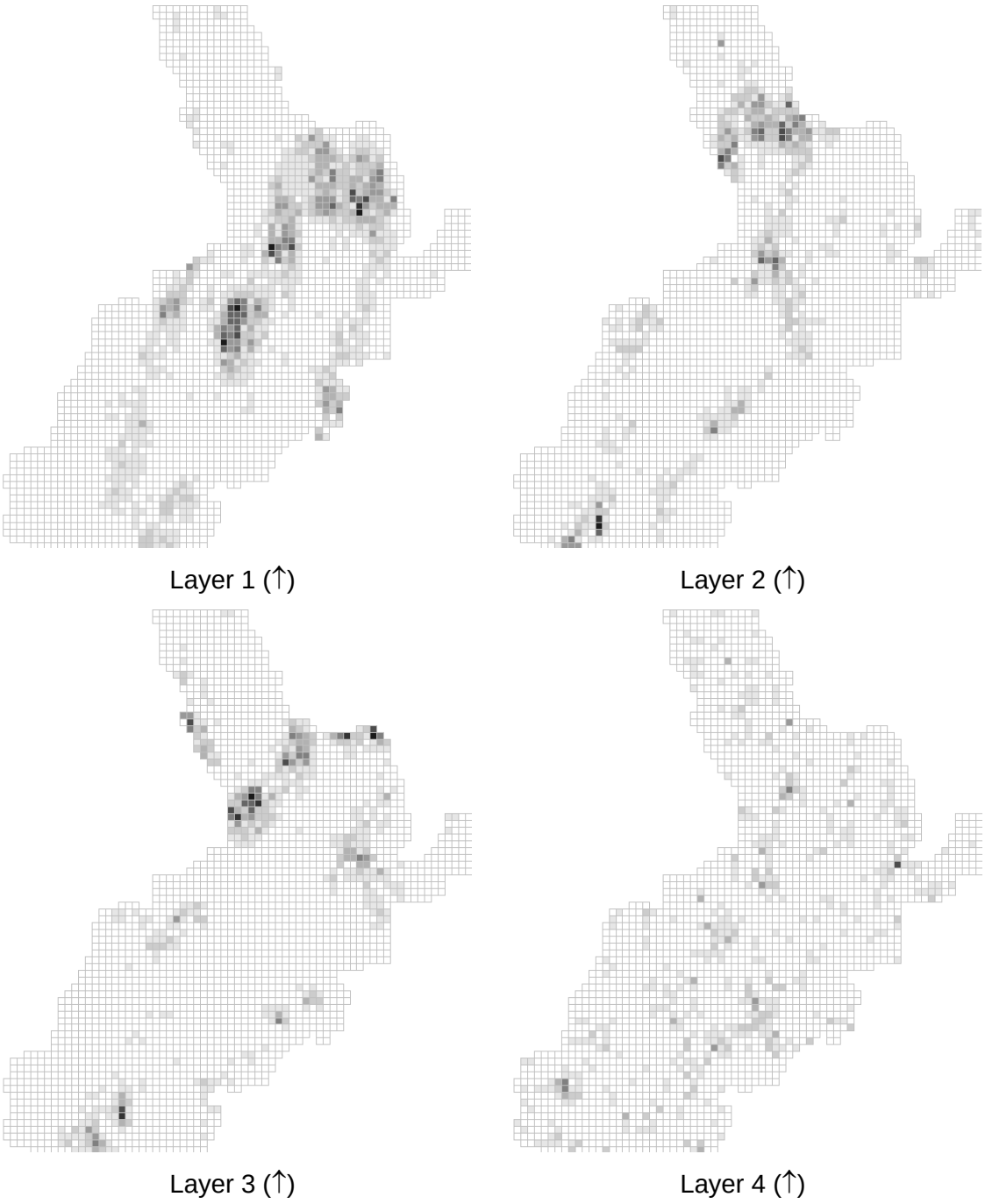

Figure 4-12 Hydraulic conductivity field for all layers in realization #6.

Figure 4-13 Hydraulic conductivity field for all layers in realization #7.

Figure 4-14 Hydraulic conductivity field for all layers in realization #8.

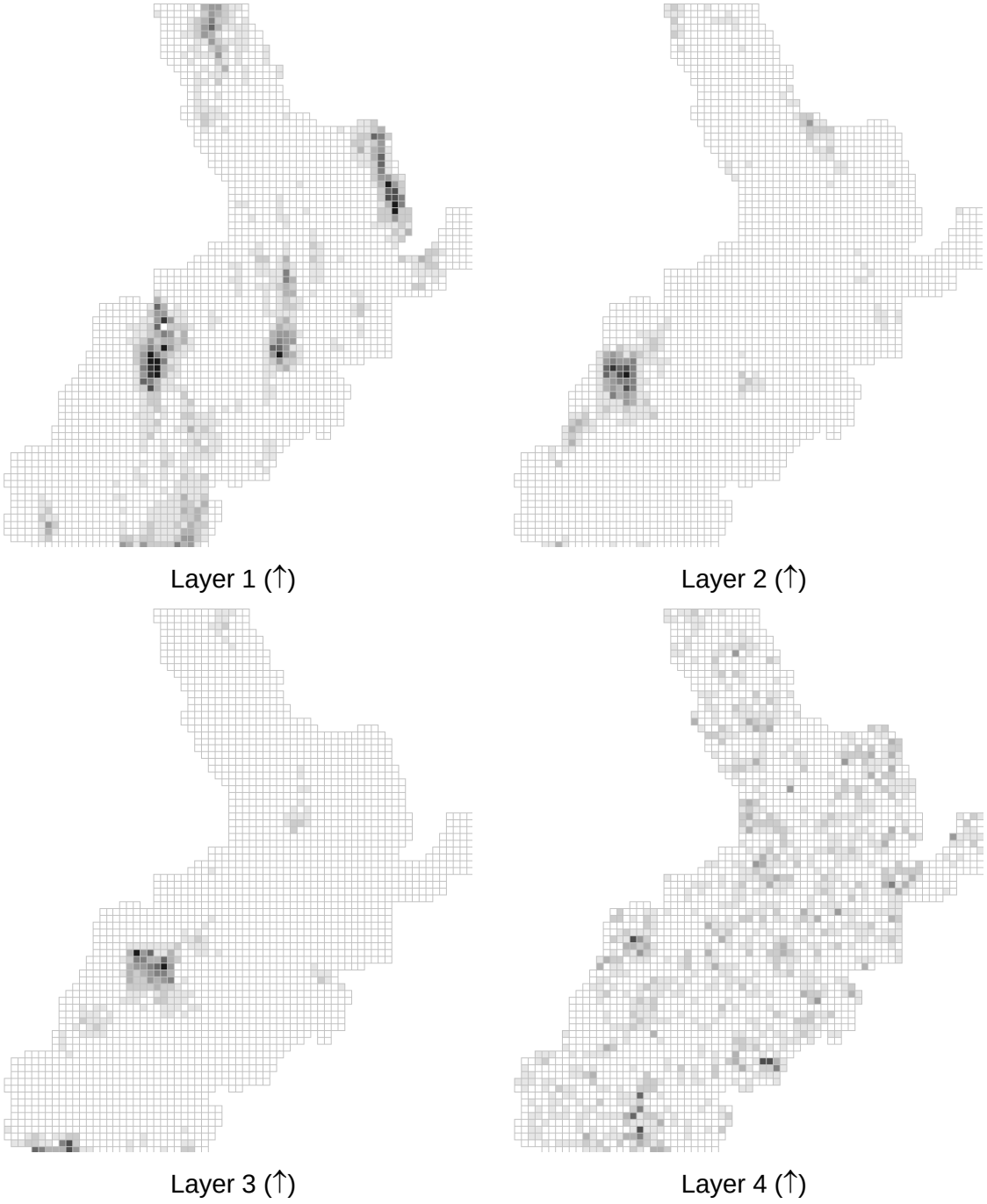

Figure 4-15 Hydraulic conductivity field for all layers in realization #9.

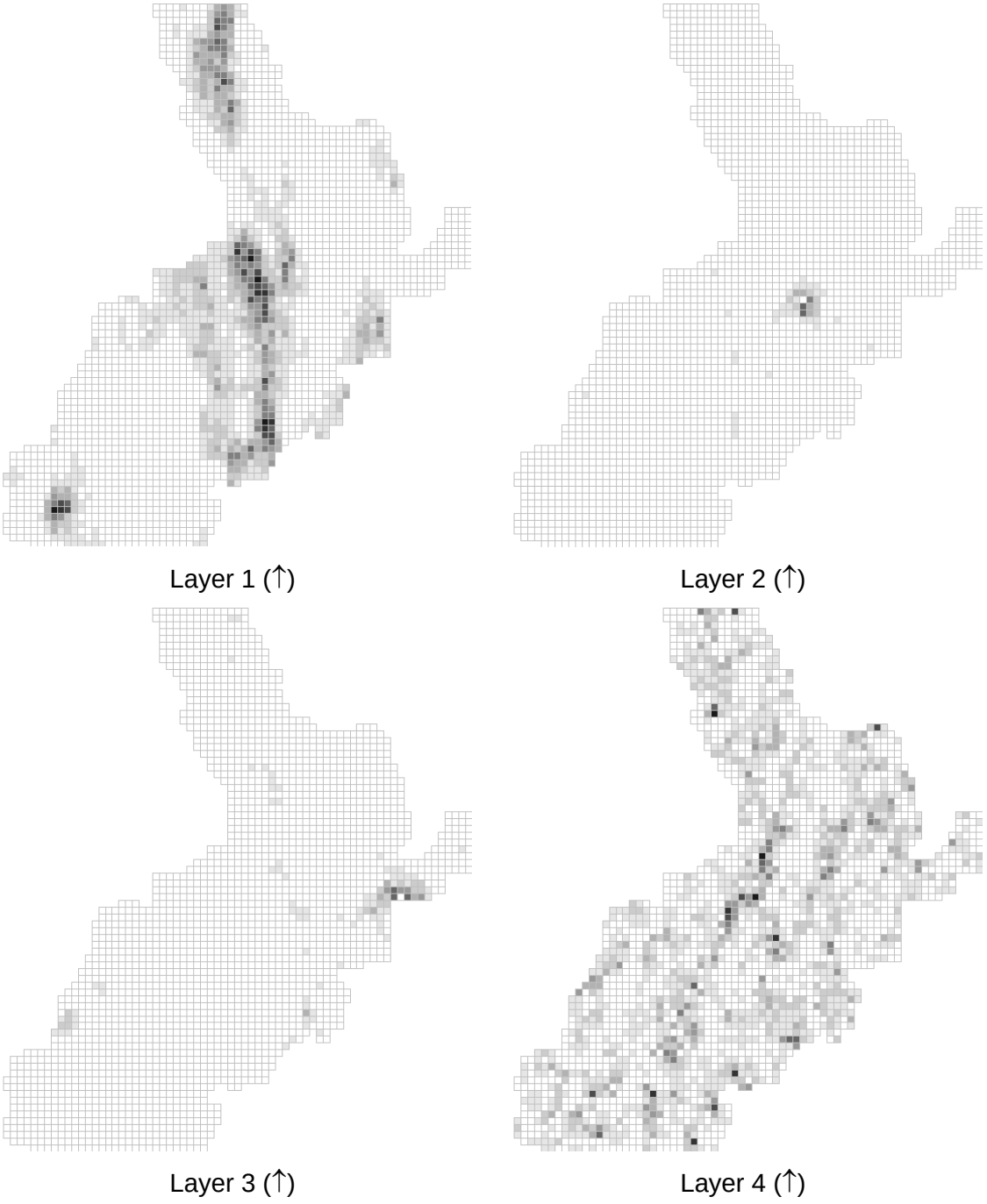

Figure 4-16 Hydraulic conductivity field for all layers in realization #10.

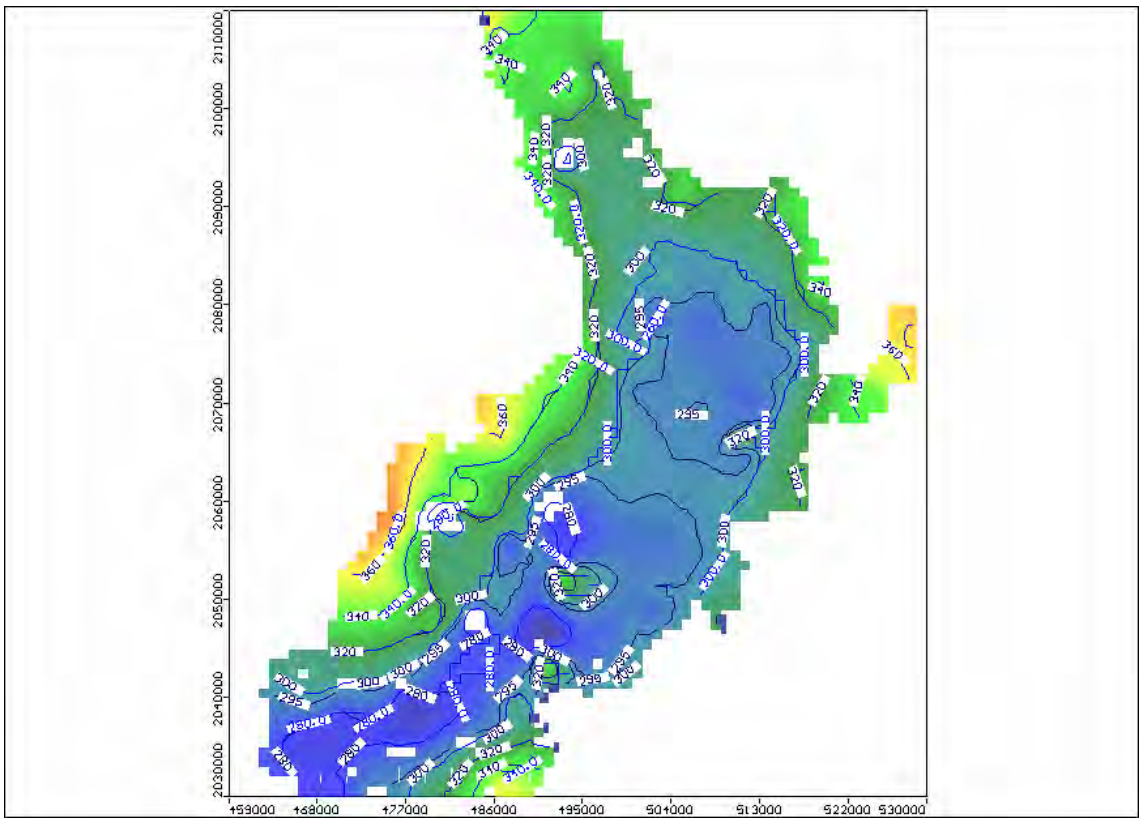

Figure 4-17 Water table elevation of realization #1

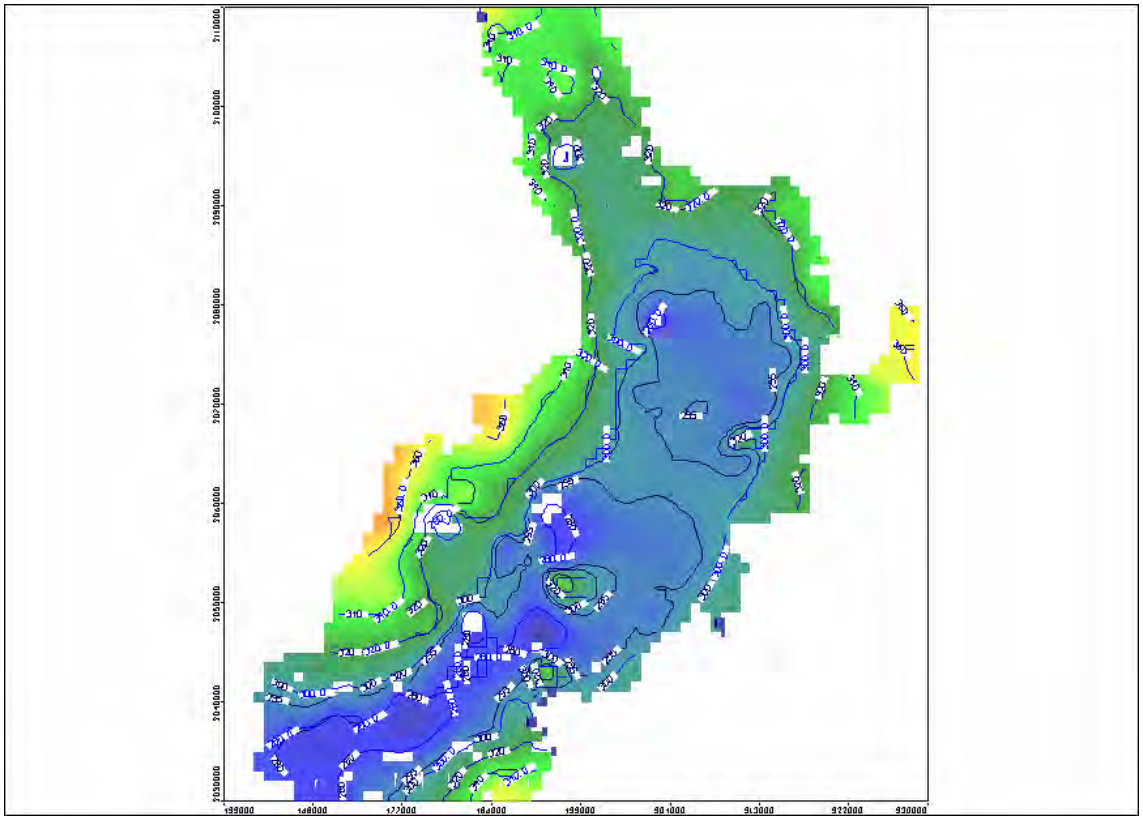

Figure 4-18 Water table elevation of realization #2

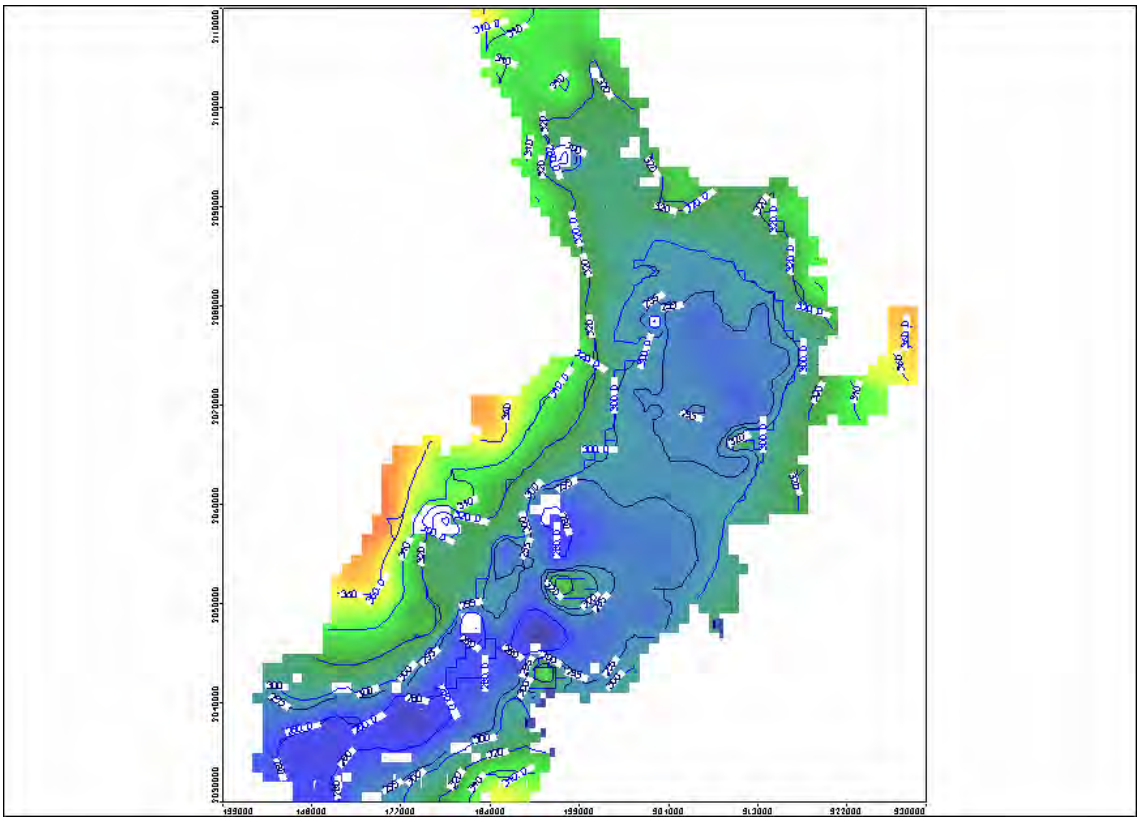

Figure 4-19 Water table elevation of realization #3

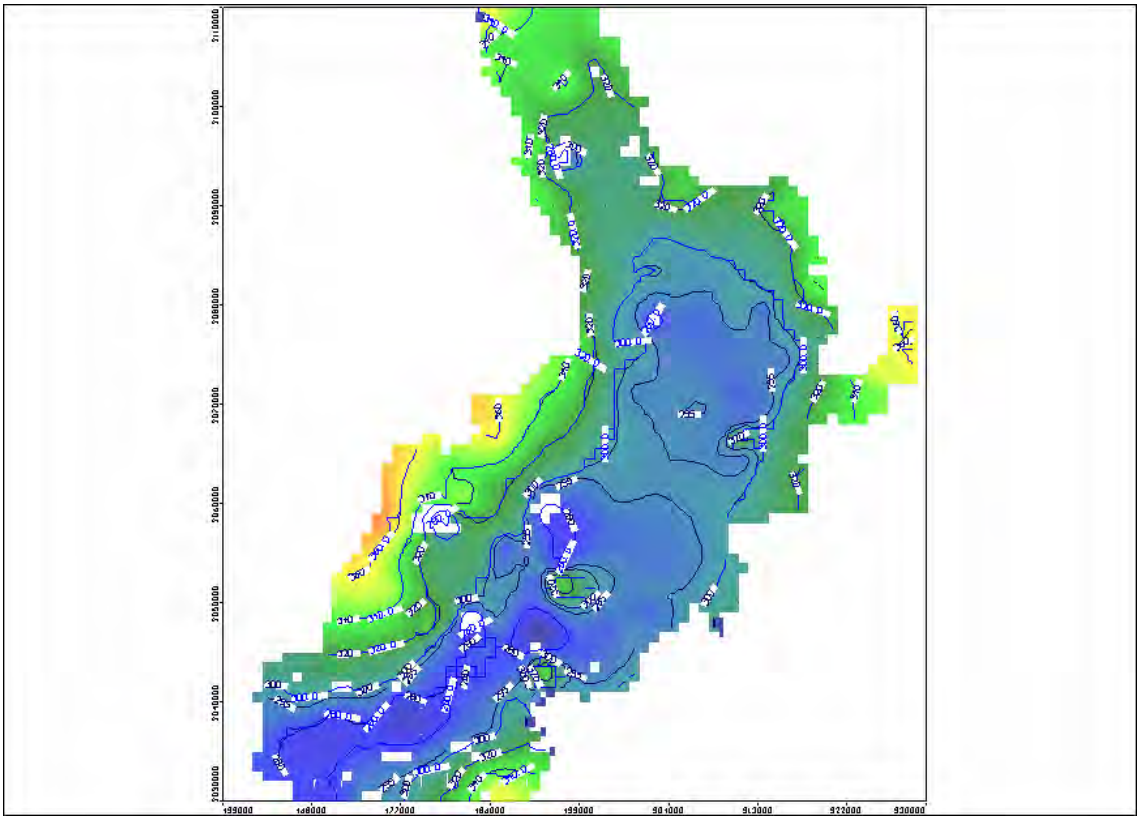

Figure 4-20 Water table elevation of realization #4

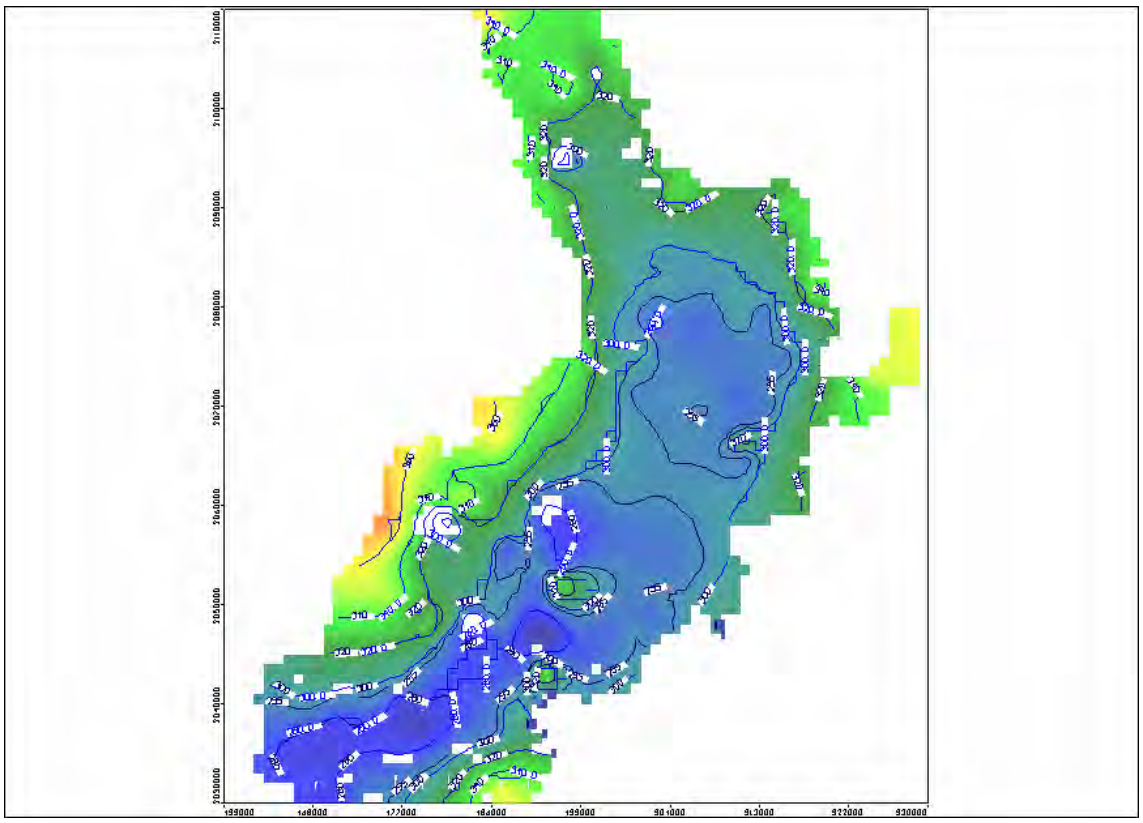

Figure 4-21 Water table elevation of realization #5

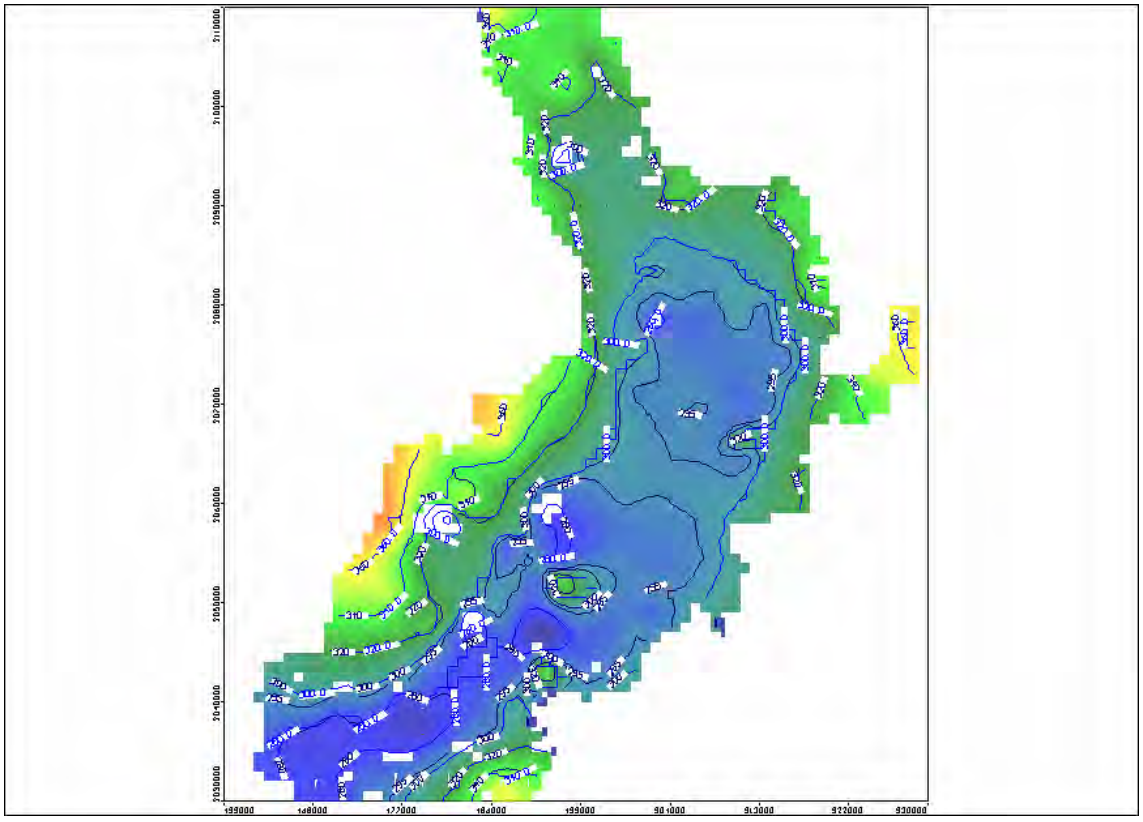

Figure 4-22 Water table elevation of realization #6

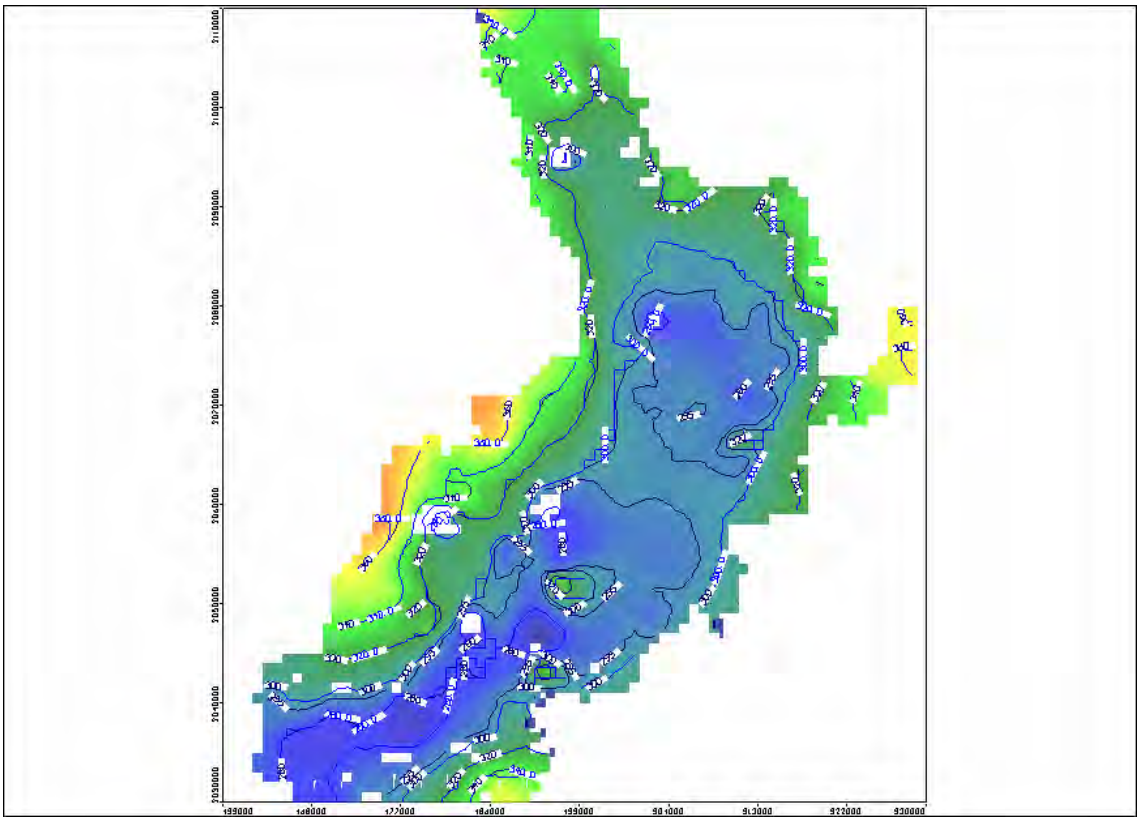

Figure 4-23 Water table elevation of realization #7

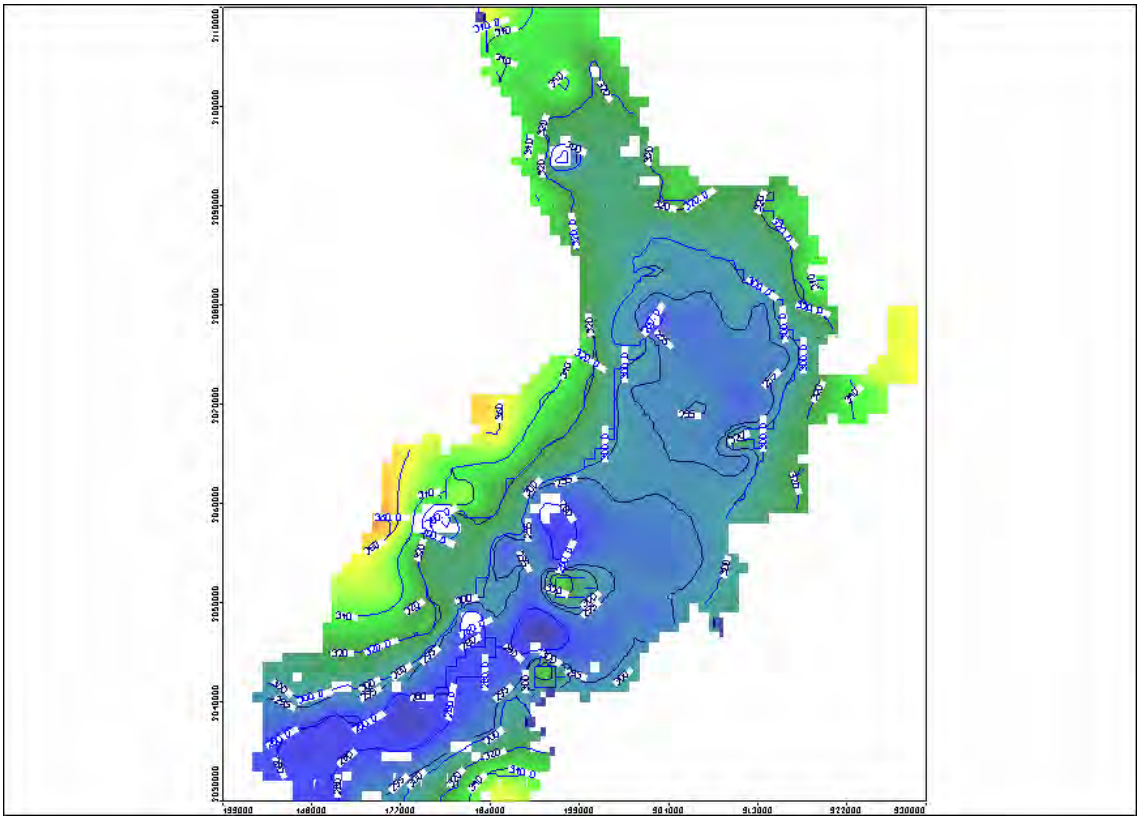

Figure 4-24 Water table elevation of realization #8

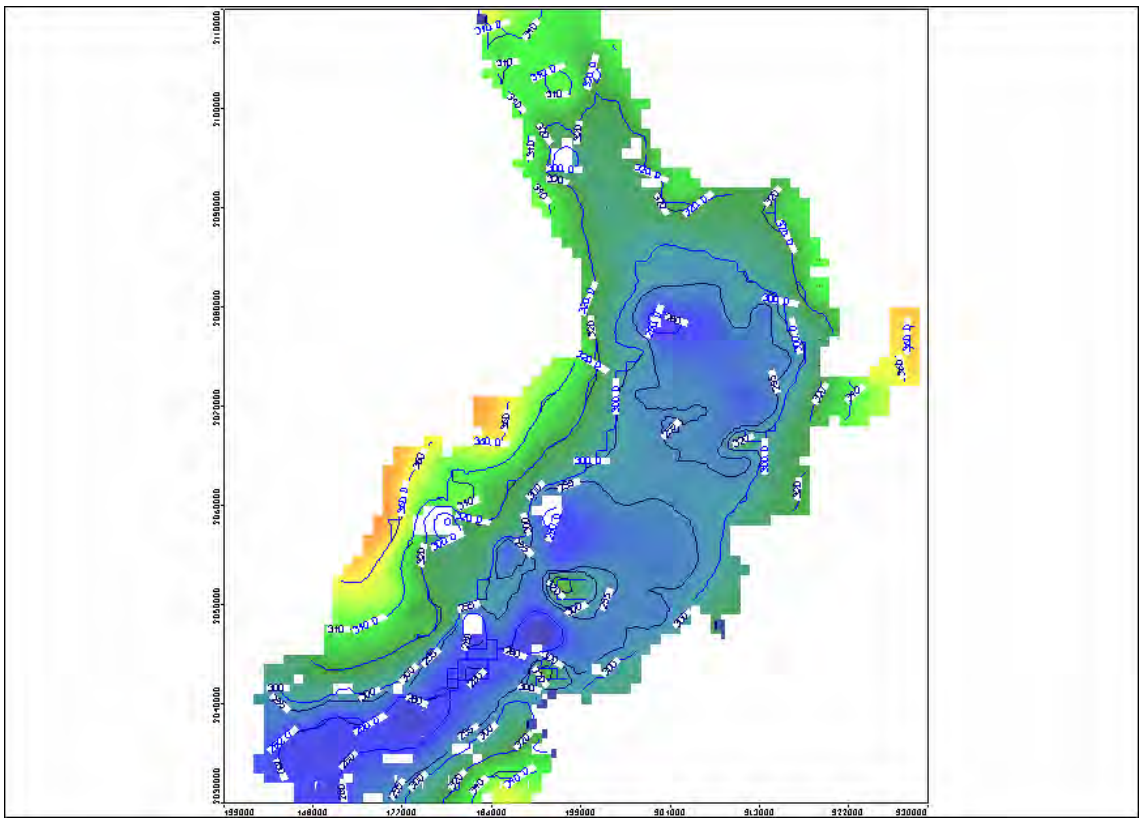

Figure 4-25 Water table elevation of realization #9

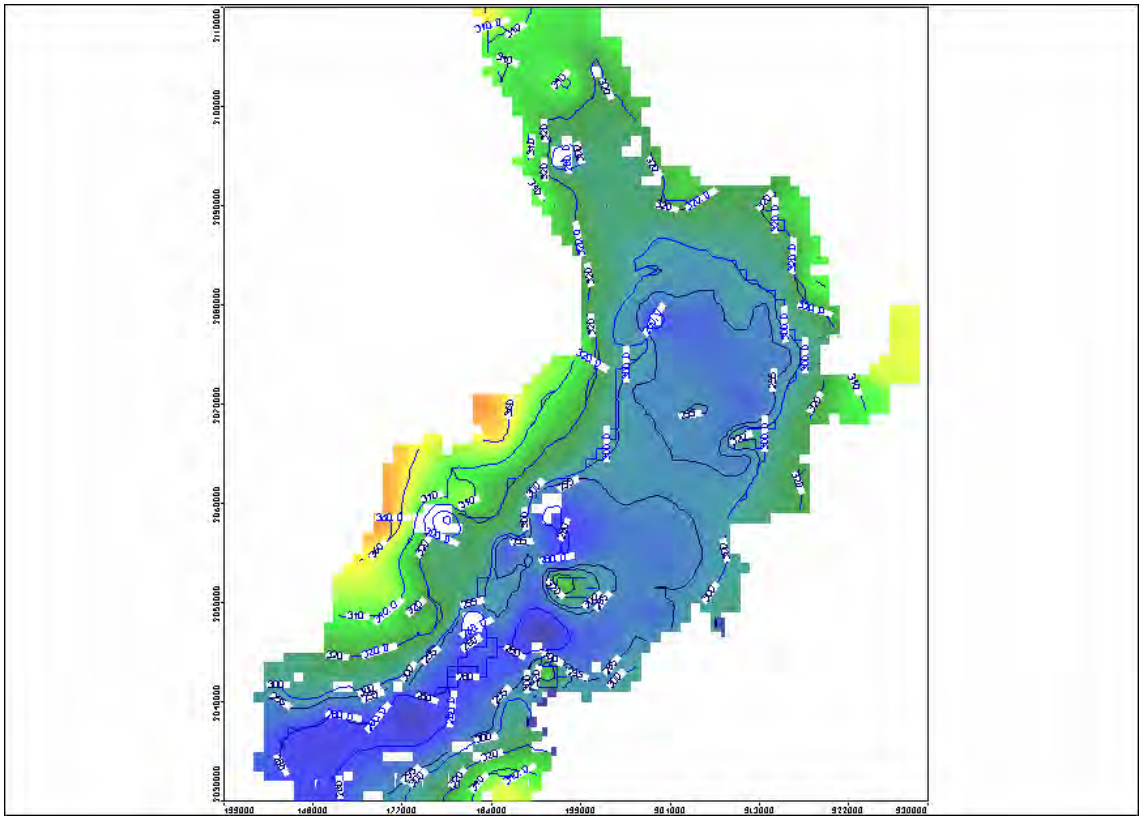

Figure 4-26 Water table elevation of realization #10

Chapter 5

Conclusions

Chapter 5: Conclusions

5.1. Summary

This research dealt with the application of stochastic methods and inverse modeling technique in setting up a comprehensive regional groundwater flow model of the Chiang Mai basin. Both deterministic and stochastic approaches were used to simulate groundwater flow regime in the semi- to unconsolidated aquifers. The flow model used in this study was a USGS finite-difference groundwater flow program called MODFLOW-2000 and the inverse modeling codes included PEST, UCODE, and PES (one of the package in MODFLOW-2000). Deterministic model simulation indicated that the annual water budget of the basin under steady-state condition was 241 Mm^3. The most sensitive parameters were hydraulic conductivity and recharge. Through stochastic simulation, the model uncertainty was evaluated. The uncertainty in water budget is $\pm$12.1 Mm^3 (95% confidence) and the average error in estimated heads was approximately $\pm$4 m.

5.2. Future Work & Recommendations

This work was based primarily on the comprehensive analyses of secondary data available through various sources. These data included lithologic and geophysical logs as well as previous model setup conducted by DGR (2003). The data was however limited and, consequently, discrepancies existed between field-measured and model-calculated hydraulic heads. Based on the findings of this research, it is recommended that characterization of aquifer's hydraulic properties is critical. If possible, comprehensive aquifer tests must be conducted to obtain more data so that model is more reliable and uncertainties in prediction can decrease.

References

References

Ahlfeld, D.P., and Heidari, Manoutchehr, 1994, Application of optimal hydraulic control to ground-water systems: Journal of Water Resources Planning and Management, v. 120, no. 3, p. 350–365.

Anderson, M.P. and W.W. Woessner. 1992. Applied groundwater modeling – Simulation of flow and advective transport. Sandiego: Academic Press, Inc.

Barlow, P.M and Moench, A.F. 1999. WTAQ – A Computer Program for Calculating Drawdowns and Estimating Hydraulic Properties for Confined and Water-Table Aquifers. U.S. Geological Survey.

Boulton, N.S. 1963, Analysis of data from non-equilibrium pumping tests allowing for delayed yield from storage: Proceedings of Institute of Civil Engineers, v. 26, p. 469–482.

Boulton, N.S., 1954, Unsteady radial flow to a pumped well allowing for delayed yield from storage: International Association of Scientific Hydrology, Rome, Publication 37, p. 472–477.

Buapeng, S., Sanghabun, S. & Lauphensri, O. (1995): Environmental Isotope Study Of Groundwater In Chiang Mai Basin, Northern Thailand. Dept. Min. Res., Ann. Techn. Meeting, Jan. 11-13, 1995; Bangkok.

Bunopas, S. & Vella, P. (1983): Opening Of The Gulf Of Thailand - Rifting Of Continental Se-Asia And Late Cenozoic Tectonics. J. Geol. Soc. Thailand, 6, 1: 1 12; Bangkok.

Bunopas, S. & Vella, P. (1992): Geotectonics And Geologic Evolution Of Thailand. Proc. Geological Resources Of Thailand: Potential For Future Development: 209 228; Bangkok.

Chaimanee, N. (1997): Some Characteristics Of Quaternary Sediments In The Chiang Mai Basin. Thai-German Technical Cooperation Project 'Environmental Geology For Regional Planning', Technical Report No. 19: 6 P.; Bangkok And Hannover.

Chuamthisong, C. (1971): Geology And Groundwater Of Chiang Mai Basin, Thailand. Master Of Science Thesis, Univ. Of Alabama; USA.

Dagan, G. 1986. Statistical theory of groundwater flow and transport: Pore to laboratory, laboratory to formation, and formation to regional scale. Water Resources Research, 22(9): 120S-134S.

Delhomme, P., 1979, Spatial variability and uncertainty in groundwater flow parameters: a geostatistical approach, WRR, vol. 15, no. 2.

Deutsch, C. and A. Journel, 1993. GSLIB Geostatistical Software Library and User's Guide, Oxford University Press, New York, 340 p.

DMR. 2000. Groundwater Map Manual Book, Chang Wat Chiang Mai & Lamphun, Division of Groundwater Resources. 2000.

DGR, 2003. Groundwater Resources Assessment Project (Chiang Mai, Upper Chao Phraya, and Mae Klong Basins). Final Report. Departmentof Groundwater Resources (Thai).

Doherty, J., 1994, PEST: Corinda, Australia, Watermark Computing, 122 p.

Dougherty, D.E., and Babu, D.K., 1984, Flow to a partially penetrating well in a double-porosity reservoir: Water Resources Research, v. 20, no. 8, p. 1116–1122.

Freeze, R., Massmann, J., Smith, L., Sperling, T., and B. James, 1990. "Hydrogeological Decision Analysis: 1. A Framework", Ground Water, v. 28, no. 5.

Gelhar, L.W. 1986. Stochastic subsurface hydrology from theory to applications. Water Resources Research, 22(9), 135S.

Greenwald, R.M., 1998, Documentation and user’s guide—MODMAN, an optimization module for MODFLOW, version 4.0: Freehold, NJ, HSI GeoTrans, 112 p.

Harbaugh, A.W., and McDonald, M.G., 1996a, User's documentation for MODFLOW-96, an update to the U.S. Geological Survey modular finite-difference ground-water flow model: U.S. Geological Survey Open-File Report 96-485, 56 p.

Harbaugh, A.W., and McDonald, M.G., 1996b, Programmer's documentation for MODFLOW-96, an update to the U.S. Geological Survey modular

finitedifference ground-water flow model: U.S. Geological Survey Open-File Report 96-486, 220 p.

Hill, M.C., 1992, A computer program (MODFLOWP) for estimating parameters of a transient, three-dimensional, ground-water flow model using nonlinear regression: U.S. Geological Survey Open-File Report 91-484, 358 p.

Hill, M.C., 1998, Methods and guidelines for effective model calibration: U.S. Geological Survey, Water-Resources Investigations Report 98-4005.

Hill, M.C., Banta, E.R., Harbaugh, A.W., and Anderman, E.R., 2000, MODFLOW-2000, the U.S. Geological Survey Modular Ground-Water Model—User guide to the observation, sensitivity, and parameter-estimation processes and three post-processing programs: U.S. Geological Survey Open-File Report 00-184, 210 p.

Konikow, L.F., Goode, D.J., and Hornberger, G.Z., 1996, A three-dimensional method-of-characteristics solute-transport model (MOC3D): U.S. Geological Survey Water-Resources Investigations Report 96-4267, 87 p.

Lefkoff, L.J., and Gorelick, S.M., 1987, AQMAN-Linear and quadratic programming matrix generator using two-dimensional ground-water flow simulation for aquifer management modeling: U.S. Geological Survey Water-Resources Investigations Report 87-4061, 164 p.

Margane, A. and Tatong, T. 1999. Aspects of the Hydrogeology of the Chiang Mai-Lamphun Basin, Thailand that are Important for the Groundwater Management. Z. angew. Geol., 45(4), 188-197.

McDonald, M.G., and Harbaugh, A.W., 1984, A modular three-dimensional finite-difference ground-water flow model: U.S. Geological Survey Open-File Report 83-875, 528 p.

McDonald, M.G., and Harbaugh, A.W., 1988, A modular three-dimensional finite-difference ground-water flow model: U.S. Geological Survey Techniques of Water-Resources Investigations, book 6, chap. A1, 586 p.

Moench, A.F. 1997, Flow to a well of finite diameter in a homogeneous, anisotropic water table aquifer: Water Resources Research, v. 33, no. 6, p. 1397–1407.

Neuman, S.P., 1972, Theory of flow in unconfined aquifers considering delayed response of the water table: Water Resources Research, v. 8, no. 4, p. 1031–1044.

Neuman, S.P., 1974, Effects of partial penetration on flow in unconfined aquifers considering delayed aquifer response: Water Resources Research, v. 10, no. 2, p. 303–312.

Peralta, R.C., 2004, Simulation/Optimization MOdeling System (SOMOS): Logan, UT, Utah State University Department of Biological and Irrigation Engineering, accessed July 28, 2004.

Poeter, E. P., and Hill, M.C., 1997, Inverse models: A necessary next step in groundwater modeling: Ground Water, v. 35(2), p. 250-260.

Poeter, E.P., and Hill, M.C., 1998, Documentation of UCODE, a computer code for universal inverse modeling: U.S. Geological Survey Water-Resources Investigations Report 98-4080, 116 p.

Polachan, S. & Saatayarak, N. (1989): Strike-Slip Tectonics And The Development Of The Tertiary Basins In Thailand. Int. Symp. Intermontane Basins, Geology And Resources: 243 253; Chiang Mai.

Theis, C.V., 1935, The relation between the lowering of the piezometric surface and the rate and duration of discharge of a well using ground-water storage: EOS, Transactions of the American Geophysical Union, v. 16, p. 519–524.

Uppasit, S. 2004. Groundwater Recharge Calculation of Chiang Mai Basin Using Water-Table Fluctuation Method. M.S. Thesis, Faculty of Science, Chiang Mai University.

Wattananikorn, K., Beshir, J.A. & Nochaiwong, A. (1995): Gravity Interpretation Of Chiang Mai Basin, Northern Thailand: Concentrating On The Ban Siep Area. Journal Of Se Asian Earth Sciences, 12: 53 64.

Wongsawat, S. 1999. Groundwater Resources of Thailand and Development, Symposium on Mineral, Energy, and Water Resources of Thailand: Towards the Year 200, 6-16, Bangkok.

Zheng, C., and Wang, P.P., 2002, MGO—A Modular Groundwater Optimizer incorporating MODFLOW and MT3DMS, Documentation and user's guide: Tuscaloosa, AL, The University of Alabama and Groundwater Systems Research Ltd., 118 p.

Zimmerman, D., Hanson, and P. Davis, 1991. Parameter Estimation Techniques and Uncertainty in Ground Water Flow Model Prediction, Sandia National Laboratories, DOE Publication DE91 000405

Appendix A

Publications

Publications

1. S. Saenton and T.H. Illangasekare. 2007. Stochastic methods for groundwater flow and contaminant transport models. *Groundwater Proceedings*. Department of Groundwater Resources. 16-27 September 2007, 111-122p.

2. S. Saenton and A. Boonton. 2007. Groundwater Model of the Wieng Haeng Basinl, Chiang Mai Province. *Groundwater Proceedings*. Department of Groundwater Resources. 16-27 September 2007, 123-131p.

3. M. Khebchareon and S. Saenton. 2007. Finite-Element Galerkin Model for Simulating Fate and Transport of Dissolved Organic Compound in Groundwater. In, *Proceedings of the 33rd Congress on Science and Technology of Thailand*. Walailak University, Nakorn Si Thammarat, Thailand. 18-21 October 2007.

Manuscripts

1. S. Saenton. 2010. Stochastic Approach for Assessment of Groundwater Potential of the Chiang Mai Basin. In preparation.

การจำลองการไหลของน้ำใต้ดินและการเคลื่อนที่ของมวลสารด้วยวิธีสโทแคสติก

Stochastic Methods for Groundwater Flow and Contaminant Transport Models

ดร. ศตวรรษ แสนทน[1]

Dr. Tissa H. Illangasekare[2]

บทคัดย่อ

ในปัจจุบัน เทคโนโลยีการจัดทำแบบจำลองการไหลของน้ำใต้ดิน แบบจำลองการเคลื่อนที่ของมวลสารในชั้นหินอุ้มน้ำ และแบบจำลองการปนเปื้อนของสารอินทรีย์ไอระเหยในดินและน้ำใต้ดิน ได้ถูกการพัฒนาขึ้นอย่างต่อเนื่องจนมีความก้าวหน้าอย่างรวดเร็ว โดยได้มีการนำแบบจำลองคณิตศาสตร์ไปประยุกต์ใช้เพื่อทำนายปรากฏการณ์ที่เกิดกับชั้นหินอุ้มน้ำทั้งในแง่ปริมาณและคุณภาพ เพื่อประโยชน์ในการบริหารและการจัดการทรัพยากรน้ำใต้ดินกันอย่างแพร่หลาย อย่างไรก็ดี การจัดทำแบบจำลองที่เกี่ยวข้องกับน้ำใต้ดินในปัจจุบัน ส่วนใหญ่ยังคงยึดหลักแนวทางดีเทอร์มินิสติก (deterministic approach) กล่าวคือ ผู้จัดทำแบบจำลองจะใช้ค่าคุณสมบัติทางชลศาสตร์ เช่น ค่าสัมประสิทธิ์ความซึมและค่าสัมประสิทธิ์การกักเก็บ ซึ่งได้จากวิเคราะห์ผลการสูบทดสอบในภาคสนามเพียงไม่กี่ตำแหน่งในพื้นที่ศึกษามาใช้ในแบบจำลอง แล้วนำผลลัพธ์ที่ได้จากแบบจำลองไปแปลผล ซึ่งส่วนใหญ่จะพบว่า ผลที่คำนวณได้ มักมีความคลาดเคลื่อนจากความเป็นจริง ทั้งนี้ เนื่องมาจากชั้นหินอุ้มน้ำมีความซับซ้อนและความไม่เป็นเนื้อเดียวกัน (heterogeneity) สูง และคุณสมบัติทางชลศาสตร์ของชั้นหินอุ้มน้ำหนึ่งๆ มีได้หลายค่า (เป็นช่วง) การใช้ค่าคุณสมบัติทางชลศาสตร์ที่ได้จากการวัดในภาคสนามเพียงไม่กี่ค่ามาใช้ในแบบจำลอง ทำให้ไม่สามารถจำลองสภาพที่แท้จริงของชั้นหินอุ้มน้ำได้ เนื่องจากของการวางตัวของชั้นน้ำยังไม่เป็นที่ทราบแน่ชัดและค่าคุณสมบัติทางชลศาสตร์ที่ใช้ในการคำนวณก็ยังมีความไม่แน่นอน บทความทางวิชาการนี้ ได้เสนอแนวทางการจัดทำแบบจำลองอีกวิธีหนึ่ง เรียกว่าวิธีสโทแคสติก (stochastic method) ซึ่งวิธีดังกล่าวสามารถใช้จำลองการไหลในชั้นหินอุ้มน้ำที่มีการวางตัวของชั้นน้ำที่ซับซ้อน โดยบทความนี้ ได้สรุปผลงานที่ได้นำเทคนิคดังกล่าว มาใช้จัดทำแบบจำลองเพื่อทำนายปรากฏการณ์ที่เกิดขึ้นกับชั้นหินอุ้มน้ำซึ่งได้จำลองขึ้นในห้องปฏิบัติการขนาดใหญ่ โดยพบว่าได้ผลการจำลองเป็นที่น่าพอใจ ผู้ศึกษาจึงได้เสนอให้มีการนำเทคนิคดังกล่าวไปใช้ควบคู่กับการจัดทำแบบจำลองน้ำใต้ดิน หรือแบบจำลองการเคลื่อนที่ของมวลสาร ในระดับมหภาคต่อไป

Abstract

Deterministic prediction of fluid flow and contaminant migration using numerical models in naturally heterogeneous subsurface media is generally infeasible due to many factors. Primary among these is it is cost prohibitive to fully characterize the relevant properties governing flow and transport at appropriate scales to use as model inputs. Model input parameters such as hydraulic conductivity, porosity and dispersivity cannot be fully defined using limited spatially distributed measurements or observations. Use of interpolated values as inputs results in

[1] ภาควิชาธรณีวิทยา คณะวิทยาศาสตร์ มหาวิทยาลัยเชียงใหม่ อ.เมือง จ.เชียงใหม่ 50200

[2] Division of Environmental Science and Engineering, Colorado School of Mines, Colorado, U.S.A.

significant uncertainty in model predictions. This uncertainty inherent in these predictions has to be taken into consideration in evaluating potential future risks to ecological and human health due to groundwater contamination. Introduction of stochastic methods to subsurface hydrology has helped regulators, subsurface hydrologists and engineers to identify such uncertainty in predictions that has implications in the use of models as management and decision tools. Stochastic approaches assign probability distributions to model input parameters and provide a means to deal with these parameter and prediction uncertainties. Successful application of stochastic methods to groundwater-related field problems has been reported. This paper discusses how stochastic theory is used in hydrogeologic studies primarily in the context of contaminant transport and migration of immiscible liquids (e.g. chlorinated solvents and petroleum waste) in the subsurface. Stochastic theory and geostatistical methods as applied to heterogeneous porous media are briefly discussed, and recent intermediate-scale laboratory studies and numerical modeling investigations are presented. The methods and tools developed in this research are currently being evaluated and validated for field applications at government owned and industrial waste sites.

1. INTRODUCTION

Groundwater constitutes an important component of domestic, industrial and agricultural water supply throughout the world. Increasing demand placed on limited supplies has made it imperative to protect scarce groundwater resources from pollution from industrial waste and agricultural chemicals. Numerical models with the capability to predict the fate and transport of these chemicals are useful as tools for management and remediation design. The accuracy of model predictions depends on the accuracy of the input parameters that characterize the flow and transport processes. Basic input parameters such as hydraulic conductivity and porosity vary in space. It is generally infeasible and cost-prohibitive to conduct detailed site characterization to obtain exact information to define this spatial variability. Hence, the distributed values of these parameters have to be inferred from observations or measurements made at discrete set of sampling points or observations that in general are sparsely distributed over the aquifer. The uncertainty associated with these undefined input parameters results in model prediction errors. Hence, it is necessary to incorporate parameter uncertainty into models to increase confidence in predictions. Stochastic approaches that assign probability distributions to these parameters provide a means to deal with these parameter and prediction uncertainties. These approaches proposed in the early eighties (Gelhar and Axness, 1983; Neuman et al., 1987) have increasingly been accepted in subsurface studies. Stochastic-based modeling provides

a *possible range* of solutions (e.g. contaminant concentrations and hydraulic heads) to groundwater-related problems accounting for uncertainty associated with flow and transport parameters.

Successful application of stochastic methods in field-scale modeling of flows and transport, and risk analysis has been reported in literature. This paper focuses on the application of stochastic methods, specifically based on geostatistical techniques in intermediate-scale laboratory studies involving fluid flow, multiphase flow in heterogeneous porous media. Controlled experiments in a laboratory allows for the study of the method more rigorously as the heterogeneity field can be defined accurately. First, the theoretical background used in developing numerical models for flow and transport in porous media is presented. This will be followed by example problems through which the application of stochastic methods is presented.

2. THEORY AND BACKGROUND

2.1 Fluid Flow in Porous Media

A porous medium can be characterized by several physical parameters, such as porosity and hydraulic conductivity. Porosity (ϕ) is the ratio of the void space to the total volume of the medium. The hydraulic conductivity (K) is a function of both the porous medium and fluid properties. The hydraulic conductivity is related to the intrinsic permeability of the medium (k) and fluid properties through $K = k\rho g/\mu$, where ρ and μ are the fluid density and dynamic viscosity, respectively. Darcy's law incorporates this hydraulic conductivity to an expression that predicts fluid flux q when the gradient of the hydraulic head dh/dx is known: $q = -K(dh/dx)$. A generalized form of Darcy's equation for a system containing multiple fluids is given by:

$$\mathbf{q}_\alpha = -\frac{k_{r,\alpha}\mathbf{k}_{ij}}{\mu_\alpha}(\nabla p_\alpha - \rho_\alpha g \nabla z), \quad (1)$$

where $\mathbf{q}_\alpha$ is the flux for α phase, $\mathbf{k}_{ij}$ is permeability tensor, p_α is pressure of phase α, z is elevation, and k_r is relative permeability. The mass conservation (i.e. continuity) equation for multiphase fluid flow system is expressed as

$$-\vec{\nabla}\cdot(\rho_\alpha \mathbf{q}_\alpha) + Q_\alpha = \frac{\partial}{\partial t}(\phi \rho_\alpha S_\alpha), \quad (2)$$

where Q_α is source-sink term, and S_α is the saturation of the α phase which is the ratio between the volume of void occupied by α phase to the total void volume. Combining Darcy's equation with mass conservation, the generalized multiphase flow equation for incompressible fluids can be obtained as:

$$\vec{\nabla}\cdot\left[\frac{k_{r,\alpha}\mathbf{k}_{ij}}{\mu_\alpha}(\nabla p_\alpha - \rho_\alpha g \nabla z)\right] + Q_\alpha = \phi\frac{\partial S_\alpha}{\partial t} \quad (3)$$

The solution of the system of equation given by Eq. (3) requires additional constitutive models that relate permeability and capillary

pressure to partial fluid saturations. A number of numerical models exist to solve this coupled, non-linear system of equations.

2.2 Contaminant Transport in Porous Media

The fate and transport of dissolved contaminants in groundwater can be described by the advection-dispersion-reaction equation:

$$\frac{\partial(\phi c)}{\partial t} = \vec{\nabla} \cdot \left(\mathbf{D_{ij}} \nabla c - \phi \overline{\mathbf{v}}_\mathbf{i} c\right) + \sum R_n \qquad (4)$$

where $\mathbf{D_{ij}}$ is dispersion coefficient tensor, R_n is a reaction term, and $\overline{\mathbf{v}}_\mathbf{i}$ is the pore velocity which can be calculated from Darcy's law given as $\overline{\mathbf{v}}_\mathbf{i} = -\mathbf{K_{ij}} \nabla h / \phi$. Advection represents the movement of a contaminant with the flowing groundwater. Hydrodynamic dispersion on the other hand, involves both molecular diffusion and mechanical mixing. The latter is a result of local variations in velocity around some mean velocity of the flow as a result of soil heterogeneity. Laboratory investigations indicate that at the macroscopic scale, dispersion is a function of pore velocity and a factor called dispersivity. The dispersion of solutes in groundwater can occur not only in the direction of groundwater flow, but also lateral to the direction of flow. The last term in Eq. (4) represents the total mass loss or generation due to other physical, chemical and biological processes such as adsorption, biodegradation, and self decay (e.g. radionuclides).

2.3 Non-Aqueous Phase Liquids

Nonaqueous phase liquid (NAPLs) are chemicals that are slightly soluble in water (e.g. petroleum products, organic solvents and wood preservatives) that remains as a separate phase for long periods of time after a spill thus contributing soils and groundwater contamination. Migration of NAPLs in the subsurface is controlled by gravity, buoyancy, and capillary forces. Lighter-than-water NAPL (or LNAPL) such as gasoline and diesel fuels, after percolating downward through unsaturated zone, can float and move on top of water table. On the other hand, denser-than water NAPLs (or DNAPL) such as organic solvents and wood treatment compounds are able to migrate downward past water table and penetrate deep into the saturated zone. During migration, a fraction of the NAPL enters pore spaces by capillary forces and they are left behind in the soil as discontinuous blobs or ganglia. When free-phase DNAPL reaches impermeable layers during migration, it may 'pool' on top of interfaces resulting in high saturation entrapment zones. These entrapped NAPLs slowly dissolve into a flowing groundwater generating a downstream plumes generating risk at receptor locations such as wells, rivers and lakes.

The presence of NAPLs in aquifers impacts groundwater quality and remediation is challenging as it is difficult to locate and

remove all of the entrapped NAPL mass. Although a number of NAPL removal technologies are currently being tested, there is mixed success in achieving cleanup goals. Uncertainty associated with achieving cleanup goals can be attributed largely to the inability to locate free-phase NAPL in heterogeneous subsurface.

2.4 Stochastic Methods

The flow and transport parameters that appeared in the equations governing equations (1)-(4), are generally measured or determined at only a few locations despite the fact that they are highly variable in space at all length scales (macroscopic to regional). A combination of sparsity of observations and measurement errors lead to uncertainty in the values of the formation properties and thus uncertainty of predictions using simulation models that solve the governing equations. The stochastic theory provides a method for evaluating these uncertainties using probability or related quantities such as statistical moments (Zhang, 2002). Material properties that define field heterogeneity are not completely random, but assumed to exhibit some correlation structure resulting from natural depositional processes that created the formation. This spatial correlation structure is defined using random space functions that are quantified using joint probability distributions or joint statistical moments.

A commonly used geostatistical approach used in stochastic formulations is to characterize the heterogeneity (in terms of permeability) of the aquifer by the first and second moments of a probability distribution function (pdf) which are referred to as mean, and variance/covariance, respectively. In modeling flow and transport, the hydraulic conductivity (K) introduces the greatest uncertainty as its value varies over a very wide range in aquifer materials. The uncertainty is not only associated with the measurement at a point but also with the uncertainty of the value at locations where it is not measured. The general approach used in developing the technique assumes that the log of K is normally distributed: $y = \ln K$. If n points in the aquifer are sampled, the estimate of the population mean is obtained from

$$\bar{y} = \frac{1}{n}\sum_{i=1}^{n} y_i \qquad (5)$$

and the estimate of the variance is given by,

$$S_y^2 = \frac{1}{n}\sum_{i=1}^{n} (y_i - \bar{y})^2. \qquad (6)$$

The pdf of the *ln K* distribution is defined by the mean and the variance. The variance measures the degree of heterogeneity of the aquifer. If the y_i is measured at a fixed set of points, and if it is necessary to estimate the value of y at other locations where measurements are not made, the mean and the standard deviation (square root of variance) can be used to provide the

most likely estimate of the un-measured value. That is, the estimated value is the mean with an uncertainty that is normally distributed with a standard deviation equal to the standard deviation of the measurements. The lognormal variable K can be described by the following pdf,

$$f_K(K) = \frac{1}{K\sigma\sqrt{2\pi}} \exp\left[-\frac{(\ln K - \mu)^2}{2\sigma^2}\right] \qquad (7)$$

where μ and σ^2 are the mean and variance of $\ln K$.

A stochastic random process is a collection of random variables that vary continuously in space (or time). The stochastic process K(x) can be thought of as a collection (or ensemble) of realizations with the same statistical properties. A realization is single observation of the spatial variation of the process. If the pdf of a spatially random process is invariant under shifts of the spatial origin, then it is considered to be second-order stationary and commonly referred to as "stationary." The importance of stationarity is the suggestion of underlying repetitive structure of the parameter. A physical description of the stationarity is captured in the covariance function that is given as,

$$\mathrm{cov}[y_1 - y_2] = E[\{y_1 - \mu_1\}\{y_2 - \mu_2\}] \qquad (8)$$

whose estimator is,

$$R_y(r) = \frac{1}{N-r}\sum_{i=1}^{n}(y_{i+r} - \bar{y})(y_i - \bar{y}) \qquad (9)$$

where $N-r$ term is the number of pairs separated by a distance r. The covariance is independent of the origin but depends on the distance between observations. The heterogeneous aquifers can be represented as a spatially correlated random field. The descriptive statistics of the random field include the mean and variance of $\ln K$ and correlation length. Spatial correlation increases the probability that a given point will have permeability similar to that of a neighboring point. K values at points that are separated by a short distance are more likely to be similar and as the separation becomes larger they are less likely to be similar. The correlation scale is a characteristic length of the average spatial persistence of $\ln K$. A geoststistical tool for the quantification of spatial structure is the experimental semivariogram (referred to as variogram). Variograms are useful in identifying the underlying spatial structure and identifying trends. The classical experimental semivaraigram estimator $\gamma(h)$, for Gaussian data is calculated as,

$$\gamma(h) = \frac{1}{2n(h)}\sum_{i=1}^{n(h)}[y(x_i + h) - y(x_i)]^2 \qquad (10)$$

where h is the separation distance between observations and $n(h)$ is the number of data pairs separated by distance h. If the $\ln K$ data are statistically homogeneous

(stationary), then the variogram is dependent only on h. A theoretical exponential model can be fitted to the variogram as,

$$\gamma(h) = \sigma^2(1 - e^{-h/\lambda}) \qquad (11)$$

The model parameter λ is the correlation length that is a measure of the distance over which the y values are correlated. Fig. 1 shows a plot of the theoretical and a measured semivariagram from a laboratory sand packing experiment conducted by Compos (1998). For a small separation distance h, the correlation between sample pairs is high and $\gamma(h)$ is small. When distance between points increases, the correlation decreases (i.e. $\gamma(h)$ increases) and variogram will eventually reach a plateau.

In general, two approaches of stochastic formulations are used. In the first approach, uncertainty analysis is incorporated directly into the model to define the predictions in terms of their mean and covariance. The second approach uses a Monte Carlo-type analysis involving a series of realizations of the uncertain parameters (Gelhar and Axeness, 1983). In our laboratory experiments and numerical studies, the second approach was used. Several realizations of hydraulic conductivity field (more correctly, log K) were generated and used for further analyses.

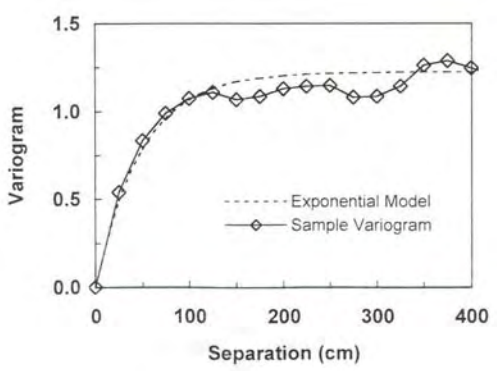

Fig. 1: Typical semivariogram for stationary process (Compos, 1998).

3. EXPERIMENTAL STUDIES

3.1 Chemical Transport in Heterogeneous Test Aquifer

Experimental investigations of the transport of dissolved species in heterogeneous porous media were conducted in both 2- and 3-dimensional test systems. Tracer experiments in either laboratory or a field site are used to characterize transport parameters of the porous medium. Barth et al. (2001a,b) conducted conservative tracer experiments in a 2-D heterogeneous porous medium (Fig. 2). Analyses based on stochastic theory and tracers test data led to the development of a guideline for selecting conservative tracer's density as a function of local hydraulic gradient which is related to $\ln K$ and $\sigma^2_{\ln K}$.

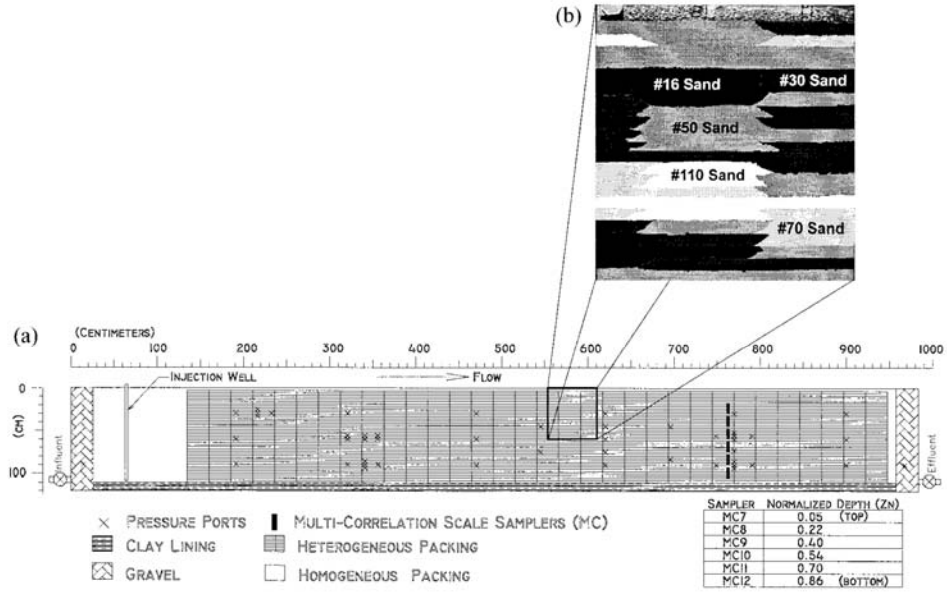

Fig. 2: Two-dimension, intermediate-scale test tank (Barth et al., 2001a & b).

Garcia et al. (2004) conducted conservative and reactive tracers test in a physically and chemically heterogeneous 3-D test aquifer (see Fig. 3). The inherent heterogeneity of the aquifer usually obscures the interpretation of field tracer tests. The goal of these experiments was to correctly evaluate transport parameters (specifically, scale-dependent dispersivity and retardation factor) of a heterogeneous aquifer that are required in the solution of advection-dispersion equation, Eq. (4). Guidelines for accurate data interpretation and determination of transport parameters from field tracers test were developed. Monte Carlo-type of simulations of tracer tests were conducted to validate and support the findings.

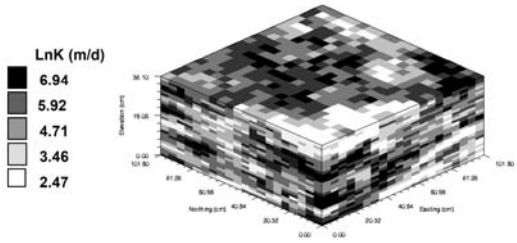

Fig. 3: Three-dimensional view of the distribution of the sand in the test aquifer (Garcia et al., 2004).

3.2 Multiphase Flow

Locating free-phase NAPL in heterogeneous subsurface is a challenging task. Estimation of highly variable saturation distribution of NAPL in the heterogeneous is required in remediation design and risk assessment. Prediction of how NAPL migrates and becomes entrapped in heterogeneous formations is of practical interest. The migration as well as the entrapment architecture (i.e. NAPL

distribution) depends strongly on porous media characteristics. Compos (1998) conducted DNAPL (trichloroethane) spreading experiments in five different permeability fields (i.e. realizations based on the same formation statistics such as mean, variance and anisotropic correlation lengths). Fig. 4 show the 2-D test cell containing a random field (packed using five different types of silica sands). It was found that NAPL entrapment architectures has spatial structure that can be defined using statistical parameters.

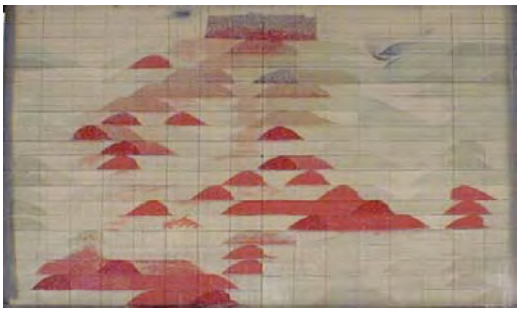

Fig. 4: Entrapment architecture created from a spill in a spatially correlated random filed (Compos, 1998).

4. NUMERICAL MODELING

4.1 Effect of Heterogeneity on Entrapment Architecture of NAPL

As mentioned earlier, soil heterogeneity can cause complex entrapment architecture of spilled NAPLs. Saenton (2003) conducted numerical experiments (80 realizations) using multiphase flow code (Delshad et al., 1996) to generate DNAPL source zone entrapment architecture. Fig. 5 shows two examples of final entrapment architecture created through model simulations. Even though all realizations have the same statistics (average ln K and variance), entrapment architecture can be significantly different. Fig. 6 shows the centers of mass for all realizations are in general clustered at the mid-depth of the spill zone, and at the center in x-direction. Their spreading however varies significantly in z-direction. In some realizations the source zones contain only high saturation pools whereas, in some cases, PCE dispersed throughout the source zone in a residual form. This observation is used in the development of up-scaling methods for mass transfer from the entrapped DNAPLs (Saenton and Illangasekare, 2007).

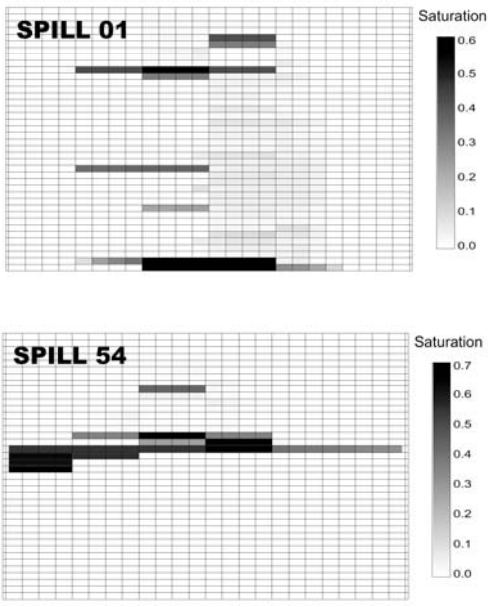

Fig. 5: Example of PCE (tetrachloroethene) spills in realizations #1 and #54.

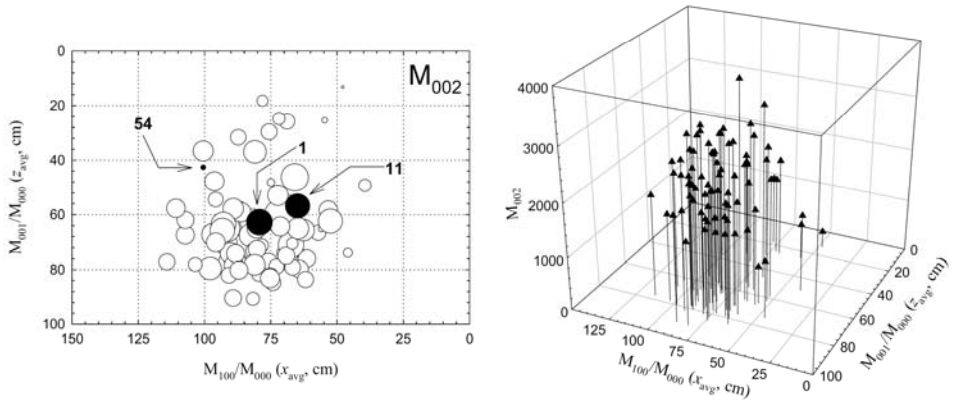

Fig. 6: Second moment (or mass spreading) in *z* direction for all 80 spills.

4.2 Effect of Entrapment Architecture on Clean-Up Efficiency

The remediation of entrapped NAPL in source zone containing different entrapment architecture can result in varying clean-up efficiency. Saenton et al. (2002) conducted a set of Monte Carlo-type numerical simulations of surfactant-enhanced NAPL remediation from the heterogeneous source zone based on 10 NAPL spills in intermediate-scale test tank. The heterogeneity was created using stochastically generated random field (Fig. 1). Fig. 7 shows the problem domain (test tank) and the simulation results. Gray lines, in Fig. 7 (right), indicate the complete delivery where the injected surfactant solution is assumed to fully sweep the entrapped NAPL. However, when by-passing due to heterogeneity is taken in to account the surfactant does not reach all the entrapped NAPL, thus affecting cleanup time significantly. A large variability in the removal efficiency was observed die to the uncertainty in delivery associated with heterogeneity.

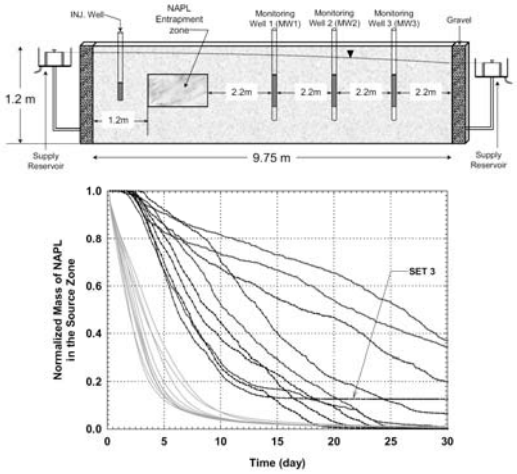

Fig. 7: (Top) Intermediate-scale test tank, and (Bottom) Normalized mass depletion as a function of time for surfactant-enhanced dissolution (incomplete delivery). The gray lines represent complete delivery cases.

5. DISCUSSION AND CONCLUSIONS

From the above numerical and laboratory study examples, it can be seen that stochastic method as applied to hydrogeology problems can be used as a tool to evaluate uncertainty in prediction and remediation efficiency. In any type of risk

assessment, uncertainty associated with parameters describing the system must always be considered. When the heterogeneity cannot be fully characterized, there exists significant uncertainty regarding the achievement of cleanup goals and the reduction of risk.

ACKNOWLEDGMENTS

The work presented here is based on research by Dr. Gilbert Barth, Dr. Daniel Fernandez Garcia, Mr. Ron Compos. The authors gratefully acknowledge their contributions. Financial support for this research was provided by the Army Research Office and Strategic Environmental Research and Development Program (SERDP) administered by the US Department of Defense. In addition, the authors would also like to thank the Faculty of Science and the Groundwater Technology Service Center (GTSC), Chiang Mai University.

REFERENCES

Barth, G.R., Illangasekare, T.H., Hill, M.C., Rajaram, H. 2001a. A new tracer-density criterion for heterogeneous porous media. Water Resources Research, 37(1): 21-31.

Barth, G.R., Illangasekare, T.H., Hill, M.C., Rajaram, H. 2001b. Predictive modeling of flow and transport in a two-dimensional intermediate-scale, heterogeneous porous medium. Water Resources Research, 37(10): 2503-2512.

Compos, R. 1998. Hydraulic conductivity distribution in a DNAPL entrapped zone in a spatially correlated random field. M.S. Thesis, University of Colorado.

Delshad, M. Pope, G.A., Sepehrnoori, K. 1996. A compositional simulator for modeling surfactant enhanced aquifer remediation. Journal of Contaminant Hydrology, 23(1-2): 303-327.

Fernndez-Garcia, D. Illangasekare, T.H., Rajaram, H. 2004. Conservative and sorptive forced-gradient and uniform flow tracer tests in a three-dimensional laboratory test aquifer. Water Resources Research. In revision.

Gelhar, L.W., Axness, C.L. 1983. Three-dimensional stochastic analysis of macrodispersion in aquifers. Water Resource Research. 19(1): 161-180.

Neuman, S.P., Winter, C.L., Newman, C.M. 1987. Stochastic theory of field-scale fickian dispersion in anisotropic porous media. Water Resource Research. 23(3): 453-466.

Saenton, S. 2003. Prediction of mass flux from DNAPL source zone with complex entrapment architecture: Model development, experimental investigation, and up-scaling. PhD Thesis, Colorado School of Mines.

Saenton, S., Illangasekare, T.H. 2007. Up-scaling of mass transfer of entrapped DNAPLs in heterogeneous aquifers: Theoretical development, numerical

implementation, and experimental validation. Water Resources Research, 43, doi:10.1029/2005WR004274.

Saenton, S., Illangasekare, T.H., Soga, K., Saba, T.A. 2002. Effect of source zone heterogeneity on surfactant enhanced NAPL dissolution and resulting remediation endpoints. Journal of Contaminant Hydrology, 53(1-2): 27-44.

Zhang, D., 2002. Stochastic Methods for Flow in Porous Media, Academic Press, pp 350.

แบบจำลองน้ำใต้ดินของแอ่งเวียงแหง จังหวัดเชียงใหม่

Groundwater Model of the Wieng Haeng Basin, Chiang Mai Province

ดร. ศตวรรษ แสนทน[1]
ผศ. ดร. อัมรินทร์ บุญตัน[2]

บทคัดย่อ

บทความนี้ได้เสนอผลการศึกษาลักษณะทางอุทกธรณีวิทยาของแอ่งเวียงแหง อ.เวียงแหง จ.เชียงใหม่ ซึ่งเป็นส่วนหนึ่งของการศึกษาประเมินผลกระทบสิ่งแวดล้อมอันเนื่องมาจากโครงการพัฒนาเหมืองถ่านหินเวียงแหง โดยได้รับการสนับสนุนงบประมาณจากการไฟฟ้าฝ่ายผลิตแห่งประเทศไทย (กฟผ.) ขั้นตอนการศึกษาประกอบด้วยการศึกษาและรวบรวมข้อมูลธรณีวิทยาเดิมที่มีอยู่แล้ว การเจาะสำรวจเพิ่มเติม การสูบทดสอบในภาคสนามเพื่อให้ได้มาซึ่งค่าคุณสมบัติทางชลศาสตร์ และการจัดทำแบบจำลองน้ำใต้ดิน จากนั้น จะนำข้อมูลทั้งหมดมาประเมินสภาพอุทกธรณีวิทยาของพื้นที่ศึกษา ผลการศึกษาพบว่า แอ่งเวียงแหงจัดเป็นแอ่งที่มีแหล่งน้ำใต้ดินศักยภาพสูง เนื่องจากปริมาณการเติมน้ำบาดาล (recharge) มีมาก และโครงสร้างทางธรณีวิทยาทำให้แอ่งมีเป็นลักษณะแอ่งปิด ส่งผลให้มีปริมาณน้ำใต้ดินสำรองสูง น่าจะสามารถพัฒนาขึ้นมาใช้ประโยชน์ได้อย่างยั่งยืน

1. บทนำ

แหล่งถ่านหินเวียงแหง อำเภอเวียงแหง จังหวัดเชียงใหม่ เป็นแหล่งที่มีศักยภาพในการนำถ่านหินมาใช้ประโยชน์ การไฟฟ้าฝ่ายผลิตแห่งประเทศไทย (กฟผ.) จึงได้ศึกษาและสำรวจทางธรณีวิทยาเพื่อประเมินความเหมาะสมและวางแผนพัฒนาแหล่งถ่านหินเวียงแหง เพื่อนำถ่านลิกไนต์ที่มีคุณภาพดี มีสารกำมะถันต่ำจากแหล่งนี้มาใช้เป็นเชื้อเพลิง ด้วยเหตุนี้ กฟผ. จึงได้ขอความร่วมมือจากมหาวิทยาลัยเชียงใหม่ในการศึกษาและวิเคราะห์ผลกระทบสิ่งแวดล้อมของโครงการพัฒนาเหมืองเวียงแหง เพื่อจัดทำรายงานและนำเสนอขอความเห็นชอบต่อสำนักงานนโยบายและแผน กระทรวงทรัพยากรธรรมชาติและสิ่งแวดล้อม ตาม พ.ร.บ.ส่งเสริมและรักษาคุณภาพสิ่งแวดล้อมแห่งชาติ พ. ศ.2535

การศึกษาลักษณะอุทกธรณีวิทยาของแอ่งเวียงแหงดังกล่าว เป็นส่วนหนึ่งของการศึกษาและจัดทำรายงานผลกระทบสิ่งแวดล้อม โดยทีมผู้ศึกษา ได้ทำการรวบรวมข้อมูลด้านธรณีวิทยา อุทกธรณีวิทยา อุทกวิทยา เพื่อนำมาจัดทำแบบจำลองคณิตศาสตร์ จำลองการไหลของน้ำใต้ดินในแอ่งเวียงแหง จากนั้นจึงได้นำแบบจำลองมาประเมินศักยภาพของแหล่งน้ำใต้ดินในแอ่งดังกล่าว

2. สภาพทั่วไปของพื้นที่ศึกษา

2.1. สภาพภูมิประเทศ

แอ่งเวียงแหง เป็นแอ่งสะสมตะกอน (Sedimentary basin) ขนาดใหญ่ของพื้นที่ในเขตอำเภอเวียงแหง ซึ่งเป็นพื้นที่ที่ประกอบด้วยชั้นตะกอนที่มีลักษณะแบบราบปิดทับอยู่บนหินฐาน มีภูเขาที่เกิดจากรอยเลื่อนทั้ง 2 ด้าน รูปร่างของแอ่งมีลักษณะคล้ายเสี้ยวพระจันทร์ รูปที่ 1 แสดงลักษณะของแอ่งเวียงแหง จุดที่สูงที่สุดของอำเภอเวียงแหงอยู่ทางด้านทิศตะวันตกเฉียงเหนือยอดดอยปกกะลา สูง 1,905 เมตร จากระดับน้ำทะเล

[1] ภาควิชาธรณีวิทยา คณะวิทยาศาสตร์ มหาวิทยาลัยเชียงใหม่ อ.เมือง จ.เชียงใหม่ 50200
[2] ภาควิชาวิศวกรรมเหมืองแร่ คณะวิศวกรรมศาสตร์ มหาวิทยาลัยเชียงใหม่ อ.เมือง จ.เชียงใหม่ 50200

และรองลงมา คือดอยดำ สูง 1,767 เมตรจากระดับน้ำทะเลอยู่บริเวณชายแดนไทย-พม่า เป็นแนวสันเขาตั้งแต่ทิศเหนือที่ช่องหลักแต่ง ตำบลเปียงหลวง ส่วนทางด้านทิศตะวันออกติดกับอุทยานแห่งชาติเชียงดาว อำเภอเชียงดาว ซึ่งเป็นจุดกำเนิดน้ำแม่แตง แม่น้ำสายสำคัญรวมทั้งลำน้ำสาขาไหลผ่านอำเภอเวียงแหง ไหลลงทางทิศใต้สู่อำเภอแม่แตงก่อนที่จะเข้าสู่เขื่อนแม่งัด รูปแบบของระบบแม่น้ำลำธารในอำเภอเวียงแหงมีลักษณะคล้ายต้นไม้ (Dendritic-pinnate pattern) ร่องน้ำสาขาไหลมาลงฝั่งตรงกันข้ามกันของแม่น้ำสายใหญ่ เป็นเพราะเนื้อหินละเอียดที่ไม่ซึมน้ำมีความ

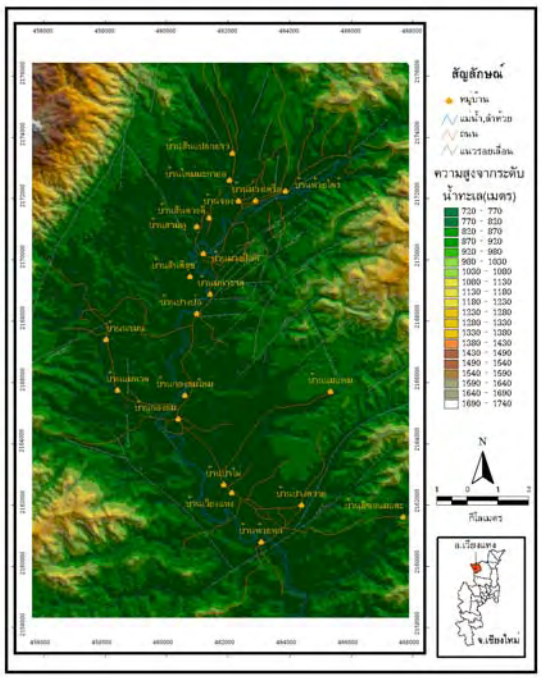

ลาดชันน้อย

รูปที่ 1 พื้นที่ศึกษา แอ่งเวียงแหง จังหวัดเชียงใหม่

2.2. ลักษณะทางธรณีวิทยา

แอ่งเวียงแหงมีลักษณะเป็นแอ่งตะกอนระหว่างภูเขา มีพื้นที่ประมาณ 100 ตารางกิโลเมตร วางตัวเกือบอยู่ในแนวเหนือ-ใต้ และเกิดจากการเคลื่อนที่ของหินตามแนวรอยเลื่อนซึ่งขนาบอยู่ด้านใดด้านหนึ่งหรือทั้งสองด้าน จากรายงานการประเมินผลธรณีวิทยาแหล่งถ่านหินปางป๋อแอ่งเวียงแหงของการไฟฟ้าฝ่ายผลิตแห่งประเทศไทย พ.ศ. 2542 สรุปว่า ลุ่มแอ่งเวียงแหงมีลักษณะเป็น Half Garben เกิดอยู่ในบริเวณที่มีโครงสร้างทางธรณีค่อนข้างซับซ้อน เนื่องจากมีรอยเลื่อนขนาดเล็กหลายทิศทางตัดผ่านบริเวณตอนกลางแอ่ง ขอบเขตด้านเหนือ และด้านใต้เป็น Fault Contacts ขอบด้านตะวันออกเป็น Angular unconformable Contact ของชั้นตะกอน ขอบเขตทางตะวันตกของลุ่มแอ่งจะเป็นรอยเลื่อน (Fault) ขนาดใหญ่ ซึ่งพบว่าเป็นหินแกรนิต อายุคาร์บอนิเฟอรัส (Carboniferous) ที่ถูกยกตัวขึ้นมาเป็นขอบแอ่ง Tertiary และพบว่ามีรอยเลื่อนขนาดเล็กที่เป็นขอบของหินแกรนิตบริเวณขอบตะวันออกของลุ่มแอ่ง สองฝั่งน้ำปรากฏตะกอนของทางน้ำปัจจุบันและตะกอนอายุไพลสโตซีน จนถึงทิวเขาสูงของหินอายุอื่น ๆ หินยุคต่าง ๆ ที่พบบริเวณแอ่งเวียงแหงประกอบด้วย หินตะกอน หินแปร และหินอัคนี อายุแก่ไปหาอ่อนได้แก่ หินยุคคาร์บอนิเฟอรัส ยุคเพอร์เมียน หินยุคเทอร์เทียรี และควอเทอร์นารี ดังแสดงในรูปที่ 2 และภาพตัดขวางในรูปที่ 3

2.3. การเรียงลำดับชั้นหินตะกอนในแอ่งเวียงแหง

หินตะกอนที่สะสมตัวในแอ่งเวียงแหงเป็นหินในมหายุคซีโนโซอิกได้แก่หินตะกอนยุค Quaternary และ Tertiary ปรากฏอย่างไม่ต่อเนื่อง ซึ่งจากข้อมูลการสำรวจและเจาะสำรวจของการไฟฟ้าฝ่ายผลิตแห่งประเทศไทยร่วมกับกรมทรัพยากรธรณี (2530) พบว่ามีการลำดับชั้นหน่วยหินดังนี้

(1) Quaternary – Recent Alluvium: พบอยู่ด้านบนสุดของแอ่ง สะสมตัวในบริเวณที่ราบน้ำท่วมถึง (Flood Plain) ของน้ำแม่แตง และลำน้ำที่แยกออกไป ประกอบด้วยตะกอนที่ยังไม่มีการอัดแน่นพวก Clay, Silt, Sand และ Gravel สีน้ำตาลปนแดงและเหลือง มีความหนาตั้งแต่ 0-27 เมตร

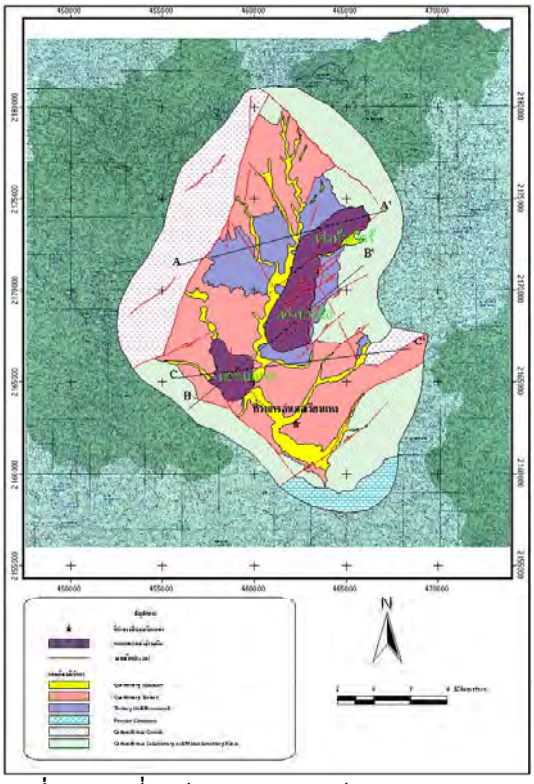

รูปที่ 2 แผนที่ธรณีวิทยาของแอ่งเวียงแหง

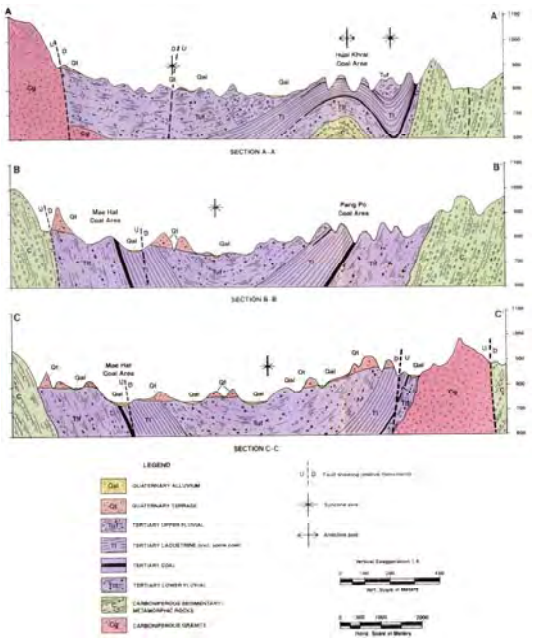

รูปที่ 3 ภาคตัดขวางแสดงการวางตัวของหินในแอ่งเวียงแหง

(2) Quaternary Terrace Unit : เป็นหน่วยหินที่แยกจากชั้น Tertiary Upper Fluvial Zone โดยรอยชั้นไม่ต่อเนื่อง (Unconformity) ประกอบด้วยตะกอน ได้แก่ Clay, Sand และ Gravel มีความหนาเพิ่มขึ้นทางทิศตะวันตก และหนามากที่สุดในบริเวณตอนกลางแอ่งค่อนไปทางทิศตะวันตก พบความหนาตั้งแต่ 0-400 เมตร

(3) Tertiary Upper Fluvial Unit : พบทั่วไปในแอ่งเวียงแหง ยกเว้นพื้นที่บริเวณขอบตะวันออกและตะวันตกเฉียงใต้ ประกอบด้วย Clay, Silt, Sand และ Gravel สีเทาปนเหลือง และน้ำตาล พบเศษหิน แกรนิตปะปน กับชั้นทรายบางบริเวณ มีความหนาประมาณ 0-120 เมตร

(4) Lacustrine Unit : เป็นหน่วยหินที่วางตัวอยู่บนหน่วยหิน Lower Fluvial Zone ประกอบด้วย Clay, Claystone, Silty Claystone, Sandy Claystone สีเขียว-เทา หรือน้ำตาล-เทา พบสีเข้มและอ่อน วางตัวแทรกสลับกัน หินชุดนี้มีชั้น Lignite สีดำ เนื้อแข็ง แทรกอยู่ในชั้น Lignite บางบริเวณพบว่า ถูกแทรกสลับด้วย Soft Lignite สีดำ Clayey Lignite สีน้ำตาลดำ และ Ligneous Clay สีน้ำตาล ความหนาของชั้น Lignite เฉลี่ยประมาณ 20 เมตร ซึ่งชั้นดิน-หินหน่วยนี้วางตัวเป็นมุมเอียงประมาณ 10-20 องศาไปทางทิศตะวันตก ความหนาของหินหน่วยนี้ประมาณ 0 ถึงมากกว่า 300 เมตร

(5) Lower Fluvial Unit : เป็นหน่วยหินที่ประกอบด้วยชั้น Clay, Silt, Sand Gravel แทรกสลับกับชั้นหินกึ่งแข็งตัว (Semi-Consolidated Rock) เช่น หิน Claystone, Sandy Claystone สีเทาอ่อนปนเหลือง Sandstone สีเทาอ่อน ขนาด Fine-Medium Grained และ Siltstone สีเทา-น้ำตาลอ่อนเป็นต้น หินหน่วยนี้วางตัวแบบไม่ต่อเนื่อง (Unconformity) บนหินแข็งรากฐาน (Basement Rock) ที่มีอายุ Carboniferous ซึ่งโผล่ทางขอบแอ่ง

ด้านตะวันออก ความหนาของหินหน่วยนี้ประมาณ 0 ถึงมากกว่า 300 เมตร

จากลักษณะของหินตะกอนที่พบแสดงให้เห็นการเปลี่ยนแปลงสภาพแวดล้อมการสะสมตัว เริ่มจากตะกอนขนาดหยาบ ซึ่งทำให้เกิดหิน Conglomerate และ Sandstone บริเวณส่วนล่าง โดยหินกรวดมนส่วนล่างสุด ซึ่งมีกรวดขนาดใหญ่จะเป็น Basal Conglomerate ลักษณะของหินเหล่านี้แสดงว่าเป็นการทับถมบริเวณขอบแอ่ง ต่อมาแอ่งทรุดตัวลงจนเกิดสภาพทะเลสาบ (Shallow Lake) เกิดการทับถมของตะกอนเนื้อละเอียดเกิดเป็นหินดินดาน (Claystone) บริเวณน้ำตื้นมีการทับถมของซากพืช ซึ่งต่อมาเปลี่ยนไปเป็นถ่านหิน ซึ่งอาจเกิดเมื่อแอ่งมีการยกตัวเป็นเหตุให้น้ำตื้น การยกตัวและการทรุดตัวของแอ่งอาจเกิดขึ้นสลับกัน โดยจะเห็นได้จากการทับถมของ Claystone เหนือชั้นถ่าน แสดงว่าระดับพื้นแอ่งอยู่ลึกลงเนื่องจากทรุดตัว ส่วนตอนบนพบชั้นทราย ซึ่งเป็นตะกอนขนาดใหญ่ บางส่วนมีชั้นถ่านบาง ๆ แทรกสลับอยู่กับหินยังไม่แข็งตัวเต็มที่ แสดงว่าเกิดเมื่อน้ำตื้นอันเนื่องจากการยกตัวอีกครั้งหนึ่ง

2.4. ลักษณะทางอุทกธรณีวิทยา

การศึกษาลักษณะทางอุทกธรณีวิทยาบริเวณแอ่งเวียงแหงนั้นมีหลายหน่วยงานที่ได้ทำการศึกษา รวมทั้งมีการขุดเจาะบ่อบาดาลเพื่อให้ประชาชนชาวเวียงแหงสามารถใช้น้ำจากชั้นน้ำบาดาลได้ ซึ่งหน่วยงานที่ได้ทำการขุดเจาะบ่อบาดาล และศึกษาในช่วงเริ่มต้นจะเป็นกรมทรัพยากรธรณี และการไฟฟ้าฝ่ายผลิตแห่งประเทศไทย โดยในช่วงเริ่มแรกกรมทรัพยากรธรณีได้ทำการเจาะบ่อบาดาลจำนวน 12 บ่อ และสำนักงานเร่งรัดพัฒนาชนบท จำนวน 9 บ่อ กรมโยธาธิการ 1 บ่อ และการไฟฟ้าฝ่ายผลิตแห่งประเทศไทย จำนวน 9 บ่อ (รูปที่ 4) หลังจากนั้นหน่วยงานอื่น ๆ ไม่ได้ทำการขุดเจาะเพิ่ม มีเพียงแต่การไฟฟ้าฝ่ายผลิตฯ ที่ยังดำเนินการศึกษา และขุดเจาะบ่อบาดาลต่อมาจนถึงปัจจุบัน

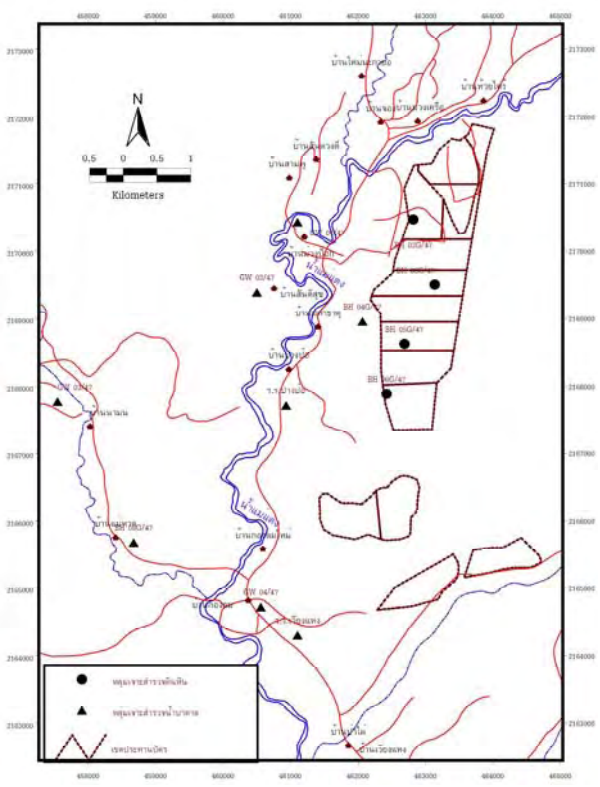

รูปที่ 4 ตำแหน่งบ่อบาดาล

จากข้อมูลการศึกษาสำรวจอุทกธรณีวิทยาของกรมทรัพยากรธรณีพบว่า ชั้นน้ำบาดาลในแอ่งเวียงแหงมีลักษณะแบ่งได้เป็น 4 ชนิด (การไฟฟ้าฝ่ายผลิตฯ, 2545) ได้แก่

ชั้นน้ำบาดาลในตะกอนกรวดโบราณ (High Terrace) ความลึกประมาณ 10-100 เมตร ให้น้ำประมาณ 5-10 ลบ.ม./ชม.

ชั้นน้ำบาดาลในชุดหิน Tertiary ความลึก 50-300 เมตร ให้น้ำน้อยกว่า 2 ลบ.ม./ชม.

ชั้นน้ำระหว่างชุดหิน Tertiary และหินแข็ง ความลึก 100-500 เมตร ให้น้ำประมาณ 5-10 ลบ.ม./ชม.

ชั้นน้ำในหินแข็ง ความลึกมากกว่า 150 เมตร ให้น้ำน้อยมากหรืออาจไม่มีน้ำ จะพบบริเวณรอยแตกของชั้นหิน

ชั้นน้ำใต้ดินทั้ง 4 ชั้น ดังกล่าวอยู่เหนือชั้นถ่านหิน โดยชั้นน้ำใต้ดินระดับตื้นเป็นชั้นดินอุ้มน้ำที่เกิดจากการตกตะกอนชั้นดินแบบลานตะพัก

น้ำ (River Terrace) อยู่ในชั้นน้ำบาดาล ตะกอนกรวดโบราณ (High Terrace) ชั้นหินอุ้มน้ำชั้นที่ 1, 2 และ 3 เกิดในสภาพแวดล้อมแบบ Fluvial Deposits เช่น จำพวกดิน ทรายปนกรวด อยู่ในช่วงความลึก 25-110 เมตร และมีปริมาณน้ำอยู่ระหว่าง 0.6-13.2 ลบ.ม./ชม.

3. การจำลองการไหลของน้ำใต้ดิน

แบบจำลองการไหลของน้ำใต้ดินเป็นเครื่องมือชนิดหนึ่งที่ใช้ช่วยในการศึกษาลักษณะอุทกธรณีวิทยา ทั้งในแง่ปริมาณและทิศทางการไหลของน้ำใต้ดินในชั้นหินอุ้มน้ำหรือในชั้นตะกอนกรวด-ทรายที่สามารถกักเก็บและจ่ายน้ำได้ ในการศึกษานี้ ผู้จัดทำได้เลือกใช้แบบจำลองคณิตศาสตร์เชิงตัวเลข (Numerical Model) ชนิด Finite-Difference ซึ่งแบบจำลองประเภทนี้มีอยู่มากมาย แต่ที่นิยมใช้ที่สุดคือแบบจำลองการไหลของน้ำใต้ดินของ United States Geological Survey หรือ USGS ที่เรียกว่า MODFLOW (Harbaugh et al., 2000)

3.1. การออกแบบกริด

ในการสร้างแบบจำลองน้ำใต้ดินของพื้นที่ๆ มีการวางตัวของชั้นหินที่ค่อนข้างซับซ้อน ควรใช้ Internal Flow Package ที่สามารถใช้จำลองการไหลในชั้นน้ำที่มีการวางตัวซับซ้อนได้ดีกว่า แพ็คเกจเดิมๆ ที่ใช้กันอยู่ ซึ่งหมายถึง Block-Centered Flow หรือ BCF (McDonald and Harbaugh, 1988) และ Layer-Property Flow หรือ LPF (Harbaugh et al., 2000) โดยในการศึกษาครั้งนี้ คณะผู้ศึกษาได้เลือกใช้ Hydrogeologic-Unit Flow หรือ HUF (Anderman and Hill, 2000)

การสร้างแบบจำลองของพื้นที่ศึกษา ที่มีการวางตัวของชั้นน้ำที่ค่อนข้างซับซ้อน (เช่น วางตัวในแนวเอียง และมีการลีบหายไปหรือ Pinch-Out) ผู้จัดทำได้เลือกแพ็คเกจ HUF (Anderman and Hill, 2000) แทนการใช้ BCF (McDonald and Harbaugh, 1988) หรือ LPF (Harbaugh et al., 2000) ซึ่งข้อดีของการใช้ HUF คือไม่จำเป็นต้องใช้กริดละเอียด ก็สามารถจำลองการไหลของน้ำใต้ดินของชั้นน้ำที่ซับซ้อนได้ ดังรูปที่ 5

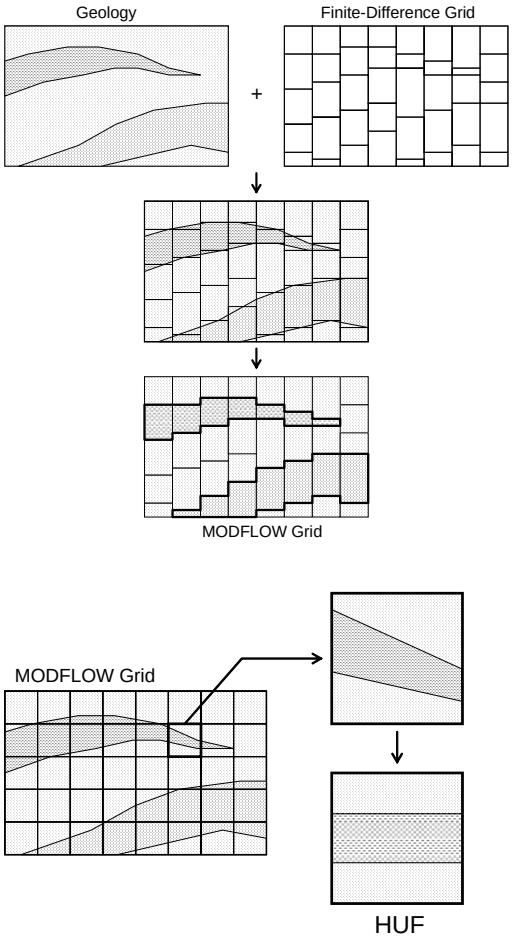

รูปที่ 5 การแบ่งกริดโดยใช้ LPF/BCF (บน) และ HUF (ล่าง)

ในการสร้างแบบจำลองคณิตศาสตร์จากรูปจำลองมโนทัศน์นี้ จะแบ่งพื้นที่ศึกษาซึ่งมีขนาด 12×15 ตร.กม. (E457000-E469000 และ N2160000-N2175000) ออกเป็น 120 คอลัมน์ (Column) ตามแนวทิศตะวันตก-ตะวันออก 150 แถว (Row) ตามแนวเหนือ-ใต้ และ 6 ชั้น (Layer) ซึ่งในแนวดิ่งหรือในแนวแกน นี้ จะมีความสูงตั้งแต่ 600 เมตร จนถึง ประมาณ 1470 เมตร (รทก.) โดยกริดที่ได้จะเป็นดัง รูปที่ 6 ตัวอย่างภาคตัดขวางของกริดสำหรับแถวที่ 84

แสดงใน รูปที่ 7 จาก Grid System ที่เห็นในรูปเหล่านี้ จะพบว่ามีข้อดีคือ ความสูงต่ำของแต่ละ Model Layer จะใกล้เคียงกับกับลักษณะภูมิประเทศและ Contact ของแต่ละหน่วยหิน

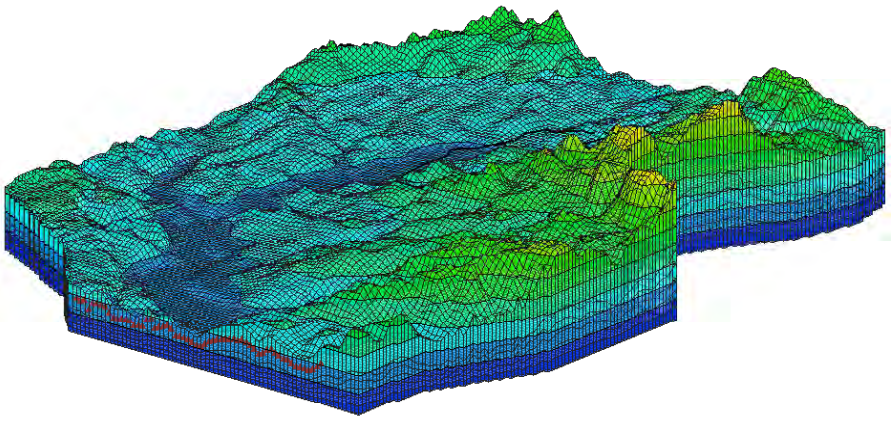

รูปที่ 6 การออกแบบกริดในแบบจำลอง

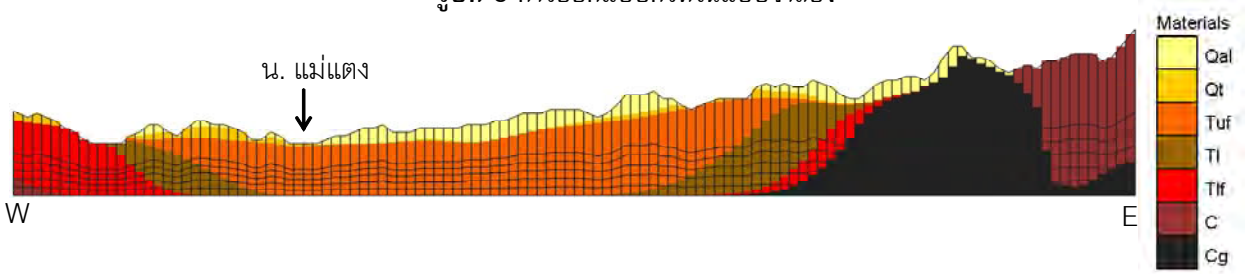

รูปที่ 7 ภาคตัดขวางของกริดในแถวที่ 84

เมื่อได้สร้างกริดสำหรับ MODFLOW เสร็จแล้ว ขั้นตอนต่อไปคือการใส่เงื่อนไขขอบและ Internal Source/Sink ต่างๆ เช่น แม่น้ำ ลำห้วยและสาขา (รูปที่ 8) Recharge Zone นอกจากนี้ขอบเขตของแบบจำลองสามด้าน ได้แก่ ด้านทิศเหนือ ใต้ และตะวันออก กำหนดให้เป็นเงื่อนไขขอบแบบ General Head Boundary (GHB) เนื่องจากขอบเขตของแอ่งที่ทำการจำลองมีขนาดใหญ่กว่าระบบกริด (Finite-Difference Grid) ของ MODFLOW ที่สร้างขึ้น จึงจำเป็นต้องใช้เงื่อนไขขอบ GHB เพื่อให้มีน้ำไหลเข้า-ออกแบบจำลองทางด้านข้างทั้งสามด้าน โดยค่า head ที่ขอบทั้งสามนั้นได้จากแผนที่ระดับน้ำใต้ดินซึ่ง ในที่นี้ ได้กำหนดไว้มีค่าเป็น 800.0, 780.0, และ 690.0 เมตร รทก. สำหรับขอบด้านทิศเหนือ ทิศตะวันตก และทิศใต้ ตามลำดับ ส่วนค่า conductance ของขอบทั้งสาม กำหนดค่าเริ่มต้นไว้ที่ 100.0 เมตร^2/วัน ซึ่งค่าที่ถูกต้องนั้น จะได้มาจากการปรับแบบจำลอง

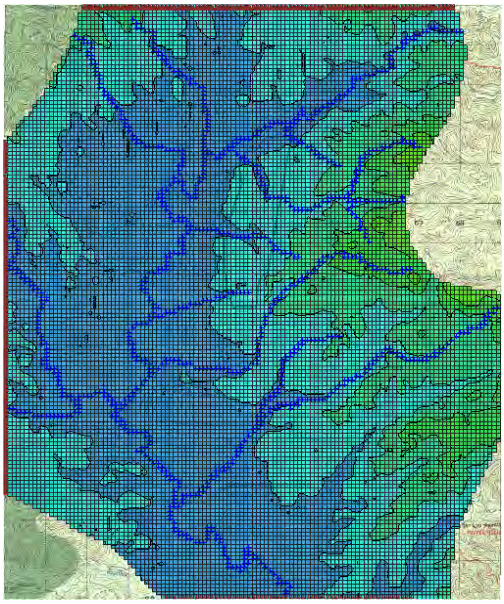

รูปที่ 8 แสดง Grid ที่เป็นแม่น้ำ/ลำห้วย

4. ผลการจำลองการไหล

เมื่อได้ Input ข้อมูลต่างๆ ลงไปในแบบจำลองแล้ว ขั้นตอนต่อไปคือทำการจำลอง (Simulate) การไหลในสภาวะคงที่ (Initial Run) ในที่นี้จะใช้ค่าสัมประสิทธิ์ความซึมหรือ Hydraulic Conductivity) ที่ได้จากการสูบทดสอบ (Pump Test) และ Falling Head Test สำหรับหน่วยหินที่ได้ทำการทดสอบ ส่วนหน่วยหินที่ไม่ได้ทำการทดสอบ โดยเฉพาะอย่างยิ่ง C และ Cg จะสุ่มค่า K เริ่มต้นไปก่อนโดยมี Guideline จาก Freeze and Cherry (1979) และสำหรับค่าของ Recharge ก็เช่นเดียวกัน จะใช้ค่าประมาณ 5% ของปริมาณน้ำฝน เมื่อทำการปรับแบบจำลองแล้วจะได้ค่าพารามิเตอร์ที่ใกล้เคียงกับความเป็นจริงมากขึ้น อัตราการใช้น้ำก็เป็นพารามิเตอร์หนึ่งที่ต้องทำการปรับ เนื่องจากในแอ่งเวียงแหงนี้มีบ่อบาดาลทั้งระดับตื้นและลึกอยู่มากมาย และการใช้น้ำของประชาชนในพื้นที่ก็ยังมีความไม่แน่นอน เนื่องจากไม่มีข้อมูลบันทึกช่วงเวลาสูบและอัตราการสูบน้ำขึ้นมาใช้ ดังนั้น ในการสร้างแบบจำลอง จึงได้กำหนดอัตราการสูบ “เฉลี่ย” เป็นพารามิเตอร์หนึ่งที่ต้องปรับเช่นเดียวกันกับ hydraulic conductivity หรือ recharge รูปที่ 9 แสดงกราฟของแรงดันน้ำ (Hydraulic Head) ที่ได้จากการจำลองเริ่มต้น (Initial Run) และจากการวัดระดับน้ำในบ่อสังเกตการณ์ จะเห็นว่าค่าที่ได้จากการคำนวณยังไม่สัมพันธ์กันกับค่าที่ได้จากการวัด ดังนั้น จะต้องมีการปรับแบบจำลอง (ปรับค่าพารามิเตอร์) เพื่อให้ผลการคำนวณใกล้ค่าจริงมากที่สุด

การปรับแบบจำลอง ได้อาศัยวิธี Automatic Parameter Estimation โดยใช้โปรแกรม PEST (Doherty, 1994) ซึ่งจะทำการปรับค่าพารามิเตอร์หลายๆ ตัวพร้อมๆ กันซึ่งแต่ละพารามิเตอร์จะถูก Update หรือเปลี่ยนไปในแต่ละ Iteration ตามค่า Sensitivity ของแต่ละตัว

รูปที่ 10 แสดงผลการปรับแบบจำลอง (Model Calibration) โดยใช้โปรแกรม PEST ซึ่งเป็นกราฟระหว่างแรงดันน้ำที่คำนวณได้จากแบบจำลองและที่ได้จากการวัด ณ บ่อสังเกตการณ์ จากรูปนี้จะเห็นว่า ค่าของ Head ในแบบจำลองใกล้เคียงกับค่าที่วัดได้ หากดูในรูปที่ 11 จะเห็นได้ชัดว่า ค่าของ Objective Function (แสดงถึงค่า Error หรือ Deviation ที่เปลี่ยนไปในแต่ละ Iteration) เริ่มลดลงเรื่อยๆ จาก Iteration ครั้งที่ 1 ถึง 19 (แต่ละ Iteration แสดงถึงการ Update ค่าพารามิเตอร์ในแต่ละครั้งของกระบวนการ Parameter Estimation)

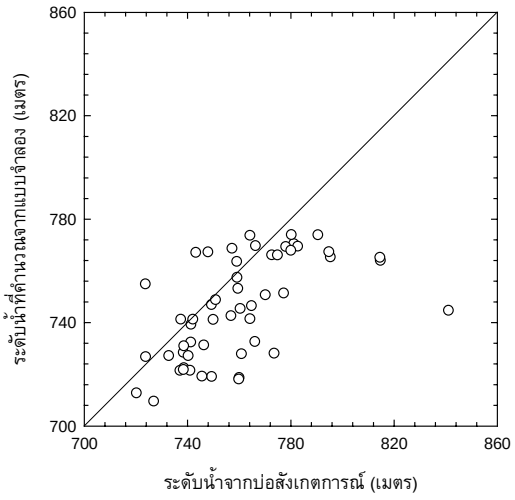

รูปที่ 9 ค่าแรงดันน้ำ ณ บ่อสังเกตการณ์ (ค่าที่วัด vs. ค่าที่คำนวณได้) ก่อนปรับแบบจำลอง

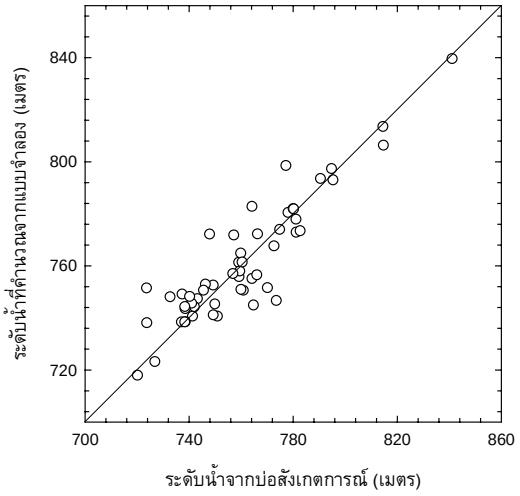

รูปที่ 10 ค่าแรงดันน้ำ ณ บ่อสังเกตการณ์ (ค่าที่วัด vs. ค่าที่คำนวณได้) **หลัง**การปรับแบบจำลอง

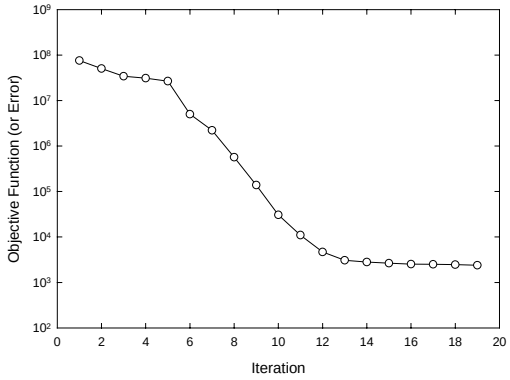

รูปที่ 11 ค่า Objective Function ของ Parameter Estimation ในการคำนวณแต่ละ Iteration

รูปที่ 12 แสดง Contour Lines ของแรงดันน้ำ (Hydraulic Head) และเส้นทางการไหลของน้ำบาดาลในแอ่ง จะเห็นว่าเส้นทางการไหลนั้นคล้ายคลึงกับรูปจำลอง Conceptual ที่ได้ออกแบบไว้ตั้งแต่แรก คือน้ำบาดาลจะไหลจากขอบแอ่งทางด้านเหนือ ตะวันตก และตะวันออก เข้าสู่ใจกลางแอ่งที่ลำน้ำแม่แตง โดยเส้นทางการไหลของน้ำบาดาล (ลูกศรสีน้ำตาล) จะไหลผ่านพื้นที่โครงการฯ เข้าสู่ลำน้ำแตง

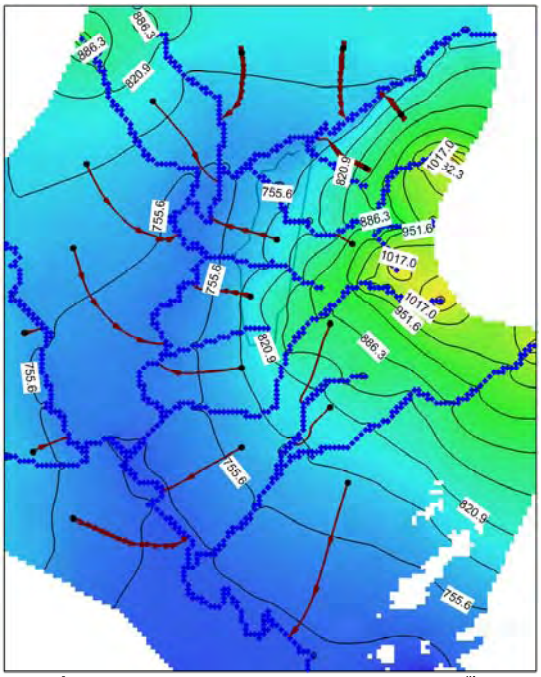

รูปที่ 12 Contour Lines ของ หรือแรงดันน้ำและเส้นทางการไหลหลังจากปรับแบบจำลองแล้ว

ในการศึกษาครั้งนี้ ถึงแม้ว่าจะมีข้อมูลอยู่ในปริมาณที่จำกัด แต่ข้อมูลเหล่านี้ (ทั้งที่เป็นข้อมูลดิบ เช่นระดับน้ำ การสูบทดสอบ ข้อมูลหลุมหยั่ง และที่เป็นข้อมูลทุติยภูมิเช่น Cross-Section หรือ Well-Log) ก็มีประโยชน์อยู่ในการสร้างแบบจำลองการไหลของน้ำใต้ดินในแอ่งเวียงแหง ตลอดจนการปรับแบบจำลองโดยใช้ข้อมูลที่มีอยู่ จนได้แบบจำลองที่พอจะเชื่อถือได้ในระดับหนึ่ง ที่จะนำไปใช้ศึกษาผลกระทบต่อปริมาณน้ำใต้ดินในพื้นที่ศึกษาจากการดำเนินโครงการในขั้นตอนต่อไป

5. เอกสารอ้างอิง

การไฟฟ้าฝ่ายผลิตแห่งประเทศไทย 2542, 2545 และ 2546 รายงานการศึกษาด้านธรณีวิทยา ธรณีวิศวกรรม และอุทกธรณีวิทยาของแอ่งเวียงแหง อ.เวียงแหง จ.เชียงใหม่

Doherty, J. 1994. PEST A Model Independent Parameter Estimation Program. Corinda, Australia, Watermark Numerical Computing. 122p.

Freeze, R.A., and J.A. Cherry. 1979. Groundwater, Prentice Hall, New York

Harbaugh, A.W., E.R. Banta, M.C. Hill, and M.G. McDonald. 2000. MODFLOW-2000, The U.S. Geological Survey Modular Ground-Water Model. User Guide to Modularization Concepts and the Ground-Water Processes. U.S. Geological Survey Open-File Report 00-92.

ผู้จัดทำขอขอบคุณการไฟฟ้าฝ่ายผลิตแห่งประเทศไทยที่ได้สนับสนุนงบประมาณและอำนวยความสะดวกในการจัดหาข้อมูงข้อมูลสำหรับการศึกษาครั้งนี้

แบบจำลองไฟไนต์อิลิเมนต์กาเลอคินสำหรับจำลองการปนเปื้อนของสารอินทรีย์ในน้ำใต้ดิน

FINITE ELEMENT GALERKIN MODEL FOR SIMULATING FATE AND TRANSPORT OF DISSOLVED ORGANIC COMPOUND IN GROUNDWATER

มรกต เก็บเจริญ,[1] ศตวรรษ แสนทน[2]

Morrakot Khebchareon,[1] Satawat Saenton[2]

[1]Department of Mathematics, Faculty of Science, Chiang Mai University, Chiang Mai, 50200. Email: mkhebcha@chiangmai.ac.th

[2]Department of Geological Sciences, Faculty of Science, Chiang Mai University, Chiang Mai, 50200. Email: ssaenton@chiangmai.ac.th

บทคัดย่อ: สารอินทรีย์ที่มีความหนาแน่นสูงกว่าน้ำ (DNAPLs) เช่นตัวทำลายชนิดต่างๆ เมื่อซึมลงไปในดินจะละลายในน้ำอย่างช้าๆ ทำให้เกิดการปนเปื้อนของน้ำใต้ดินระดับตื้นเป็นวงกว้าง การออกแบบระบบบำบัดฟื้นฟูน้ำใต้ดินซึ่งถูกปนเปื้อน จะต้องใช้แบบจำลองคณิตศาสตร์ที่อธิบายกระบวนการต่างๆ อาทิ การไหลของน้ำใต้ดิน การละลายของสารอินทรีย์ การเคลื่อนตัวและการแพร่กระจายของสารอินทรีย์ในชั้นหินอุ้มน้ำ ซึ่งแบบจำลองดังกล่าวเป็นระบบสมการเชิงอนุพันธ์ย่อยที่ต้องอาศัยการประมาณคำตอบด้วยระเบียบวิธีเชิงตัวเลข ในการศึกษาครั้งนี้ผู้ศึกษาได้จัดทำแบบจำลองคณิตศาสตร์เชิงตัวเลขชนิดไฟไนต์อิลิเมนต์กาเลอคินสำหรับแก้ระบบสมการดังกล่าวในหนึ่งและสองมิติ โดยระบบที่มีโดเมนเป็นหนึ่งมิตินั้น แบบจำลองได้รับการยืนยันจากผลเฉลยในรูปฟังก์ชันวิเคราะห์ (analytical solution) และจากข้อมูลผลการทดลองในห้องปฏิบัติการ ส่วนผลเฉลยในรูปฟังก์ชันวิเคราะห์ของปัญหาในสองมิติสำหรับปัญหาประเภทนี้ไม่มี ดังนั้น จึงได้เพียงเปรียบเทียบกับผลการจำลองกับวิธีไฟไนต์ดิฟเฟอเรนซ์ โดยในอนาคตจะทดสอบแบบจำลองในสองมิติกับผลการทดลองจากห้องปฏิบัติการอีกครั้งหนึ่ง

Abstract: Dense, non-aqueous phase liquids (DNAPLs) are common organic contaminants in subsurface environment. Once spilled or leaked underground, they slowly dissolved into groundwater and generated a plume of contaminants. In order to manage the contaminated site and predict the behavior of dissolved DNAPL in heterogeneous subsurface requires a comprehensive numerical model. In this work, the Crank-Nicolson finite-element Galerkin (CN-FEG) numerical scheme for solving a set coupled system of partial differential equations that describes fate and transport of dissolved organic compounds in one- and two-dimensional domain was developed and implemented. In case for 1-D model, the code was verified with analytical solutions and tested with experimental data. Although no analytical solution exists for code verification in 2-D case, the results from CN-FEG scheme were comparable to the solutions obtained from an experimentally validated finite-difference program. Future work includes validation of the model using experimental data of DNAPL dissolution in 2-D test cell.

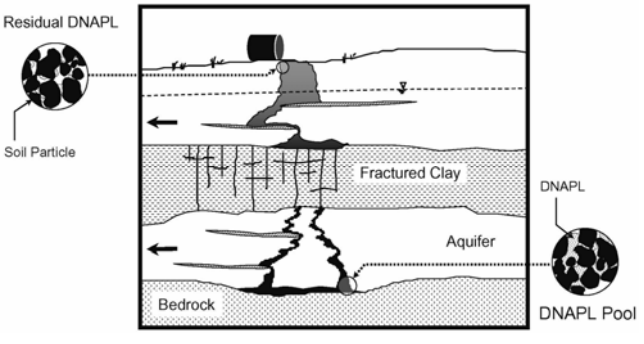

Introduction: Dense Non-aqueous phase liquids (DNAPLs) are organic compounds that are immiscible in water, and they present another phase of concern in groundwater contamination problems [3]. They present special problems for the hydrogeologists, regulators, and engineers because their fate and transport are difficult to simulate and because they may follow irregular flow paths in heterogeneous porous media. Most NAPLs are health hazard and some are known to be carcinogens. Once they leaked or spilled into soils, as shown in picture (above), significant fraction of DNAPL remained entrapped and

slowly dissolve into the flowing groundwater. Partial or full exposure to polluted groundwater results in a high risk for those who are located downstream of the DNAPL source zone. Although aqueous solubility of components in NAPLs is low, its concentration level is much higher than the regulated drinking water standards. Therefore there is the need for immediate action to clean-up contaminated aquifers. Several active remediation schemes such as pump-and-treat, in situ chemical oxidation, surfactant-enhanced dissolution, and bioremediation have been proposed and implemented to clean-up NAPL sources but result in mixed success. This is particularly due to an inability to locate NAPL source zone as well as the implementation of the clean-up technology. In addition, slow dissolution kinetics of organic components from NAPLs to a flowing groundwater lengthens NAPL source's life, thus prolonging and extending groundwater contamination. In order to predict NAPL source's longevity or to estimate the clean-up duration of the selected remediation technologies, a validated numerical model is needed. This study therefore aims to develop a validated numerical code that is capable of simulating groundwater flow, contaminant transport, and mass transfer processes in NAPLs contaminated aquifers.

Methodology: Governing equations describing the groundwater flow, DNAPL dissolution and advection-dispersion of dissolved DNAPL in aquifer are shown in (1.1)-(1.3);

$$S_s \frac{\partial h}{\partial t} = \vec{\nabla} \cdot (\mathbf{K} \nabla h) + W \tag{1.1}$$

$$\frac{\partial C}{\partial t} = -\vec{\nabla} \cdot (\mathbf{v} C - \mathbf{D} \nabla C) - \frac{\partial}{\partial t}(\rho_n \phi_0 S_n) \tag{1.2}$$

$$\frac{\partial}{\partial t}(\rho_n \phi_0 S_n) = -k_{La}(C - C_s) \tag{1.3}$$

where S_s, h, $\mathbf{K}$, and W are specific storage, hydraulic head, hydraulic conductivity tensor, and source/sink, respectively. In the mass transport equations, parameters C, $\mathbf{v}$, $\mathbf{D}$, S_n, k_{La}, ρ_n, and ϕ_0 are contaminant concentration, groundwater velocity ($\mathbf{v} = -\mathbf{K}\nabla h / (1 - S_n)\phi_0$), dispersion coefficient tensor, DNAPL saturation, mass transfer coefficient, DNAPL density, and initial porosity of an aquifer, respectively. In finite-element Galerkin method a domain of interest was discretized into small regions called elements and each element consists of nodes. In this research, a linear element was used for 1-D domain while a linear triangular domain was used in case of 2-D. The minimization of weighted residuals resulted in the following system of linear algebraic equations as shown in (2) and (3).

GW Flow:

$$\begin{aligned}([S] + \omega\Delta t[K])\{h\}_{t+\Delta t} &= ([S] - (1-\omega)\Delta t[K])\{h\}_t \\ &+ \Delta t\,(\omega\{F\}_{t+\Delta t} + (1-\omega)\{F\}_t)\end{aligned} \tag{2}$$

Transport:

$$\begin{aligned}([A] + \omega\Delta t[D])\{C\}_{t+\Delta t} &= ([A] - (1-\omega)\Delta t[D])\{h\}_t \\ &+ \Delta t\,(\omega\{F\}_{t+\Delta t} + (1-\omega)\{F\}_t) \\ &+ \Delta t\,\{M\}\end{aligned} \tag{3}$$

The above expressions are called finite-element Galerkin scheme for solving groundwater flow and contaminant transport (with DNAPL dissolution) equations. A parameter ω is used to change the scheme from fully-implicit (ω = 1.0) to fully-explicit schemes (ω = 0.0). If ω = 0.5, ascheme is called Crank-Nicolson finite-element Galerkin or CN-FEG scheme. The terms [A], [D], [S], and [K] refer to adsorption, advection-dispersion, storage, and conductance matrices, respectively; where {F}, and {M} are flux and dissolution vectors. The above scheme was

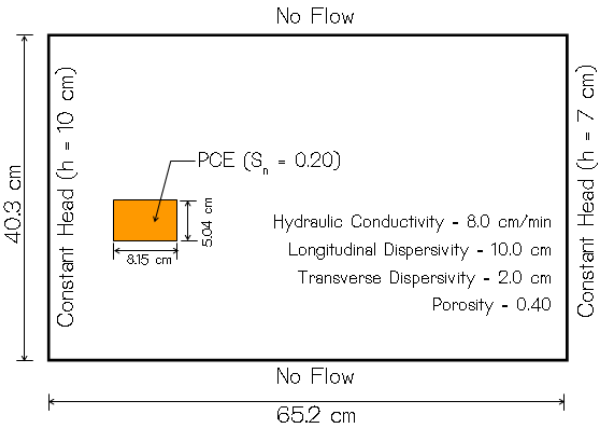

implemented by modifying the computer codes developed by Istok [1]. The developed scheme was also successfully tested using 1-D analytical solution and 1-D column experimental data [2,5]. In this paper, a solution from CNFEG scheme was compared to solutions obtained from finite-difference method [4] using a hypothetical test problem in 2-D domain as shown in picture (above).

Results: Simulation of rate-limited mass transfer and advective-dispersive transport of dissolved PCE for both finite-element and finite-difference programs are shown in Fig. 1. These pictures show contour lines (or color shades) of equal PCE concentration after 10 minutes (using k_{La} = 10 min^{-1}). As expected, dissolved PCE plume moves from left to right according to hydraulic gradient and it also diffuses around the source zone due to dispersion. Although both solutions were comparable, it is however not possible assess the accuracy or validity of the results since analytical solution does not exist in order to make direct comparison. Our future work will include validating the code using experimental data.

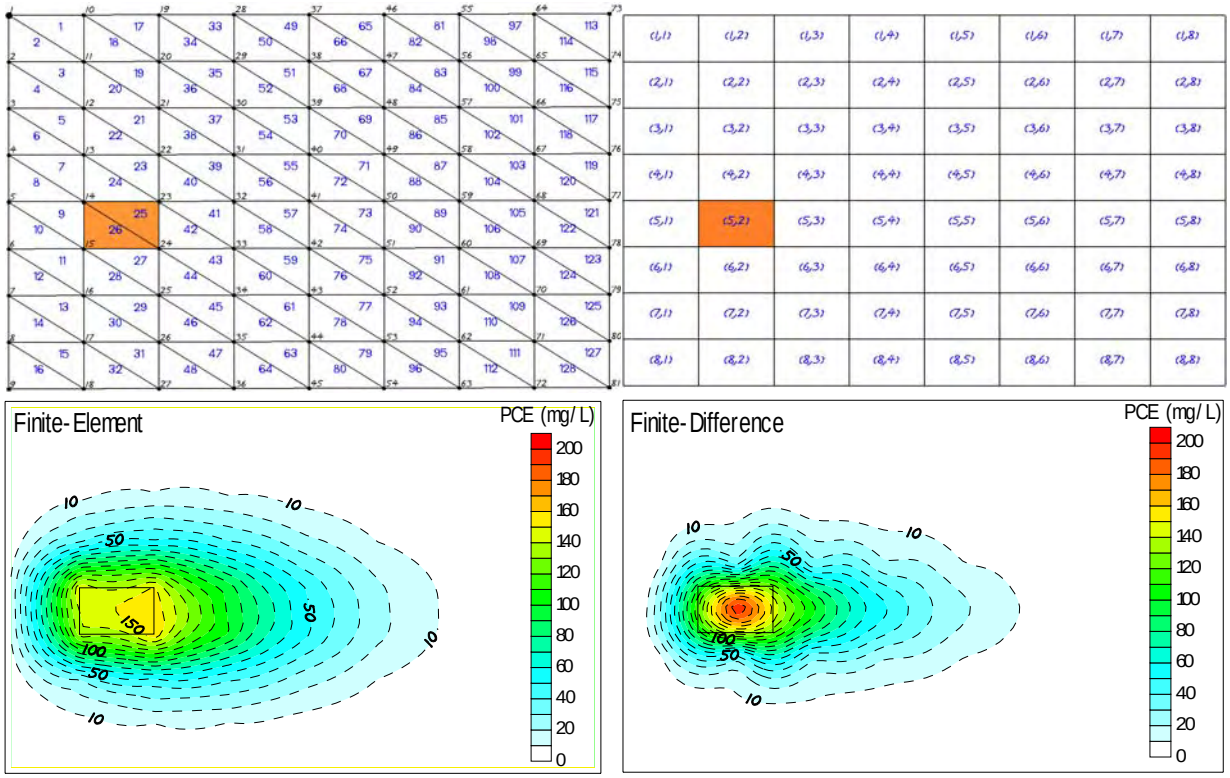

Figure 1 Simulation of PCE dissolution using CN-FEG scheme and finite-difference method.

References:

1. J. Istok. Groundwater Modeling by the Finite Element Method. Water Resources Monograph. American Geophysical Union, 1989.
2. M. Khebchareon and S. Saenton. Finite element solution for 1-D groundwater flow, advection-dispersion, and interphase mass transfer: I. Model development. Thai Journal of Mathematics, 3(2):223-240, 2005.
3. J.W. Mercer and R.M. Cohen. A review of immiscible fluids in the sub- surface: Properties, models, characterization and remediation. Journal of Contaminant Hydrology, 6:107-163, 1990.
4. S. Saenton. Prediction of Mass Flux from DNAPL Source Zone with Complex Entrapment Architecture: Model development, Experimental Validation, and Up-Scaling. PhD thesis, Colorado School of Mines, U.S.A., 2003.
5. S. Saenton and M. Khebchareon. Finite element solution for 1-D groundwater flow, advection-dispersion, and interphase mass transfer: II. Experimental validation. Chiang Mai Journal of Science, 33(2):161-168, 2006.

Keywords: finite-element Galerkin, Crank-Nicolson, groundwater, DNAPL, tetrachloroethene, modeling

Acknowledgements: Authors gratefully acknowledge the financial support from the Thailand Research Fund (TRF) Grant nos. MRG4980128 and MRG4980079.

Appendix B

Groundwater Budgets & Calibration Results for 10 Realizations

Groundwater Budget & Calibration Results for Realization #1
(Time = day, Length = meter)

VOLUMETRIC BUDGET FOR ENTIRE MODEL AT END OF TIME STEP 1 IN STRESS PERIOD 1

CUMULATIVE VOLUMES	L**3	RATES FOR THIS TIME STEP	L**3/T
IN:		IN:	
STORAGE =	0.0000	STORAGE =	0.0000
CONSTANT HEAD =	0.0000	CONSTANT HEAD =	0.0000
WELLS =	0.0000	WELLS =	0.0000
RIVER LEAKAGE =	106400.1250	RIVER LEAKAGE =	106400.1250
ET =	0.0000	ET =	0.0000
HEAD DEP BOUNDS =	852.8888	HEAD DEP BOUNDS =	852.8888
RECHARGE =	569915.6875	RECHARGE =	569915.6875
TOTAL IN =	677168.6875	TOTAL IN =	677168.6875
OUT:		OUT:	
STORAGE =	0.0000	STORAGE =	0.0000
CONSTANT HEAD =	0.0000	CONSTANT HEAD =	0.0000
WELLS =	212257.7188	WELLS =	212257.7188
RIVER LEAKAGE =	114725.7109	RIVER LEAKAGE =	114725.7109
ET =	317929.8438	ET =	317929.8438
HEAD DEP BOUNDS =	771.6244	HEAD DEP BOUNDS =	771.6244
RECHARGE =	0.0000	RECHARGE =	0.0000
TOTAL OUT =	645684.8750	TOTAL OUT =	645684.8750
IN - OUT =	31483.8125	IN - OUT =	31483.8125
PERCENT DISCREPANCY =	4.76	PERCENT DISCREPANCY =	4.76

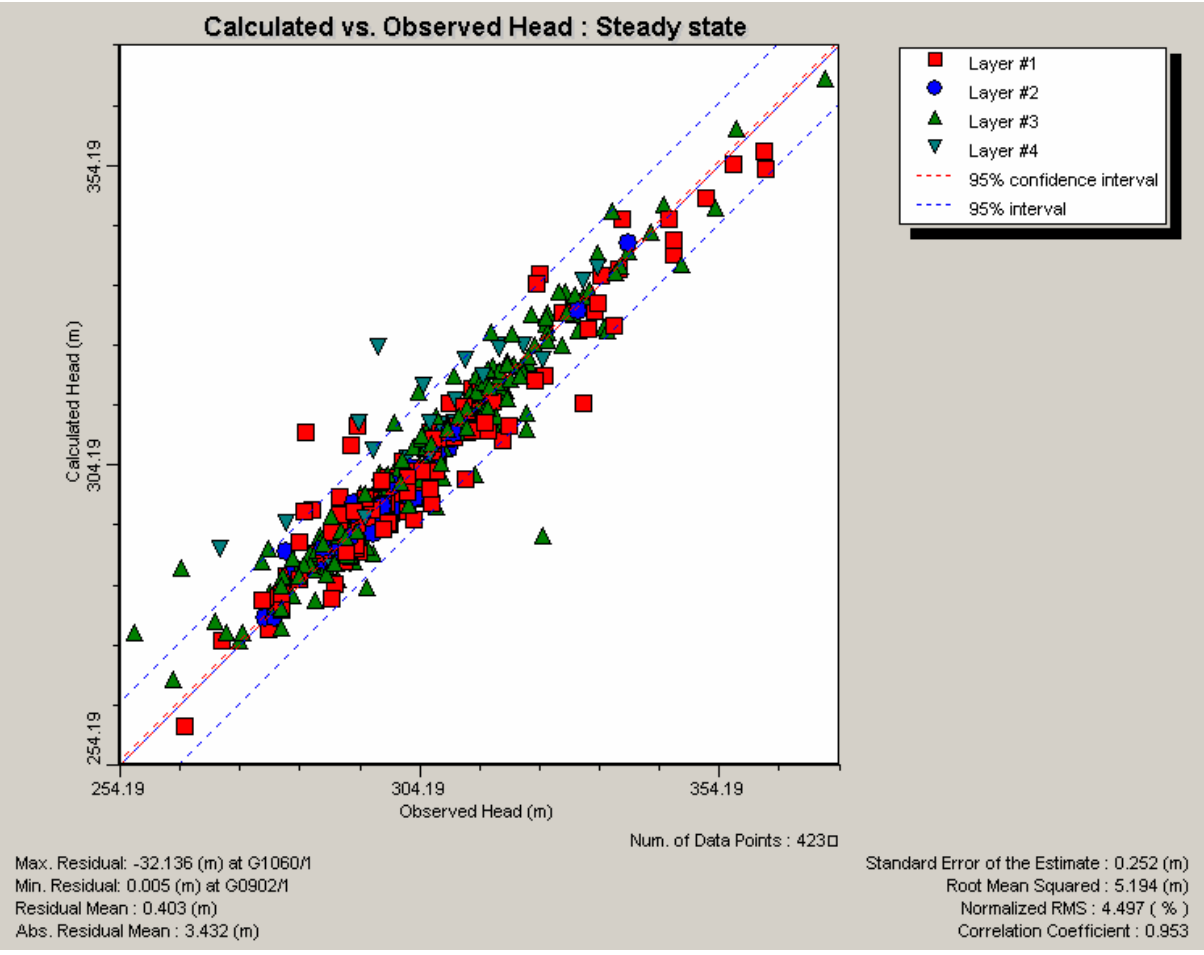

Groundwater Budget & Calibration Results for Realization #2
(Time = day, Length = meter)

VOLUMETRIC BUDGET FOR ENTIRE MODEL AT END OF TIME STEP 1 IN STRESS PERIOD 1

CUMULATIVE VOLUMES	L**3	RATES FOR THIS TIME STEP	L**3/T
IN:		IN:	
STORAGE =	0.0000	STORAGE =	0.0000
CONSTANT HEAD =	0.0000	CONSTANT HEAD =	0.0000
WELLS =	0.0000	WELLS =	0.0000
RIVER LEAKAGE =	105313.7266	RIVER LEAKAGE =	105313.7266
ET =	0.0000	ET =	0.0000
HEAD DEP BOUNDS =	877.1571	HEAD DEP BOUNDS =	877.1571
RECHARGE =	569915.6875	RECHARGE =	569915.6875
TOTAL IN =	676106.5625	TOTAL IN =	676106.5625
OUT:		OUT:	
STORAGE =	0.0000	STORAGE =	0.0000
CONSTANT HEAD =	0.0000	CONSTANT HEAD =	0.0000
WELLS =	212257.7188	WELLS =	212257.7188
RIVER LEAKAGE =	111640.7188	RIVER LEAKAGE =	111640.7188
ET =	313814.3125	ET =	313814.3125
HEAD DEP BOUNDS =	766.8383	HEAD DEP BOUNDS =	766.8383
RECHARGE =	0.0000	RECHARGE =	0.0000
TOTAL OUT =	638479.5625	TOTAL OUT =	638479.5625
IN - OUT =	37627.0000	IN - OUT =	37627.0000
PERCENT DISCREPANCY =	5.72	PERCENT DISCREPANCY =	5.72

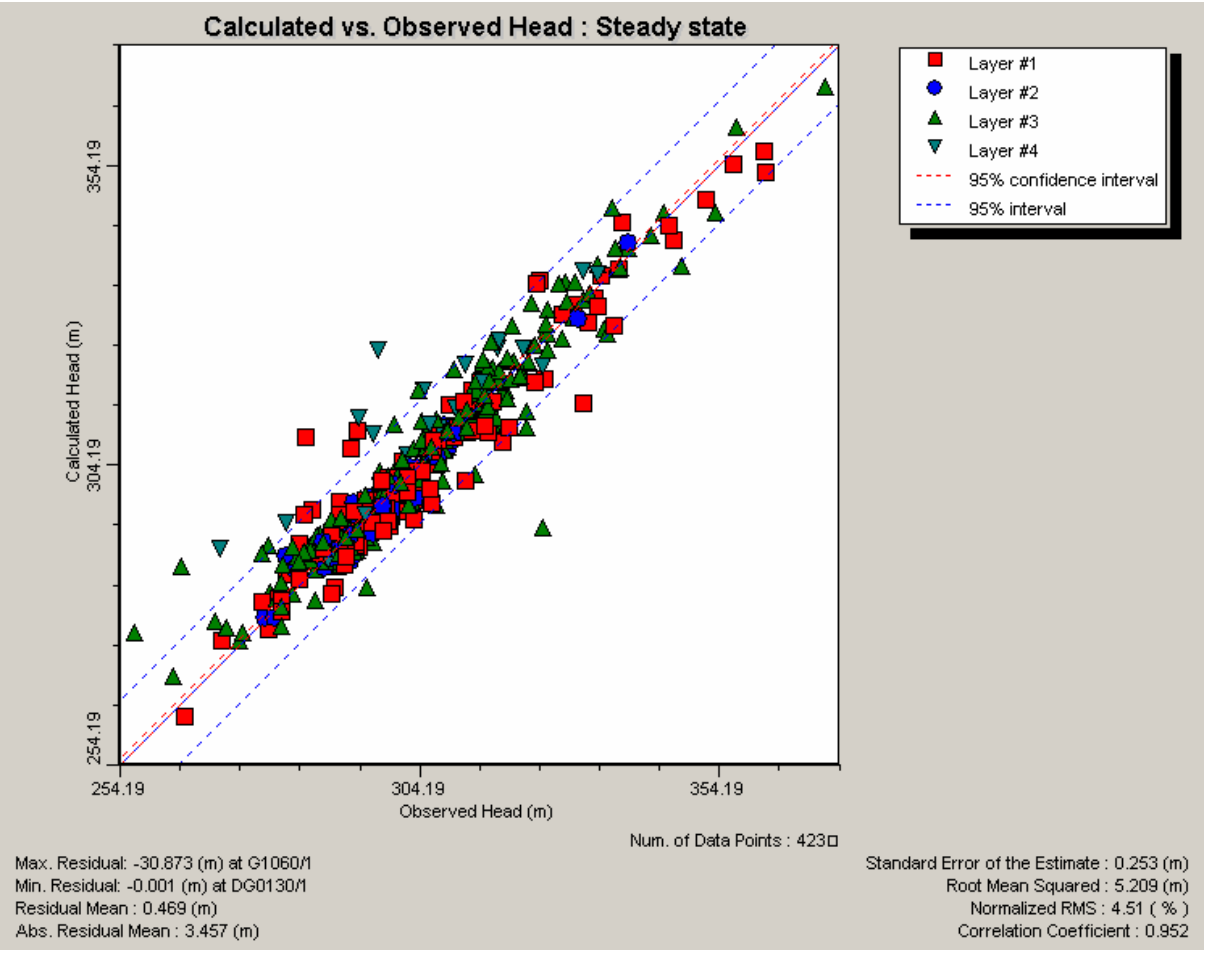

Groundwater Budget & Calibration Results for Realization #3
(Time = day, Length = meter)

VOLUMETRIC BUDGET FOR ENTIRE MODEL AT END OF TIME STEP 1 IN STRESS PERIOD 1

CUMULATIVE VOLUMES	L**3	RATES FOR THIS TIME STEP	L**3/T
IN:		IN:	
STORAGE =	0.0000	STORAGE =	0.0000
CONSTANT HEAD =	0.0000	CONSTANT HEAD =	0.0000
WELLS =	0.0000	WELLS =	0.0000
RIVER LEAKAGE =	106729.4453	RIVER LEAKAGE =	106729.4453
ET =	0.0000	ET =	0.0000
HEAD DEP BOUNDS =	850.1711	HEAD DEP BOUNDS =	850.1711
RECHARGE =	569915.6875	RECHARGE =	569915.6875
TOTAL IN =	677495.3125	TOTAL IN =	677495.3125
OUT:		OUT:	
STORAGE =	0.0000	STORAGE =	0.0000
CONSTANT HEAD =	0.0000	CONSTANT HEAD =	0.0000
WELLS =	212257.7188	WELLS =	212257.7188
RIVER LEAKAGE =	115212.1719	RIVER LEAKAGE =	115212.1719
ET =	319637.5000	ET =	319637.5000
HEAD DEP BOUNDS =	778.3486	HEAD DEP BOUNDS =	778.3486
RECHARGE =	0.0000	RECHARGE =	0.0000
TOTAL OUT =	647885.7500	TOTAL OUT =	647885.7500
IN - OUT =	29609.5625	IN - OUT =	29609.5625
PERCENT DISCREPANCY =	4.47	PERCENT DISCREPANCY =	4.47

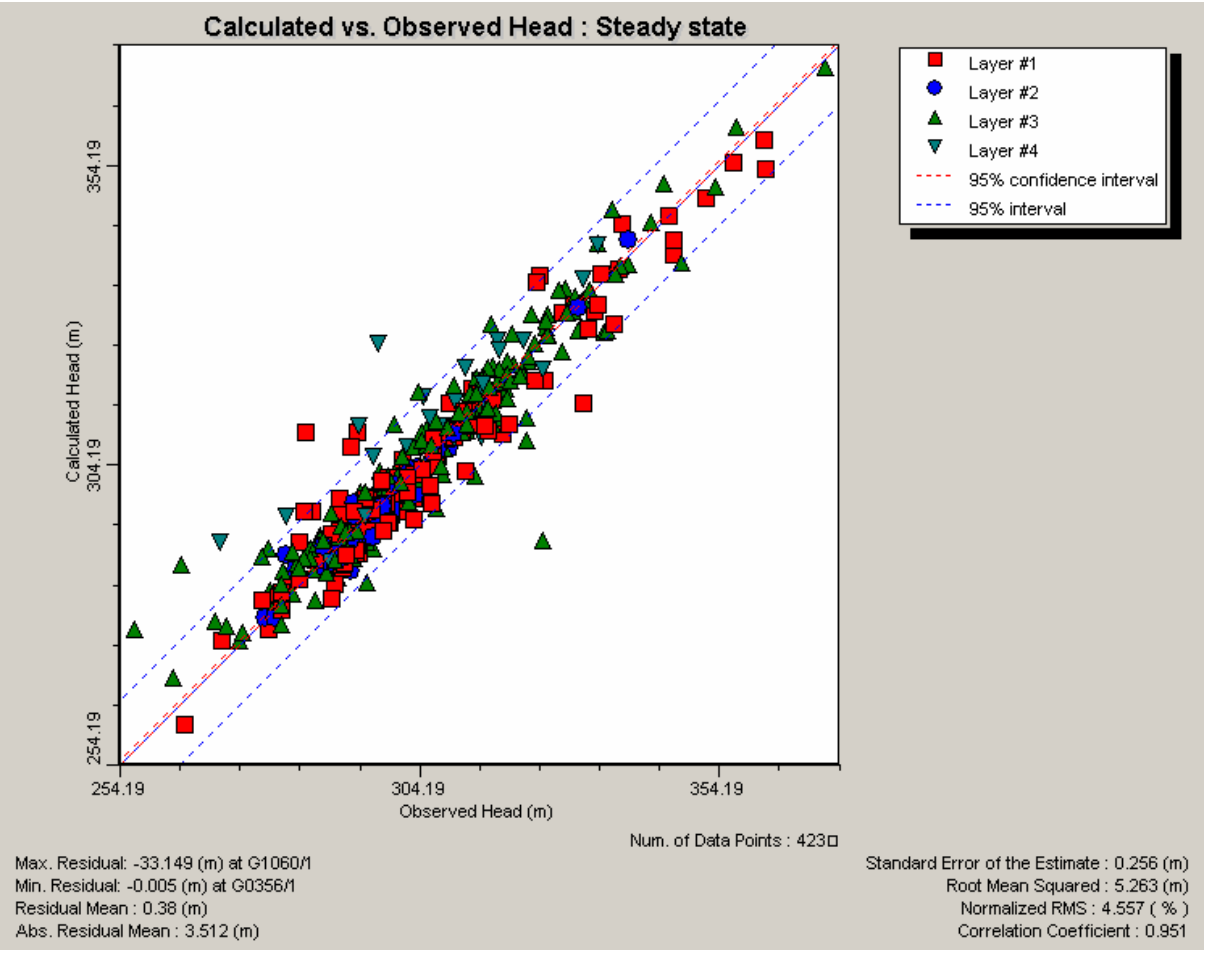

Groundwater Budget & Calibration Results for Realization #4
(Time = day, Length = meter)

VOLUMETRIC BUDGET FOR ENTIRE MODEL AT END OF TIME STEP 1 IN STRESS PERIOD 1

CUMULATIVE VOLUMES	L**3	RATES FOR THIS TIME STEP	L**3/T
IN:		IN:	
STORAGE =	0.0000	STORAGE =	0.0000
CONSTANT HEAD =	0.0000	CONSTANT HEAD =	0.0000
WELLS =	0.0000	WELLS =	0.0000
RIVER LEAKAGE =	107765.5781	RIVER LEAKAGE =	107765.5781
ET =	0.0000	ET =	0.0000
HEAD DEP BOUNDS =	837.7482	HEAD DEP BOUNDS =	837.7482
RECHARGE =	569915.6875	RECHARGE =	569915.6875
TOTAL IN =	678519.0000	TOTAL IN =	678519.0000
OUT:		OUT:	
STORAGE =	0.0000	STORAGE =	0.0000
CONSTANT HEAD =	0.0000	CONSTANT HEAD =	0.0000
WELLS =	212257.7188	WELLS =	212257.7188
RIVER LEAKAGE =	114635.7266	RIVER LEAKAGE =	114635.7266
ET =	315725.5938	ET =	315725.5938
HEAD DEP BOUNDS =	774.3561	HEAD DEP BOUNDS =	774.3561
RECHARGE =	0.0000	RECHARGE =	0.0000
TOTAL OUT =	643393.3750	TOTAL OUT =	643393.3750
IN - OUT =	35125.6250	IN - OUT =	35125.6250
PERCENT DISCREPANCY =	5.31	PERCENT DISCREPANCY =	5.31

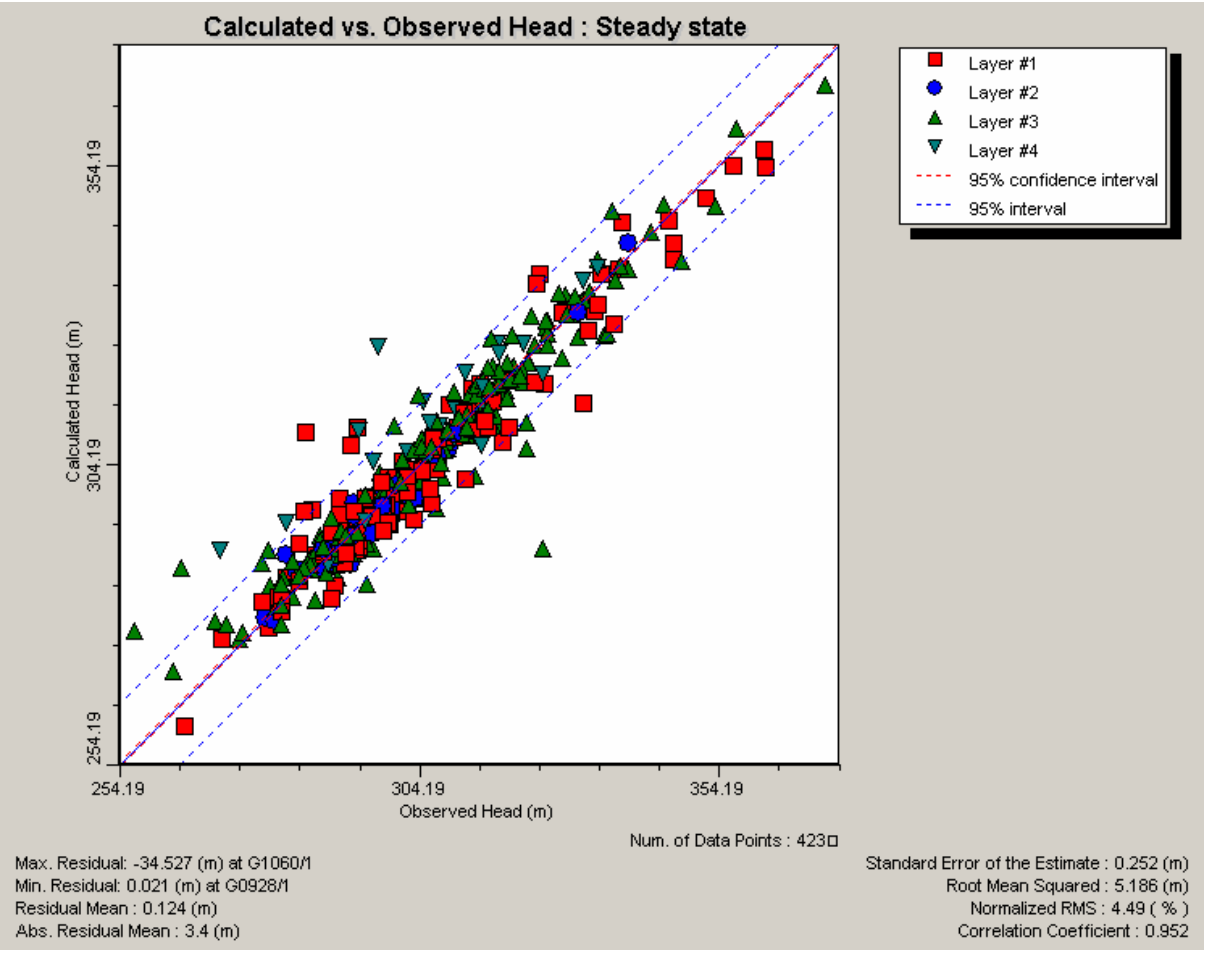

Groundwater Budget & Calibration Results for Realization #5
(Time = day, Length = meter)

VOLUMETRIC BUDGET FOR ENTIRE MODEL AT END OF TIME STEP 1 IN STRESS PERIOD 1

CUMULATIVE VOLUMES	L**3	RATES FOR THIS TIME STEP	L**3/T
IN:		IN:	
STORAGE =	0.0000	STORAGE =	0.0000
CONSTANT HEAD =	0.0000	CONSTANT HEAD =	0.0000
WELLS =	0.0000	WELLS =	0.0000
RIVER LEAKAGE =	108295.5547	RIVER LEAKAGE =	108295.5547
ET =	0.0000	ET =	0.0000
HEAD DEP BOUNDS =	869.0826	HEAD DEP BOUNDS =	869.0826
RECHARGE =	569915.6875	RECHARGE =	569915.6875
TOTAL IN =	679080.3125	TOTAL IN =	679080.3125
OUT:		OUT:	
STORAGE =	0.0000	STORAGE =	0.0000
CONSTANT HEAD =	0.0000	CONSTANT HEAD =	0.0000
WELLS =	212257.7188	WELLS =	212257.7188
RIVER LEAKAGE =	115196.0000	RIVER LEAKAGE =	115196.0000
ET =	316574.0312	ET =	316574.0312
HEAD DEP BOUNDS =	761.5087	HEAD DEP BOUNDS =	761.5087
RECHARGE =	0.0000	RECHARGE =	0.0000
TOTAL OUT =	644789.2500	TOTAL OUT =	644789.2500
IN - OUT =	34291.0625	IN - OUT =	34291.0625
PERCENT DISCREPANCY =	5.18	PERCENT DISCREPANCY =	5.18

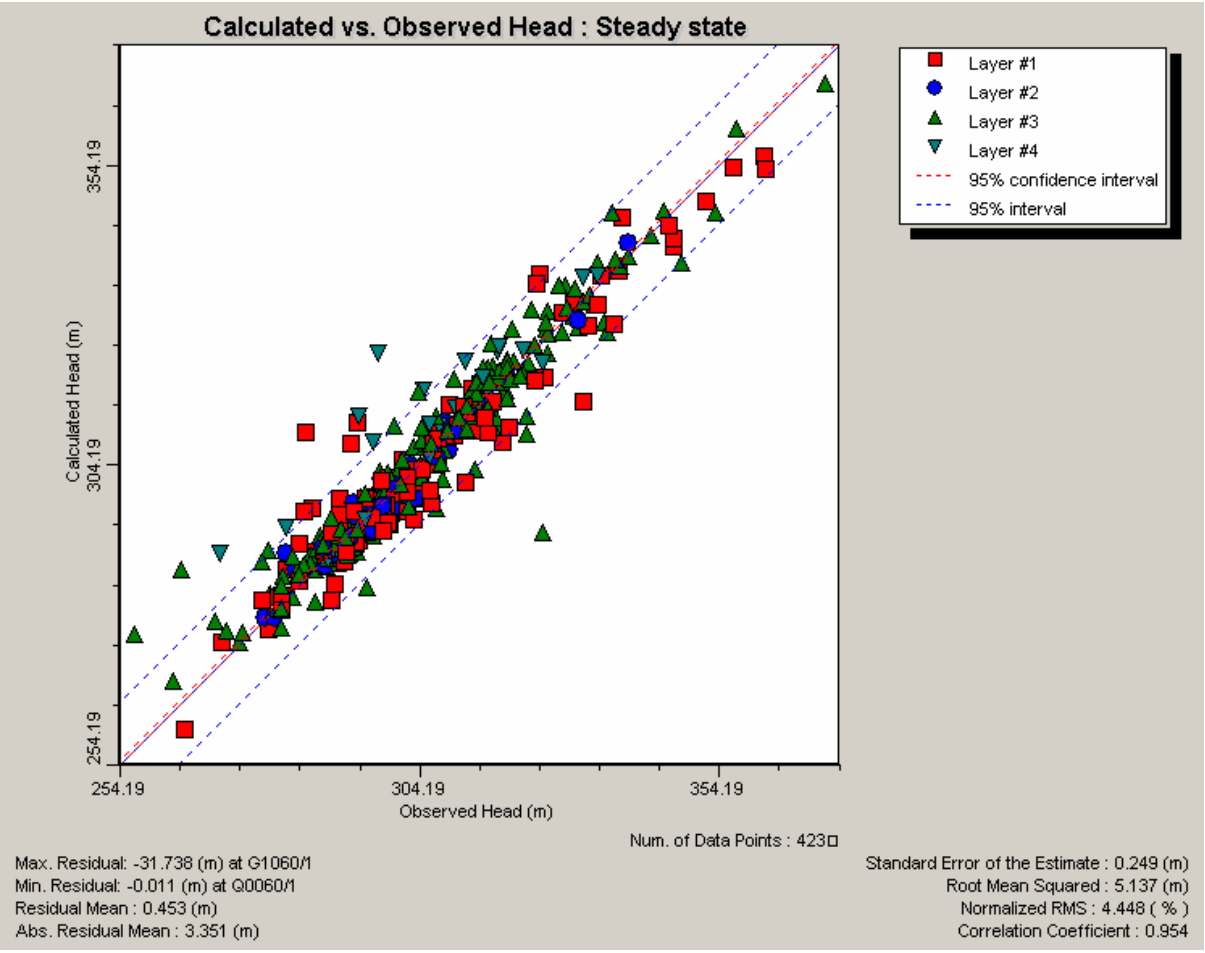

Groundwater Budget & Calibration Results for Realization #6
(Time = day, Length = meter)

VOLUMETRIC BUDGET FOR ENTIRE MODEL AT END OF TIME STEP 1 IN STRESS PERIOD 1

CUMULATIVE VOLUMES	L**3	RATES FOR THIS TIME STEP	L**3/T
IN:		IN:	
STORAGE =	0.0000	STORAGE =	0.0000
CONSTANT HEAD =	0.0000	CONSTANT HEAD =	0.0000
WELLS =	0.0000	WELLS =	0.0000
RIVER LEAKAGE =	107988.6641	RIVER LEAKAGE =	107988.6641
ET =	0.0000	ET =	0.0000
HEAD DEP BOUNDS =	873.0763	HEAD DEP BOUNDS =	873.0763
RECHARGE =	569915.6875	RECHARGE =	569915.6875
TOTAL IN =	678777.4375	TOTAL IN =	678777.4375
OUT:		OUT:	
STORAGE =	0.0000	STORAGE =	0.0000
CONSTANT HEAD =	0.0000	CONSTANT HEAD =	0.0000
WELLS =	212257.7188	WELLS =	212257.7188
RIVER LEAKAGE =	115074.0938	RIVER LEAKAGE =	115074.0938
ET =	316707.5000	ET =	316707.5000
HEAD DEP BOUNDS =	759.7283	HEAD DEP BOUNDS =	759.7283
RECHARGE =	0.0000	RECHARGE =	0.0000
TOTAL OUT =	644799.0625	TOTAL OUT =	644799.0625
IN - OUT =	33978.3750	IN - OUT =	33978.3750
PERCENT DISCREPANCY =	5.13	PERCENT DISCREPANCY =	5.13

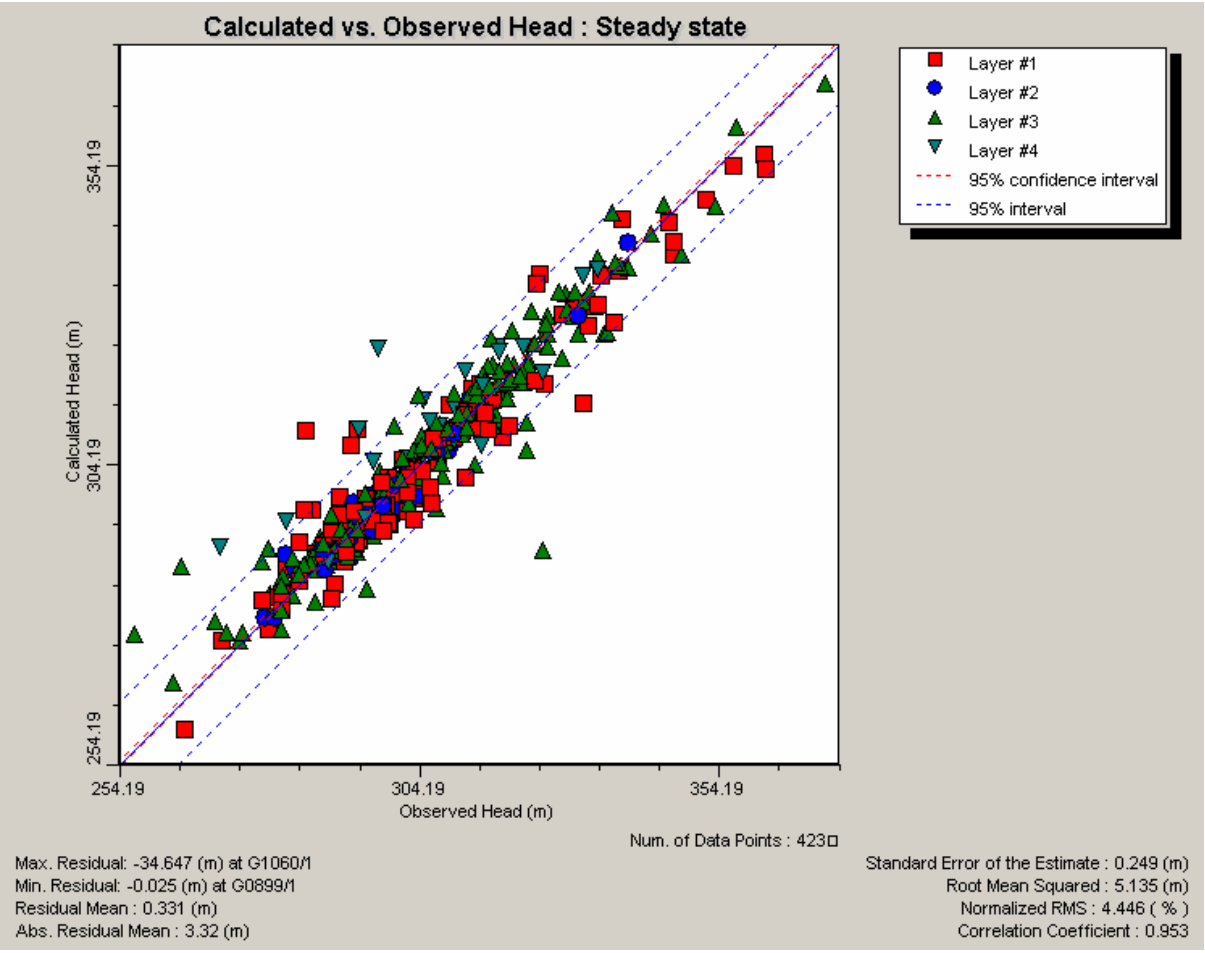

Groundwater Budget & Calibration Results for Realization #7
(Time = day, Length = meter)

VOLUMETRIC BUDGET FOR ENTIRE MODEL AT END OF TIME STEP 1 IN STRESS PERIOD 1

CUMULATIVE VOLUMES	L**3	RATES FOR THIS TIME STEP	L**3/T
IN:		IN:	
STORAGE =	0.0000	STORAGE =	0.0000
CONSTANT HEAD =	0.0000	CONSTANT HEAD =	0.0000
WELLS =	0.0000	WELLS =	0.0000
RIVER LEAKAGE =	103850.6797	RIVER LEAKAGE =	103850.6797
ET =	0.0000	ET =	0.0000
HEAD DEP BOUNDS =	838.7792	HEAD DEP BOUNDS =	838.7792
RECHARGE =	569915.6875	RECHARGE =	569915.6875
TOTAL IN =	674605.1250	TOTAL IN =	674605.1250
OUT:		OUT:	
STORAGE =	0.0000	STORAGE =	0.0000
CONSTANT HEAD =	0.0000	CONSTANT HEAD =	0.0000
WELLS =	212257.7188	WELLS =	212257.7188
RIVER LEAKAGE =	109954.7656	RIVER LEAKAGE =	109954.7656
ET =	313018.8125	ET =	313018.8125
HEAD DEP BOUNDS =	758.5044	HEAD DEP BOUNDS =	758.5044
RECHARGE =	0.0000	RECHARGE =	0.0000
TOTAL OUT =	635989.8125	TOTAL OUT =	635989.8125
IN - OUT =	38615.3125	IN - OUT =	38615.3125
PERCENT DISCREPANCY =	5.89	PERCENT DISCREPANCY =	5.89

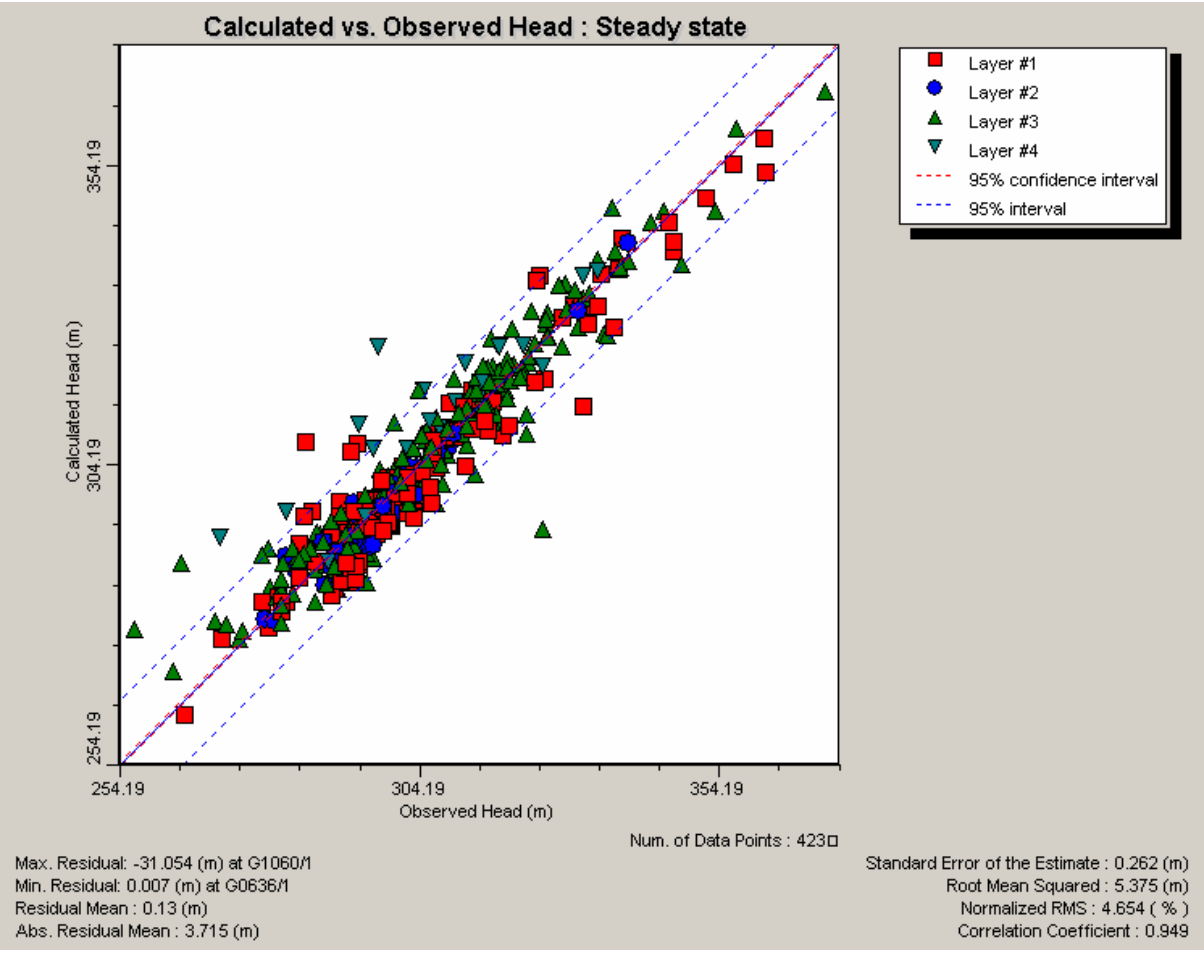

Groundwater Budget & Calibration Results for Realization #8
(Time = day, Length = meter)

VOLUMETRIC BUDGET FOR ENTIRE MODEL AT END OF TIME STEP 1 IN STRESS PERIOD 1

CUMULATIVE VOLUMES	L**3	RATES FOR THIS TIME STEP	L**3/T
IN:		IN:	
STORAGE =	0.0000	STORAGE =	0.0000
CONSTANT HEAD =	0.0000	CONSTANT HEAD =	0.0000
WELLS =	0.0000	WELLS =	0.0000
RIVER LEAKAGE =	107938.0156	RIVER LEAKAGE =	107938.0156
ET =	0.0000	ET =	0.0000
HEAD DEP BOUNDS =	857.0347	HEAD DEP BOUNDS =	857.0347
RECHARGE =	569915.6875	RECHARGE =	569915.6875
TOTAL IN =	678710.7500	TOTAL IN =	678710.7500
OUT:		OUT:	
STORAGE =	0.0000	STORAGE =	0.0000
CONSTANT HEAD =	0.0000	CONSTANT HEAD =	0.0000
WELLS =	212257.7188	WELLS =	212257.7188
RIVER LEAKAGE =	114935.8750	RIVER LEAKAGE =	114935.8750
ET =	315645.3125	ET =	315645.3125
HEAD DEP BOUNDS =	767.3380	HEAD DEP BOUNDS =	767.3380
RECHARGE =	0.0000	RECHARGE =	0.0000
TOTAL OUT =	643606.2500	TOTAL OUT =	643606.2500
IN - OUT =	35104.5000	IN - OUT =	35104.5000
PERCENT DISCREPANCY =	5.31	PERCENT DISCREPANCY =	5.31

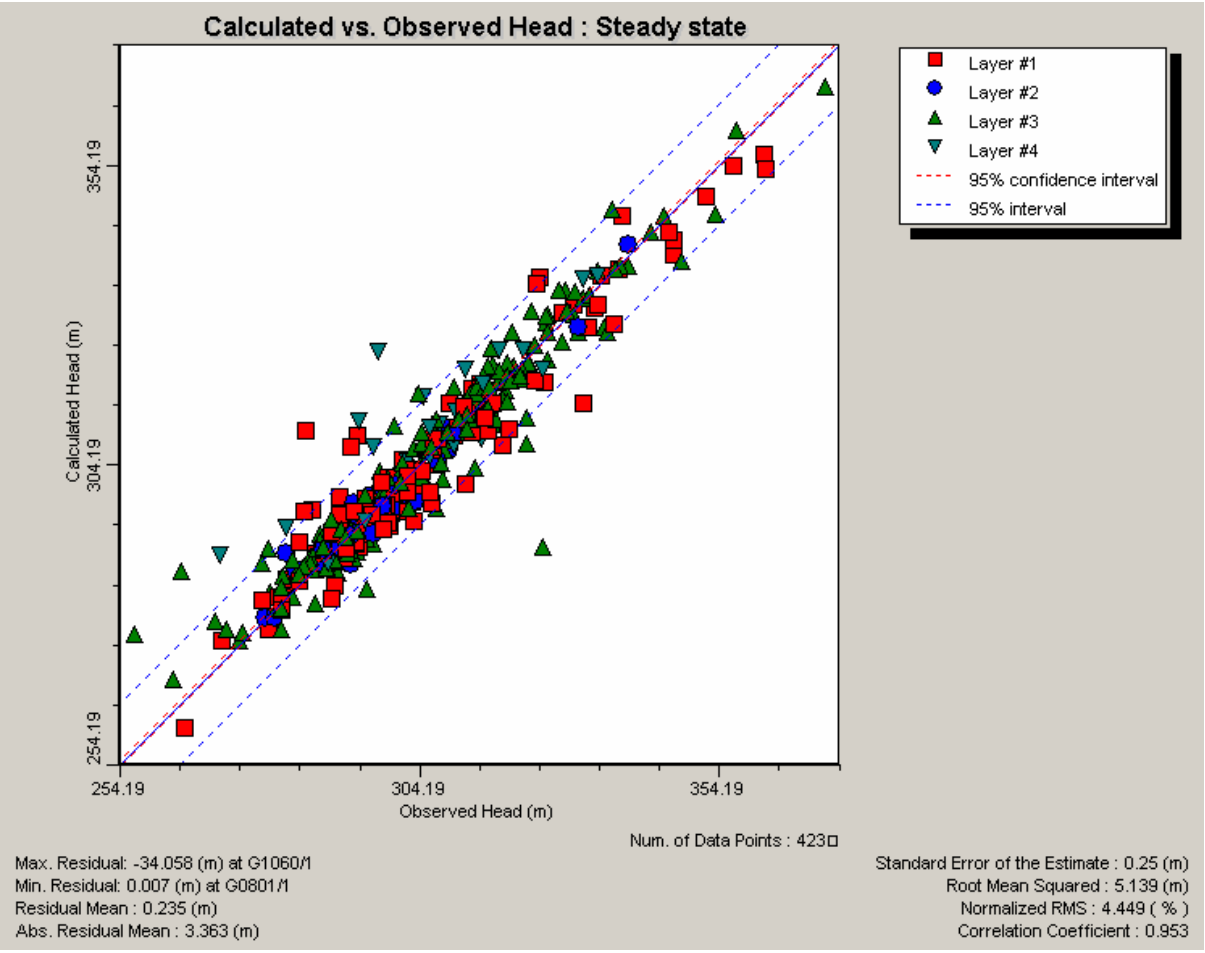

Groundwater Budget & Calibration Results for Realization #9
(Time = day, Length = meter)

VOLUMETRIC BUDGET FOR ENTIRE MODEL AT END OF TIME STEP 1 IN STRESS PERIOD 1

CUMULATIVE VOLUMES	L**3	RATES FOR THIS TIME STEP	L**3/T
IN:		IN:	
STORAGE =	0.0000	STORAGE =	0.0000
CONSTANT HEAD =	0.0000	CONSTANT HEAD =	0.0000
WELLS =	0.0000	WELLS =	0.0000
RIVER LEAKAGE =	99281.3281	RIVER LEAKAGE =	99281.3281
ET =	0.0000	ET =	0.0000
HEAD DEP BOUNDS =	869.8982	HEAD DEP BOUNDS =	869.8982
RECHARGE =	569915.6875	RECHARGE =	569915.6875
TOTAL IN =	670066.9375	TOTAL IN =	670066.9375
OUT:		OUT:	
STORAGE =	0.0000	STORAGE =	0.0000
CONSTANT HEAD =	0.0000	CONSTANT HEAD =	0.0000
WELLS =	212257.7188	WELLS =	212257.7188
RIVER LEAKAGE =	106364.0547	RIVER LEAKAGE =	106364.0547
ET =	310962.3125	ET =	310962.3125
HEAD DEP BOUNDS =	753.3288	HEAD DEP BOUNDS =	753.3288
RECHARGE =	0.0000	RECHARGE =	0.0000
TOTAL OUT =	630337.4375	TOTAL OUT =	630337.4375
IN - OUT =	39729.5000	IN - OUT =	39729.5000
PERCENT DISCREPANCY =	6.11	PERCENT DISCREPANCY =	6.11

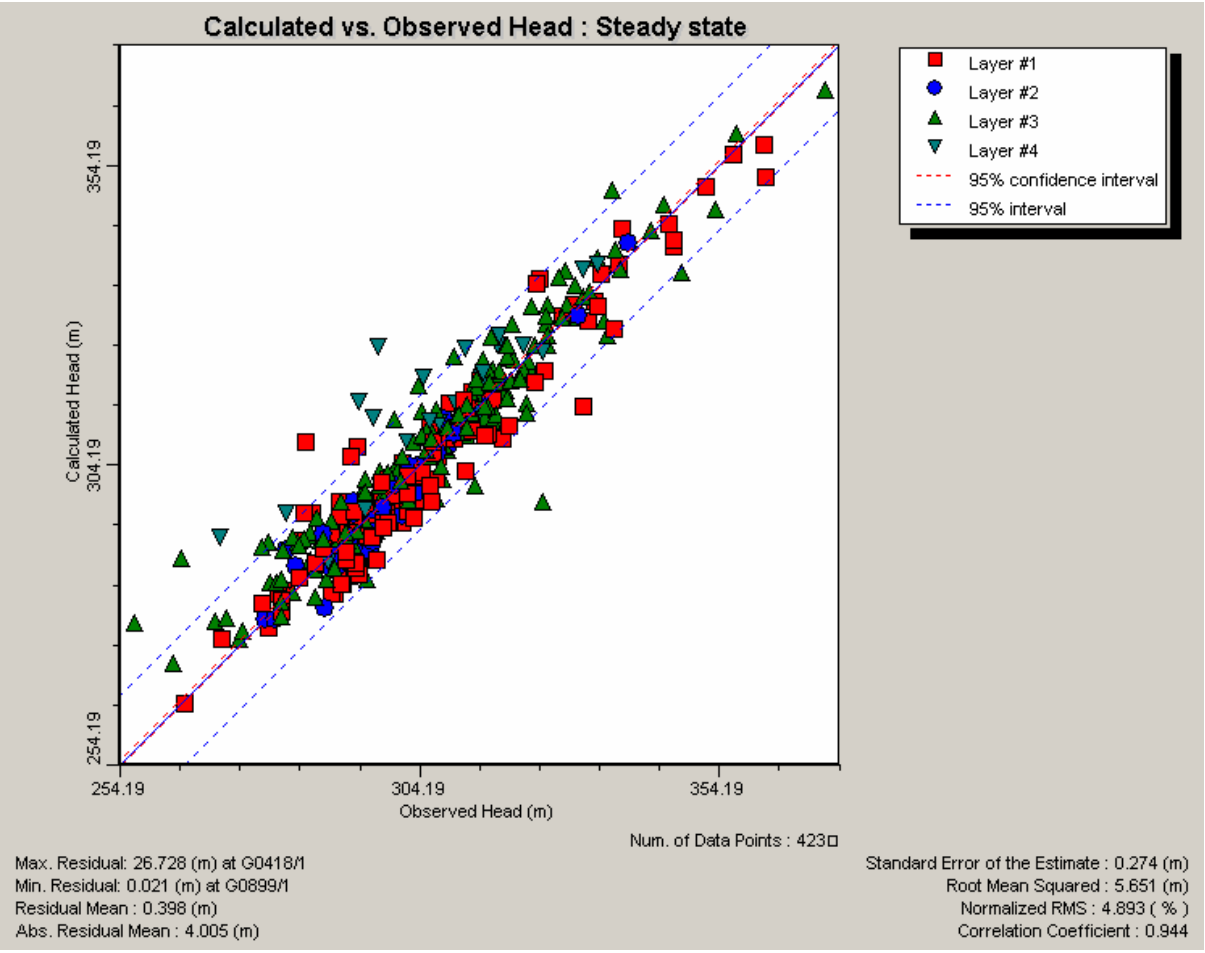

Groundwater Budget & Calibration Results for Realization #10
(Time = day, Length = meter)

VOLUMETRIC BUDGET FOR ENTIRE MODEL AT END OF TIME STEP 1 IN STRESS PERIOD 1

CUMULATIVE VOLUMES	L**3	RATES FOR THIS TIME STEP	L**3/T
IN:		IN:	
STORAGE =	0.0000	STORAGE =	0.0000
CONSTANT HEAD =	0.0000	CONSTANT HEAD =	0.0000
WELLS =	0.0000	WELLS =	0.0000
RIVER LEAKAGE =	106464.6328	RIVER LEAKAGE =	106464.6328
ET =	0.0000	ET =	0.0000
HEAD DEP BOUNDS =	859.4398	HEAD DEP BOUNDS =	859.4398
RECHARGE =	569915.6875	RECHARGE =	569915.6875
TOTAL IN =	677239.7500	TOTAL IN =	677239.7500
OUT:		OUT:	
STORAGE =	0.0000	STORAGE =	0.0000
CONSTANT HEAD =	0.0000	CONSTANT HEAD =	0.0000
WELLS =	212257.7188	WELLS =	212257.7188
RIVER LEAKAGE =	113343.3828	RIVER LEAKAGE =	113343.3828
ET =	316047.8125	ET =	316047.8125
HEAD DEP BOUNDS =	764.8276	HEAD DEP BOUNDS =	764.8276
RECHARGE =	0.0000	RECHARGE =	0.0000
TOTAL OUT =	642413.7500	TOTAL OUT =	642413.7500
IN - OUT =	34826.0000	IN - OUT =	34826.0000
PERCENT DISCREPANCY =	5.28	PERCENT DISCREPANCY =	5.28